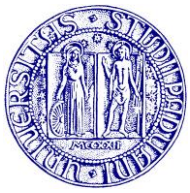

UNIVERSITY OF PADUA

DEPARTMENT OF PHARMACEUTICAL AND PHARMACOLOGICAL SCIENCES

DESIGN AND DEVELOPMENT OF A PVA COMPOSITE SCAFFOLD FOR PERIPHERAL NERVE REGENERATION

PhD Thesis

Borgio Luca

UNIVERSITÀ
DEGLI STUDI
DI PADOVA

UNIVERSITY OF PADUA

DEPARTMENT OF PHARMACEUTICAL AND PHARMACOLOGICAL SCIENCES

PhD SCHOOL IN BIOLOGY AND REGENERATIVE MEDICINE

BIOLOGY OF INTERCELLULAR INTEGRATION

XXV° CYCLE

PhD THESIS

DESIGN AND DEVELOPMENT OF A PVA COMPOSITE SCAFFOLD FOR PERIPHERAL NERVE REGENERATION

PhD School Director: Prof. Maria Teresa Conconi

Curriculum Coordinator: Dr. Luisa Dalla Valle

Supervisor: Prof. Claudio Grandi

PhD student: Dr. Luca Borgio

To my Family and myself

INDEX

ABBREVIATIONS

A	Absorbance
abs	abs
APO E	Apolipoprotein E
APS	Ammonium Persulfate
BDNF	Brain Derived Nervous Factor
BSA	Bovine Serum Albumin
CGRP	Calcitonin Gene-Related Peptide-
CNTF	Ciliary Neurotrophic Factor
CNTFRα	Receptor CNTFα
DAPI	4 ',6-Diamidino-2-phenylindole
DDS	Drug Delivery System
DLS	Dynamic Light Scattering
DNFH	Dinitrophenylhydrazine
DNF-hydrazone	dinitrophenylhydrazone
DSC	Differential Scanning Calorimetry
DTT	Dithiothreitol
ECM	Extracellular Matrix
ERK	Extracellular signal-regulated Kinase
FBS	Fetal Bovine Serum
FCS	Fetal Calf Serum
FDA	Food and Drug Administration
FGF	Fibroblast Grow Factor
GDNF	Glial Cell-Derived Factor Grow
HRP	Horseradish Peroxidase
HR	Horse Serum
IGF	Insulin-like Grow Factor
IL-1	Interleukin 1
IL-6	Interleukin 6
IMAC	Imobilyzed Metal Ion Affinity Chromatography
IPTG	Isopropyl-β-D-tiogalactopiranoside
LB	Luria Broth
LIF	Leukemia Inhibitory Factor
MAG	Myelin-Associated Glycoprotein

MBP	Myelin Basic Protein
MeCN	Acetonitrile
MMP	Matrix Metal Proteinase
MTT	3 - (4,5-dimethylthiazol-2-yl) -2,5-diphenyltetrazolium bromide
NEAA	Not Essential Aminoacids
NGF	Nerve Grow Factor
NRG-1	Neuregulin 1
NTFs	Neurotrophic factors NTFs
NT-3	Neurotrophin 3
NT-4	Neurotrophin 4
NT-5	Neurotrophin 5
OSM	Oncostatin M
PBS	Phosphate Buffer Saline
PCL	Polycaprolactone
PC12	Murine stabilized Pheochromocytoma cells
PEG	Polyethylene glycol
Pen-Strep	Penicillin and Streptomycin
PGA	Polyglycolic acid
PLA	Poly-Lactic Acid
PMP22	Peripheral Myelin Protein 22
PU	Polyurethane
PVA	Polyvinyl alcohol
P0	Protein zero
SDS-PAGE Gel	Sodium Dodecyl Sulfate Polyacrilamide Electrophoresis
SEM	Scanning Electron Microscope
SHSY5Y	Human stabilized neuroblastoma cells
CNS	Central Nervous System
SNP	Peripheral Nervous System
TEMED	Tetramethylethylenediamine
TFA	Trifluoroacetic Acid
ε	Molar absorptivity coefficient

RIASSUNTO

Le lesioni dei nervi periferici rappresentano il 2,8 % dei traumi totali annui. Più di 360.000 persone all'anno negli USA e più di 300.000 in Europa vanno incontro a questo genere di lesione, che spesso può portare ad una condizione di disabilità permanente (Ciardelli e Chiono, 2005).

La causa principale è rappresentata dagli incidenti automobilistici e pratica sportiva; ciò nonostante lacerazioni da coltelli, vetri, metalli e fratture ossee ricoprono il 30 % della casistica. Anche la stessa chirurgia, specialmente quella ortopedica degli arti superiori, è spesso causa di lesione nervosa, come lo sono anche le manovre di trazione che vengono effettuate durante il parto, che ricoprono il 0,12 % della totalità delle lesioni (Ichiara et al, 2008).

Sebbene nella maggior parte dei casi si ricorra alla chirurgia, l'ingegneria tissutale, basata su conoscenze di ingegneria dei materiali, fattori di crescita proteici e cellule (sia staminale che somatiche) si sta affermando sempre più come una valida, ed a volte, unica possibilità di riparazione delle lesioni nervose periferiche (Geuna et al,2007).

Basandosi su queste considerazioni è stato ideato, costruito, sviluppato e testato, da un punto di vista chimico, fisico e biologico uno scaffold tubulare di polivinilalcol (PVA). Il PVA è un polimero sintetico, idrosolubile, biocompatibile, resistente, poco costoso e difficilmente degradabile. Al fine di favorire una migliore cinetica di degradazione, il materiale è stato modificato chimicamente, mediante una reazione di tipo ossidativo. Questa stessa reazione si è dimostrata, inoltre, idonea a favorire il rilascio di fattori neurotrofici, tra cui TAT-CNTF, la cui attività è fondamentale nelle varie tappe del processo rigenerativo dei nervi periferici.

Il percorso di lavoro svolto, dalla ossidazione del materiale fino al prodotto finito (attraverso la tecnica di freese thawing) ha prodotto uno scaffold polimerico tubulare coperto da brevetto come invenzione industriale ((No: **VI2013A000019,** classe: A61K) depositato presso "Camera di Commercio Industria, Artigianato e Agricoltura" di Vicenza.

ABSTRACT

The peripheral nerve injuries represent 2.8% of the total annual trauma. More than 360.000 people at year in the U.S.A. and more than 300.000 in Europe undergo this type of lesion, which often can lead to a condition of permanent disability (Ciardelli and Chiono, 2005).

The main cause is represented by motor vehicle and sports accidents, nevertheless knives, glass, metal lacerations and bone fractures cover as much as 30% of the total cases. Even the same surgery, especially orthopedic on upper limb, it is often due to nerve injury, as they are traction maneuvers that are performed in childbirth, which cover a rate of 0.12% in all lesions (Ichiara et al , 2008).

Although surgery is a frequent medical practice in most of the cases, tissue engineering, based on knowledge and used of engineering materials, growth factors and cells (both staminal or somatic cells) is becoming more and more like a viable, and sometimes, only possibility of repair the peripheral nerve lesions (Geuna et al, 2007).

Based on these considerations it has been designed, built, developed and tested a composed tubular scaffold in polyvinyl alcohol (PVA) from chemical, physical and biological point of view. The PVA is a synthetic polymer, water-soluble, biocompatible, durable, inexpensive and hardly degradable. In order to facilitate a better kinetic of degradation of the material it has been chemically modified, by a oxidative reaction. This same reaction has been shown, moreover, to promote the release of neurotrophic factors, including TAT-CNTF, whose activity is known to be essential in the various stages of the peripheral nerves regeneration process.

The work course, from the material oxidation to the final product (through the freeze thawing technique) has developed a tubular polymer scaffold which is a patented industrial invention (No: **VI2013A000019,** class: A61K) deposited in “Camera di Commercio Industria, Artigianato e Agricoltura” of Vicenza, Italy.

INTRODUCTION

1) PERIPHERAL NERVE REGENERATION

1.1. Peripheral nerves anatomy

The nerves are tube-shaped branched anatomical structures, formed by bundles of myelinated and unmyelinated nerve fibers that connect the central nervous system to the periphery of the body, transmitting sensory and motor stimuli, or effector stimuli, or stimuli to control the smooth muscles of the viscera and blood vessels, myocardium and glandular secretion. Each nerve is covered by three concentric layers of connective tissue: the epineurium, the perineurium and the endoneurium (Fig. 1).

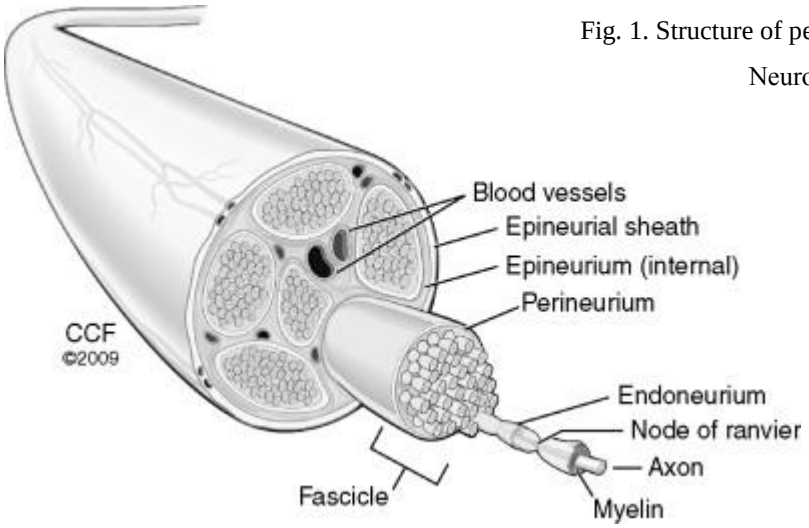

Fig. 1. Structure of peripheral nerve (from "International Review of Neurobiology". 87: 141-172. 2009).

The epineurium layer is placed externally and is formed by loose connective tissue of collagen fibers, fibroblasts and adipocytes. It is penetrated by blood and lymph vessels, which then branch out in the perineurium. In the perineurium can be distinguished an outer layer, said circumferential, and an inner, said interfascicular.

The structure of the nerve perineurium into sets, which are groups of axons. E 'consists of several layers of collagen fibers united to endothelial cells. The capillaries that pass through the perineurium continue in the endoneurium and ensure the necessary supply of oxygen and substances to axons and Schwann cells.

The endoneurium is the innermost layer. It consists of loose connective tissue and fibers of type I collagen, which run parallel to the axis of the axons; addition to these elements are present fibroblasts, macrophages and mast cells. The endoneurium surrounds the axon and Schwann cells, which represent the part of the peripheral nervous system glial: if they form only the neurilemma, is

a simple sheath around the monolamellar neuritis, the fibers will be of type amyelinic; if, instead, the plasma membrane of the Schwann cell goes to wrap the neuritis a variable number of times, there will be a sheath plurilamellar and the fiber will be of type myelin. The fiber myelin allows the saltatory conduction of the impulse, so as to increase the speed of transmission of the pulse from the periphery to the central nervous system and vice versa.

The nerve fibers of the peripheral nerves, then, in addition to being distinct in myelinated and unmyelinated, can be also classified according to the type and direction of stimulus, and according to the diameter.

Considering the type and direction of the pulse, we can distinguish between:

• Effector (drive or efferent) fibre, centrifugal flow in the central nervous system to the periphery; are divided into somatic, aimed at voluntary striated muscle, and visceral, with direct synaptic interruption of the sympathetic ganglia, the smooth muscles of internal organs, vessels , myocardium and glands.

• Sensitive (or related or afferent) fibre, a centripetal course from the periphery to the central nervous system; are divided into somatic, leading to nervous centers transduced sensory impulses from receptors sensitive skin, muscles and joints and visceral, leading to nervous center transduced sensory impulses from sensory receptors found in the viscera.

• Sensitive specific (or special sensory) fibre, leading to the nervous centers pulses transduced at the level of the sense organs.

If we refer to the diameter, this is directly proportional to the size of the cell body to which it belongs and to the length of the fiber itself. Therefore are distinguished:

• A fibres, myelinated, with a diameter of 3-22 μm;

• B fibres, myelinated, with diameter 1.5-3 μm;

• C fibres, unmyelinated, with a diameter of 0.3 to 1.5 μm.

The peripheral nerves include cranial nerves (12 pairs) and spinal nerves (33 pairs).

The spinal nerves are divided into eight cervical nerves, twelve thoracic nerves, 5 lumbar, 5 sacral and 3 coccygeal, of which the last two rudimentary. The spinal nerves unite the brain and spinal cord, constituting the central nervous system (CNS), to the peripheral tissues.

The spinal nerve is formed by the union of a nerve root front, which exits from the lateral-ventral furrow of the vertebral canal, and a rear, that comes out from the groove lateral-dorsal aspect of the spinal canal. Each posterior root has a swelling, called dorsal root ganglia and site of the sensory neuron called pseudo-unipolar ganglion neuron while the anterior root host axons of motor neurons α and Y located in the anterior horn of the spinal cord (Fig. 2).

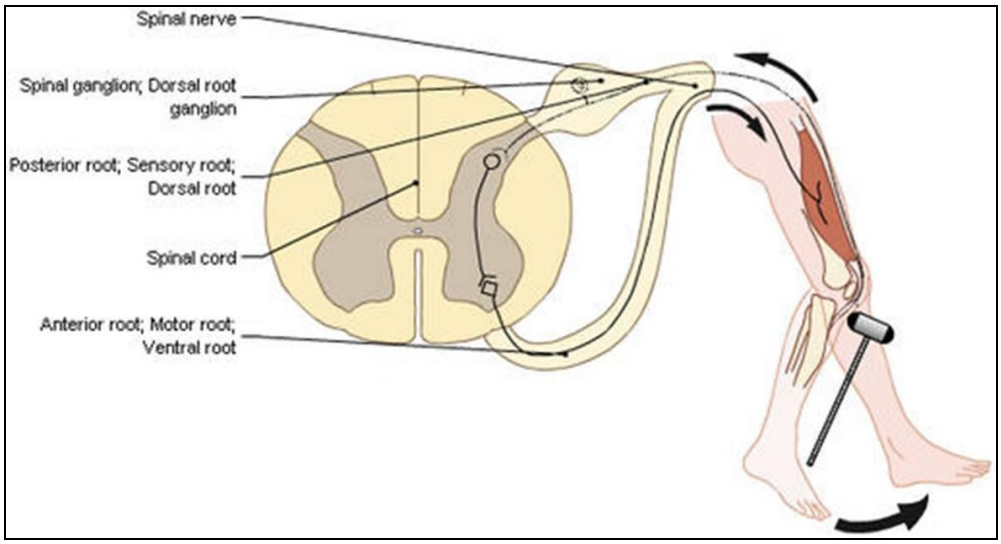

Fig. 2. Anterior and posterior root of the spinal nerve (from "Anatomy of the spinal cord", Micheau A. 2009).

The spinal nerve, which occupies the intervertebral foramen, is little more than 1 cm and includes both efferentand afferent nerve fibers. The output of the foramen, called the spinal nerve, divides into a dorsal branch (or rear) and a ventral (or anterior).

The dorsal branch is in turn divided into smaller branches, which will go to innervate the erector muscles of the spine and the skin overlying the muscles of the back. The dorsal branch have a segmental distribution and will go to innervate a specific region of the body surface called dermatome.

The ventral branch is also divided into a series of smaller diameter branches that innervate the muscles and skin of the front side of the body. From these smaller branches, originate also nerve plexuses, masses of fibers that take their name from their positions within the human body, and we can identified the cervical (Fig. 3A.), brachial (Fig. 3B.), lumbar and sacral plexus. From these plexuses originate from the real and actual peripheral nerves, which will extend to the whole organism.

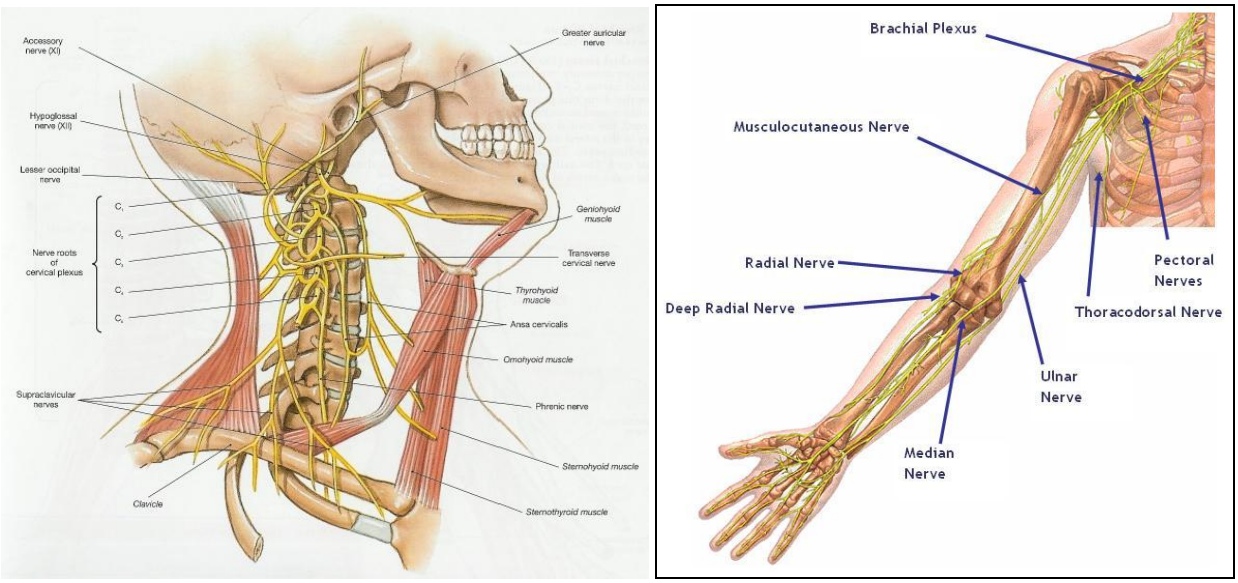

Fig. 3. Cervical (A) and brachial (B) plexuses.

1.2. Peripheral nerves lesion

Lots of knowledge about peripheral nerve lesions were acquired during war periods. For example the neurologist S. Weir Mitchell studied systematically this type of lesion during the American Civil War (Campbell, 2008).

The peripheral nerve injuries are very common and represent as much as 2.8% of the total annual trauma and may result in partial or complete loss of motor function, sensory and autonomic, and very often can induce a long-term disability for the patient (Ciardelli and Chiono, 2005).

The etiology of these lesions is quite varied, but the causes are mostly represented from bruises, sprains, lacerations with sharp objects, broken bones, car accidents, sports injuries; a case study is less represented by thermal damage, electrical, radiation, and percussion by compressions (that may give rise to phenomena of ischemic type). In some cases, the lesion can be connected to neoplasms, systemic diseases, immune and inflammatory reactions; very often the origin of nerve injury may be of iatrogenic type.

Nerve injuries can be divided into two types based on two classification: the classification of Seddon and that of Sunderland (Campbell, 2008).

In the Seddon classification injuries can be of three types:

• Neurapraxia: the nerve undergoes a loss of motor function and sensory, mainly due to ischemic or compression damage. The nerve is anatomically intact and, consequently, does not meet to Wallerian degeneration, but is not functional and therefore will not be able to transmit pulses: consequently it will also have a paralysis of the body part innervated with possible due to disuse atrophy. Generally the lesion resolves in three to six months with remyelination.

• Axonotmesis: axons within the nerve is damaged or destroyed but the structure of the surrounding connective tissue remain intact. Distal stump of the nerve undergoes Wallerian degeneration, while the proximal stump undergoes retrograde degeneration. The transmission pulse is compromised, as well as the functionality of the connected area of the body. The reinnervation depends on the degree of internal injury and the distance of this from the muscle. The absence of lesion of nerve connective structures makes it unnecessary surgery.

• Neurotmesis: the nerve is completely severed and there is no continuity between it and the stump, the connective tissue is damaged severely. Even in this case the proximal stump undergoes retrograde degeneration, while the distal to Wallerian degeneration. In this type of injury the spontaneous regeneration is slow and, very often, not functional: it is, therefore, necessary surgery to ensure speed and quality of the regeneration process, as well as to avoid complete degeneration, with consequent atrophy of the muscle.

The classification according Sunderland is much more complex and identifies five degrees of lesion (Campbell, 2008): the first, the second and the fifth match neuraprassia, axonotmesis and neurotmesis of Seddon, while the third and fourth represent two subclasses of axonotmesis.

The third degree of lesion involves axonotmesis with damage not only of the axon, but also of endonevrium, while the perineurium is not compromised. In this type of injury Schwann cells are not able to organize themselves into columns and the surrounding environment to the region of the axon is damaged and less favorable to regeneration. Even in this case the distal stump undergoes Wallerian degeneration and the proximal to a much more extensive retrograde degeneration. The reinnervation will be less efficient with respect to a lesion of the second degree and can lead to a recovery rarely around 60-80% of the initial functionality.

In the fourth degree of injury the internal structure of the nerve is completely destroyed and is unaffected only the epineurium. The continuity of the nerve structure is maintained only by fibrous scar, due to the activity of fibroblasts at the point of injury. The presence of this scar hinders axonal regeneration contributing, instead, to the formation of a mass of fibers said neuroma in continuity,

that will not allow the recovery of the function. Even in this case it becomes necessary to surgery in order to remove the fibrotic tissue and promote optimum regeneration (Fig. 4.).

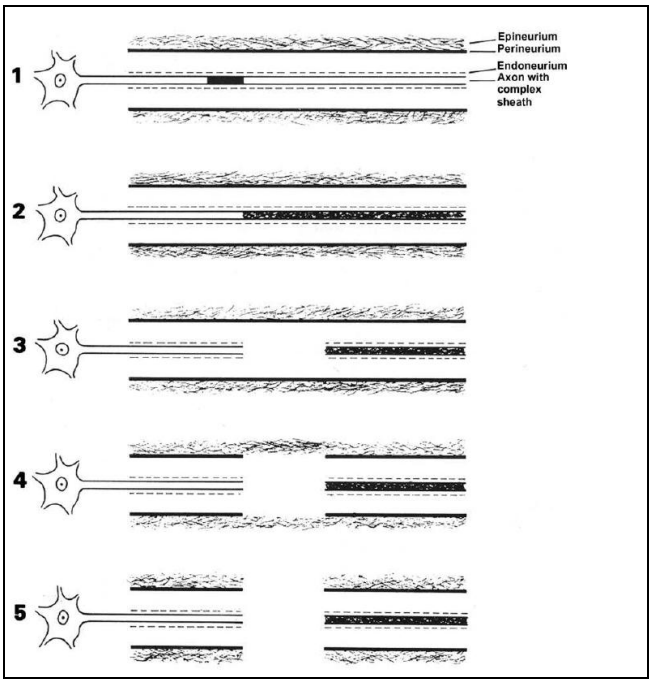

Fig. 4. Summary outline of the wound according to 5 degrees of Sunderland classification (Campbell, 2008).

In lesions of mixed type can coexist various signs of lesions already described above; are very common and are undoubtedly the most complicated from a surgical point of view: this group is known as the sixth degree of lesion.

The two classifications just explained very often create difficulties of interpretation and can make confusion. For this purpose it has been proposed a criterion which divides the lesions of peripheral nerves in degenerative and non-degenerative lesions: not degenerative type don't involve impairment of the axon, while the degenerative lesions include partial nerve impairment, with or less maintenance of endonevrium, and the total transection type (Campbell, 2008).

1.2.1. Cellular and molecular bases of peripheral nerves regeneration

In the central nervous system (CNS) there is no regeneration, except for a few areas such as the olfactory cortex, the hippocampus and the subventricular zone; if the site of the lesion is not localized in these areas, there will never be a recovery of functionality but rather other undamaged areas will fulfill the functions of the injured area (nervous plasticity) (Campbell, 2008).

The peripheral nervous system (PNS), instead, is able to regenerate spontaneously. The regeneration is based, fundamentally, on three mechanisms: remyelination, sprouting from the distal axons not damaged and the regeneration from the site of the lesion. If the lesion involves approximately 20-30% of axons repair is based on the collateral sprouting from undamaged axons, if the lesion involves more than 90% of the axons primarily involved in the repair mechanism that involves the regeneration directly from the site of the lesion (Campbell , 2008).

In peripheral nerve injury death of neurons can be stimulated by several factors, including a small diameter axons, the age and the proximity of the cell body to the area of injury (Hall, 2005 and Navarro et al, 2007). The recovery of the function depends on several factors, intrinsic and extrinsic to the neuron; in the first place, the neurons survivors will have to adapt to the new situation and for this will have to switch from mediators of signal to them of growth, secondly the environment at the level of the abutment will provide sufficient support to the distal axon regeneration and finally target must be satisfactory reinnervated to ensure full recovery of the function (Ichihara et al, 2008).

Most nerve injuries cause breakage of the fibers and already in the 24 hours after this event you can see the first phenomena of degeneration, which can last for weeks. At the level of the residual limb distal axons and myelin coatings undergo a process of degradation and fragmentation, said Wallerian degeneration. In this phase the myelin is transformed into neutral lipid compounds that will be eliminated by the combined action of Schwann cells de-differentiated, of blood monocytes that manage to infiltrate at endonevrium site becoming damaged and macrophages from a population of macrophages already present in the nerve (Campbell, 2008). For regeneration purposes is also important the degradation of proteins that inhibit regeneration, like the myelin associated glycoprotein (MAG) (Fig. 5).

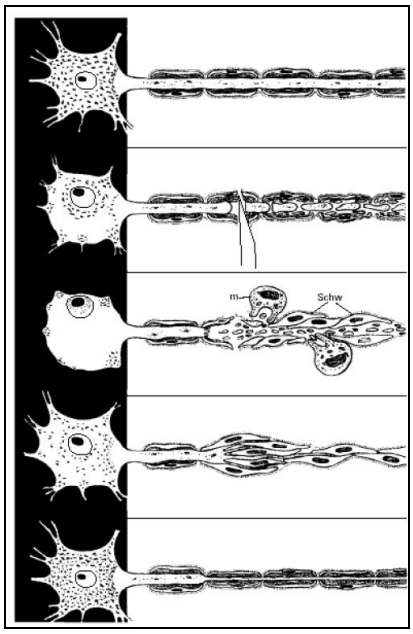

Fig. 5. Summary diagram of neuronal changes after injury (Hall, 2005).

A fundamental role in the process of regeneration is accomplished by Schwann cells: early in the regenerative process they are detached from the distal stump and de-differentiate to the stage of pre-myelinating cells. The same cells, within 48 hours after injury, also reduce the expression of genes coding for the typical proteins of the myelin such as myelin basic protein (MBP), the myelin protein zero (P0), the peripheral myelin protein 22 (PMP22); there was also a decrease of proteins such as connexin 32 and the E-cadherin, fundamental for the organization of nodes and internodes, as well as of caveolin, essential for the transport of cholesterol to the cell.

After three or four days after injury, Schwann cells de-differentiated enter into an intense proliferative phase, at the level of the distal stump, probably also stimulated by the activity of mitogenic macrophages, involved in the release of neurotrophic factors and neurotropic.

Wallerian degeneration is in fact related to an intense inflammatory response that, in some way, promotes the regeneration process. In a few hours, at the level of the distal stump, can be an increase in the levels of cytokines, chemokines, tumor necrosis factor (TNF), interleukin 1 (IL-1) depending from Schwann, mast cells (which increase the permeability of blood vessels in order to facilitate the migration of macrophages), macrophages (which are able to increase the levels of IL-1 action stimulating the production of nerve grow factor (NGF) and secrete apolipoprotein E (Apo E), able to collect the lipids from debrids of cells and direct it to the Schwann cells during regeneration) and from activated endothelial cells (Hall, 2005).

Another important factor favoring the proliferation is the increased production of erythropoietin, which stimulates mitotic activity of Schwann cells through the activation of an autocrine mechanism that includes the phosphorylation of JAK proteins 2 and of the extracellular signal-regulated kinase (ERK) as well as the downregulation of the metal-matrix proteinases (MMP-3), which normally act on fibronectin to generate a fragment that involves inhibition of the division of Schwann cells (Hall, 2005).

Subsequently Schwann cells undergo in a proliferative state and migrate towards the proximal part of the injured nerve and go to form the columnar structures, real binary, said columns of Bunger, which act as support for the regeneration. The columns of Bunger are formed at the level of the basal lamina in formation and promote neuronal regeneration in a favorable growth environment (Ichiara et al, 2008). The columns of Bunger are maintained until you will have a satisfactory regeneration of the nerve, which will occur when the sprouts emerged from the proximal stump and penetrate in the endonevrium of the distal stump and grow distally in close contact with the basal lamina and Schwann cells de-differentiated associated with it (Johnson et al, 2005). For innervation occurred Schwann cells will multiply even so as to be able to rely on a large number of cells to myelinate the axon; subsequently re-differentiated to the stage of myelinating cells and begin to produce layers of myelin wrapping around the axon.

In the regenerative phase Schwann cells are able to promote increased synthesis and secretion of neurotrophic factors (NTFs), essential in the regeneration, since it can attract and guide the axons; they include the nerve grow factor (NGF), brain-derived nerve grow factor (BDNF), neurotrophin 4 and 5 (NT 4 and 5), glial-cell-line derived neurotrophic factor (GDNF), ciliary neurotrophic factor (CNTF) and insulin-like grow factor (IGFs).

Simultaneously to changes of the Schwann cells, also the proximal stump and the soma undergo a series of morphological and functional changes.

In the soma, after the lesion, occurs an increase in cytoplasmic RNA simultaneously with an increase in the production of lysosomal acid phosphatase, which are essential for digestion of axonal fragments. The soma also meets chromatolysis, process in which there is an increase in cell volume and dispersion of the “tigroid” substance (or Nissl), due to increased metabolic activity. Subsequently the soma promotes an increase in the synthesis of proteins intended for axon growth and during this process can occur a retraction of synapses from the cell body (Johnson et al, 2005).

In the portion proximal to the lesion, although there is retrograde degeneration limited to the first node or a little more, the proximal stump is able to survive because there is no interruption of

continuity with the soma. During the phase immediately subsequent to the lesion are witnessing an increase in the intracellular concentration of Ca^{2+} ions and of vasoactive peptides such as calcitonin gene-related peptide (CGRP) which together with the degranulation of mast cells are responsible of the hyperaemia in the area of the damage. The increase of intracellular Ca^{2+} also promotes the activation of proteolytic enzymes Ca^{2+}-dependent (as phospholipases and calpains) that promote the degeneration of the cytoskeleton (Hall, 2005) and its subsequent remodeling in order to encourage the formation of a " cone "of growth, one for axon, capable of emitting pseudopodia which ramify advancing distally. The axonal sprouting is favored by the release, by the Schwann cells, macrophages and from the distal stump of the same substances chemoattractant, such as, for example, neuronal growth factors.

The regeneration also needs a basal lamina, a particular type of extracellular matrix, which acts as a "scaffold" for the cells in regeneration.

The basal lamina, which mediates the contact between the axon in the process of regeneration and Schwann cells de-differentiated, is rich of adhesion molecules, such as fibronectin, laminin and collagen able to promote axon elongation in via regeneration (Ichiara et al, 2008).

The repair of a minor injury and medium-sized start immediately, and regeneration occurs quite quickly, and if the injury is serious, however, the repair and regeneration have timing protracted and very often you will have to resort to surgery to ensure recovery optimal functionality.

1.2.2. Treatment of peripheral nerve injuries

Unlike the CNS, injuries to the SNP can be resolved by the application of different surgical techniques. At first, the most common approach is based on simple sutures between the two nerve stumps, leading to poor recovery of function, and then, with the introduction of grafts in surgical practice and tubulization cases of complete recovery increased significantly. It’s important to remember that the suture is not possible without the absence of tension at the site of union and that is always important the alignment of the files nervous, and, by considerable distances between the two ends it is essential to use a " guide ", which allows the correct axonal growth without formation of neuroma (IJkema-Paassen et al, 2004).

The peripheral lesions can be divided into incomplete, without loss of substance, and total, with or without loss of substance.

The techniques used for the repair of incomplete lesions include:

• Epinevrial suture terminal-to-end: in this technique the lesion can intervene at epinevrium, the proximal and distal stumps are immobilized to avoid creating tension in the stitches. After carefully aligned the two nerve stumps, is practiced on a single suture around the whole circumference of the nerve. The elements within the nerve remain intact, there may be some minimal fibrosis intraneuronal. It is practicable in lesions size of less than 5 mm (Daly et al, 2012).

• Perinevrial terminal-to-end suture: this technique involves the alignment of the nerve fibers and the suture at the level of files, on the perineurium within the nerve will then present foreign material that will favor the onset of fibrosis. This technique is also particularly difficult for the alignment of files at the level of the two nerve stumps since it is important to avoid the creation of tensions at the point of suture to prevent further fibrosis, compressions of axons in the process of regeneration and problems to microcirculation.

• Epinevrial suture: this technique is the set of the preceding in which the suture is performed to realign the dossiers nerve, by passing the thread through the epineurium and the perineurium.

The techniques used for the repair of total injuries include:

• Suture termino-terminal under tension: the two nerve stumps, although they are physically separated, are sutured under tension; the same tension is greater as much as greater is the distance between the two nerve terminals. In point of suture usually occurs a fibrous expanded that inhibits correct axonal regeneration (Battiston et al, 2005).

• Suture termino-lateral: the technique is employed in the case of not accessibility to the proximal stump following a lesion with loss of substance (Beris et al, 2006). In this case it exploits the epineurium of a healthy nerve close to that lesioned that will act as a "bridge" to axons in the process of regeneration. Seen that the Wallerian degeneration is a fundamental process for the start of regenerative processes, it becomes necessary the incision of the healthy epinevrium in order to stimulate all those phenomena, such as the release of neurotrophic factors from Schwann cells, which, in the meantime, have migrated in the healthy epinevrium, required to collateral sprouting. The incision of a healthy nerve may cause, in turn, serious consequences. For this reason, at times, especially if the healthy nerve is not very close to that lesioned, it is possible the use of pipes of silicone to rejoin the two nerve stumps. These devices must be enriched in cellular elements and/or pro-regenerative factors. Very often, in order to avoid the application of sutures, with consequent possibility of onset of fibrotic scar and damage to the healthy nerve, is used fibrin glue.

• Grafts: the graft is a connection of various nature that connects the two ends of the injured nerve, without tension. They are generally used in case of nerve lesions of size greater than 5 mm, for which the simple suture would cause an excessive tension on the point of reunification between the two stumps (Johnson et al, 2008).

These structures act as trophic and mechanical support and are able to drive the neuronal regrowth: in fact they contribute to direct sprouting from the proximal stump of the injured nerve, create a system for the diffusion of growth factors released from the injured nerve and reduce the onset of fibrosis.

Depending on the origin of the material used for the graft creation it is possible to distinguish:

• Autograft: the material comes from the same patient from injury;

• Allograft: the material comes from external donors, often by dead people;

• Xenograft: the material comes from different species.

The allograft and xenograft are more available but often cause immunogenicity, thus making necessary immunosuppressive therapies.

The best regeneration occurs using autograft: they have many advantages, including the biocompatibility between tissues, the low toxicity and the ability to promote adhesion and cell migration. The autograft also entails some considerable drawbacks, such as the need of an additional step to collect the material to be used as graft and the possible loss of functionality of the area of the body from which is picked up the material for the construction of the graft. Very often the length of the material withdrawn is not sufficient to repair the lesion and the recovery of the full functionality is not always granted. It is applicable to lesions smaller than 5 cm (Daly et al, 2012).

The graft is generally constituted by a portion of a vein, muscle or nerve. The repair of nerve injuries through the use of venous materials have reported many successes, comparable to those obtained by the use of nerves, especially in terms of recovery of sensitivity. The use of venous grafts can only find application in cases of nerve injury of small size (less than 30 mm): for this reason it has been studied a "mixed" graft, consisting of a fragment of vein filled with a piece of muscle or nerve (Fig. 6.) (called “muscle into vein” or “nerve into vein”), which gave satisfactory results in nerve lesions larger than 30 mm (Battiston et al, 2005).

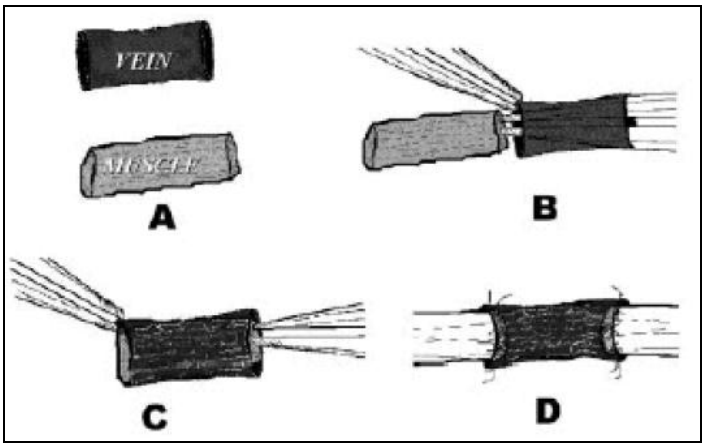

Fig. 6. Scheme of the preparation of the "muscle into vein" (Battiston et al, 2005).

The use of skeletal muscle as a material for a simple decellularized or filler mixture of graft is motivated by the presence in the muscle of proteins, such as laminin, fibronectin and collagen, able to promote axonal elongation (IJkema-Paassen et al, 2004). However a graft consisting of a fragment nervous is the best choice, especially if the fragment comes from the same patient. It is an ideal scaffold, which will contain all the cellular and molecular elements (Schwann cells, basal lamina, endoneurium and growth factors) capable of favoring the neuronal growth. Generally are used fragments of the sural and saphenous nerve, whose injury does not involve serious loss of functionality and sensitivity. Despite the great potential, also the use of a nervous graft involves certain disadvantages including the narrowness of the nerves of possible use and their length (often insufficient to join the two stumps in a nerve injury), surgical interventions, loss of sensitivity, the inadequate support for axonal growth and the possibility that the recovery is less than 40% (Ichihara et al, 2008).

Given the multiple disadvantages, microsurgery is oriented towards innovative repair systems, including the tubulization.

2) BIOMATERIALS AND NERVE REGENERATION

2.1. The tubulization in the peripheral nerves regeneration process

The tubulization is a technique used for a long time in surgery of peripheral lesions, although the greatest development has been in the last twenty years. Already in the nineteenth century was aware

of the possibility of using a fragment, not nervous, to reunite two separate nerve ends. The first materials used were of human origin and only secondarily was thought of a possible use of synthetic materials for regenerative purpose (Battiston et al, 2005).

The tubulization is a technique based on the creation of true and proper tubular pipes consist of materials with inorganic, natural or synthetic origins which have the task of ensuring continuity between the proximal and distal nerve stump. It's use is increasingly frequent, given the larger limits to the use of the graft, the interesting mechanical properties and the ability to induce a chemical stimulation in axonal regeneration (Ciardelli and Chiono, 2005). This technique brings many advantages in nerve repair: reduces the infiltration of the myofibroblasts, the appearance of neuroma and fibrotic, favors collateral sprouting and the accumulation of neurotrophic factors (Daly et al, 2012). They are therefore employed tubular prostheses in cases of injury with loss of substance and allows to guide axonal sprouting from the proximal end of the severed nerve, favors the diffusion of neurotropic and neurotrophic factors secreted by the distal stump and restricts the onset of fibrosis (Johnson et al, 2005) (Fig. 7.).

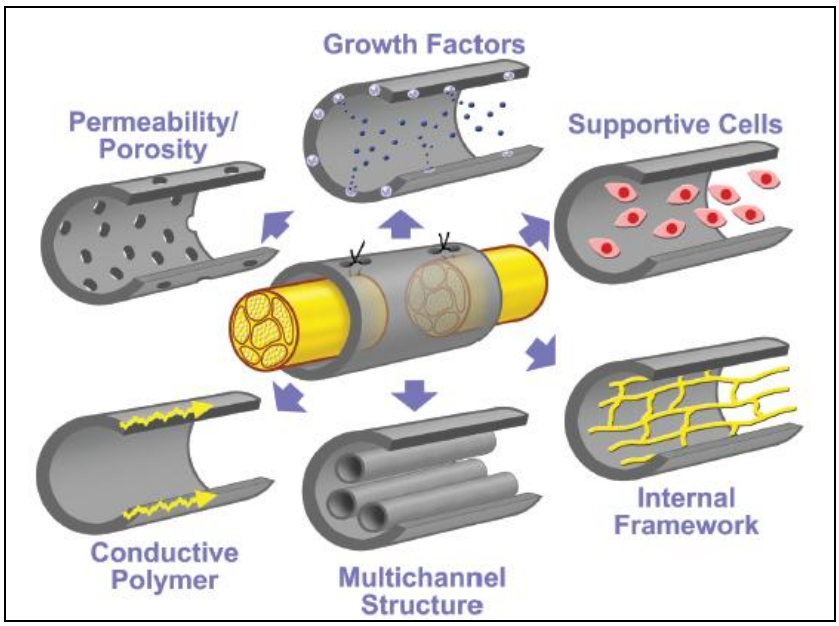

Fig.. 7. Diagram of possible properties of a tubular scaffold in nerve regeneration application (De Ruiter et al, 2009).

To ensure the regeneration, the scaffold must possess certain characteristics such as:

• Appropriate support for axonal regeneration: it must have excellent flexibility and mechanical strength;

• Being semi-permeable, so as to promote vascularization, the exchange of nutrients and pro-rigenerative factors between the tube and the external environment and the elimination of waste substances;

• Biodegradable and bioabsorbable: a tube which is degraded too quickly is not able to ensure the mechanical and trophic support useful to regenerate; products derived from the degradation must, furthermore, be absorbable and non-toxic, while a tube that degrades too slowly will remain in the site of application as a foreign body, stimulating the inflammatory response and/or immune, without favoring the regeneration;

• Biocompatible with the organism in which it is implanted and non-toxic;

• Must have a three-dimensional structure to mimic the native nerve structure;

• Must promote the adhesion, proliferation and cell migration;

• Must be manufactured in a simple way and be cheap.

Obviously, the choice of a system must be determined also by the nature and extent of the lesion (Tabesh et al, 2009). If the lesion is small, an efficient regeneration can be obtained by the use of a simple hollow tube. The regeneration generally develops into five different phases: in the fluid phase there is a reversal of plasma exudate from both stumps of injured nerve, rich in pro-regenerative factors and molecular precursors of the extracellular matrix. Then enter the phase "matrix", which there is the formation of a fibrin network between the proximal and distal stumps without cells. This process takes about a week. The third step involves cell migration: endothelial cells, fibroblasts and Schwann cells migrate, proliferate and align along the fibrin network. It is followed by the axonal phase, in which occurs the sprouting of axons in the process of regeneration. The last step provides for the re-myelination of axons (Daly et al, 2012) (Fig. 8.).

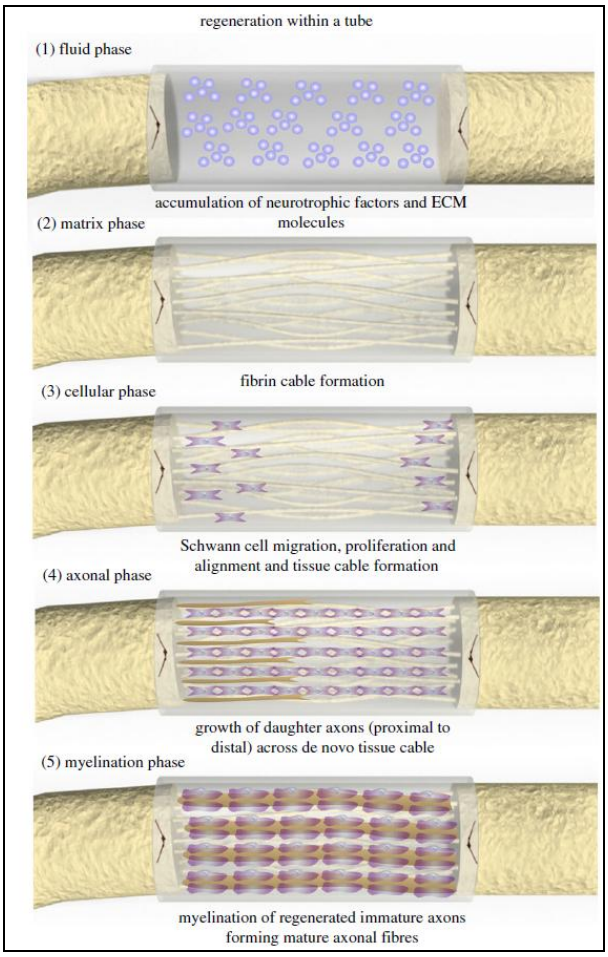

Fig. 8. Stages of regeneration with the application of hollow tubes (Daly et al, 2012).

If the lesion is extended it is necessary to implant a full pipe to prevent that the external structure collapses on itself and to avoid the lacking in cell migration in the site of injury, due, very often, to inadequate formation of the fibrin network in regenerative process. A current strategy for nerve repair involves the addition of an intraluminal structure (filler) which can act both as a support for the fibrin network and the elongation of axonal sprouts and cellular migration and proliferation (Daly et al, 2012). As fillers may be used synthetic and natural materials in the form of gels, sponges, films, fibers and filaments.

The repair of a clinically relevant nerve lesion generally requires a year to allow the complete regeneration of the nerve. Therefore, the materials used for the construction of scaffolds for nerve regeneration must be slowly degradable and reduce in thickness but maintain the flexibility and an adequate mechanical strength.

2.2. Biomaterials characteristics in peripheral nerves regeneration

The use of biomaterials in tubulization of two nerve stumps was born as an alternative to the techniques of grafting; the first articles about treated the properties of some inert metals, cellulose esters, gelatin, most of which turned out to be unsatisfactory for nerve regeneration. Only in the last two decades there has been a real improvement in knowledge of biomaterials and their properties.

The use of biomaterials is part of tissue engineering applications: it can be defined as a new therapeutic approach and can improve the regeneration and repair of damaged tissues relying on natural healing potential of the patient himself. It can be considered a viable alternative to both the reconstructive surgery and the organ transplantation, fundamental practices but with quite a few drawbacks.

Therapy of tissue regeneration has three main objectives: the first is to act as a new therapeutic strategy. The second is to broaden the scope of conventional therapies and the last is the desire to combat the deterioration typical of degenerative diseases. Therapy of tissue regeneration has two possible approaches: the first is to transplant cells with high proliferative potential in the site affected by the damage by infusion or injection. The effectiveness of this practice is limited because only few cells can survive. The second approach is based on the use of biomaterials, able to create an ideal environment to the cellular proliferation and differentiation.

In tissues, there are two fundamental elements, cells and the extracellular matrix (ECM), the latter can be regarded as a natural scaffold inside the body able to promote the cellular proliferation and differentiation. The tissue regeneration generally takes place using one or both elements in an appropriate combination. Biomaterials play a key role in the creation of substitutes of the extracellular matrix for the preparation of scaffolds and substrates for cell culture, DDS and progress in the research of stem cell biology. The biomaterials suitable for the regeneration of the peripheral nerve are chosen according to some characteristics which must be fulfilled, such as:

• Adaptability to mechanical stress and strain at the site of injury;

• Biocompatibility and lack of immunogenicity;

• Biodegradability, therefore the capacity of being degraded or solubilized by any process that allows for the elimination from the implantation site. The degradation of a biomaterial can occur in two ways: the first comprises phenomena of hydrolysis and enzymatic digestion, involving progressive loss of mass of the scaffold to its complete elimination. The second involves the splitting of the material, chemically cross-linked, water-soluble into fragments;

• Stability, from a mechanical and chemical point of view;

• Non-toxic;

• Processing, and suitable for the construction of various devices;

• To promote the release of bioactive components, such as DDS.

These characteristics can be found in polymers (Tab. 1 and 2), both natural and synthetic, while other materials such as metals or ceramics (inorganics) have shown little properties for tissue regeneration.

TABLE 1. COMMON MATERIALS USED TO CONSTRUCT NERVE GUIDANCE CHANNELS

Material	*Degradable or nondegradable*	*In vivo studies in the CNS?*	*Source*	*Cell adhesive*	*Electrically active?*	*Comments*
Silicone	Nondegradable	No	Synthetic	No	No	Provides a means to isolate regeneration environment
PAN/PVC	Nondegradable	Yes	Synthetic	No	No	Used mainly for delivery of Schwann cells or olfactory ensheathing glia
PTFE	Nondegradable	No	Synthetic	No	Sometimes	Highly inert and considered physiologically compatible
PHEMA	Nondegradable	Yes	Synthetic	No	No	Similar mechanical properties to the spinal cord
Poly(α-hydroxyacids)	Degradable	Yes	Synthetic	No	No	Family of synthetic polymers that display a spectrum of mechanical properties
Chitosan	Degradable	No	Insects and crust-aceans	Sometimes	No	Cationic nature may improve neuronal adhesion
Collagen	Degradable	Yes	Animals	Yes	No	Proven to enhance growth and differentiation of many cell types
PHB	Degradable	No	Bacteria and algae	Yes	No	Contains longitudinally oriented fibers for neuron and glial cell guidance
PVDF	Nondegradable	No	Synthetic	No	Yes	Provides electrical stimulation without an external source
PP	Nondegradable	No	Synthetic	No	Yes	Used with controlled external electrical stimulation

TABLE 2. FDA-APPROVED PNS NERVE GUIDANCE CHANNELS (ADAPTED FROM SCHLOSSHAUER ET AL., 2006)

Material	*Name*	*Degradable or nondegradable*	*Description*	*Diameter (mm)*	*Length (cm)*	*Company*
PGA	GEM Neurotube®	Degradable	Porous, corrugated, woven mesh tube	2.3–8	2–4	Synovis Micro Companies Alliance Inc., Birmingham, AL
Type 1 collagen	NeuroMatrix™	Degradable	Semipermeable tube composed of dense fibers	2–6	2.5	Collagen Matrix, Inc., Franklin Lakes, NJ
Type 1 collagen	Neuroflex™	Degradable	Semipermeable, flexible tube composed of dense fibers	2–6	2.5	Collagen Matrix, Inc., Franklin Lakes, NJ
PLCL	Neurolac®	Degradable	Flexible, transparent tube	1.5–10		Polyganics BV, The Netherlands
Type 1 collagen	NeuraGen®	Degradable	Semipermeable tube composed of crosslinked collagen fibers	1.5–7	2–3	Integra™ NeuroSciences, Plainsboro, NJ
Type 1 collagen	NeuraWrap™ Nerve Protector	Degradable	Wrap composed of cross-linked collagen fibers with a porous outer layer and a semipermeable inner layer	3–10	2–4	Integra™ NeuroSciences, Plainsboro, NJ
Poly-vinyl alcohol hydrogel	SaluBridge™	Nondegradable	Flexible hydrogel with similar mechanical properties to human tissue	2–10	6.35	SaluMedica™, LLC, Atlanta, GA

Tab. 1 and 2. List of some of the most common natural and synthetic biomaterials (De Ruiter et al, 2009).

There are substantial differences between natural and synthetic polymers: in the first place, the synthetic polymers are degraded by hydrolysis, while the natural by enzymatic process. Synthetic polymers are easily modified, both chemically and physically, and are more adaptable, while the natural polymers, deriving from peptides, polysaccharides or nucleic acids are difficult to handle.

From the chemical point of view, instead, the synthetic polymers are more hydrophobic than the natural type, and are more rigid, but more mechanical resistance, when compared to natural: this

makes them less degradable. The majority of them have also poor adhesion and pro-survival cellular properties. To cover these problems, the surface of synthetic materials can be modified by chemical reaction; on the other hand also the natural one can be physically, enzymatically and chemically cross-linked to improve mechanical stability and strenght.

Therefore the biomaterials used in the context of nerve regeneration may be employed both biological materials that synthesis:

- ***Biological Materials***

The natural polymers usually derived from proteins or carbohydrates, are biodegradable, non-toxic, mechanically similar to the tissue to be replaced and promote cellular adhesion and migration (Tabesh et al, 2009).

Collagen is considered to be the ideal material in tissue regeneration since it is the most abundant component of the extracellular matrix; as a support to the tissues and interacts with the cells to promote adhesion, migration and proliferation. The material is isolated from animal tissues and is characterized by mechanical strength, biocompatibility and low immunogenicity. It's a fibrous protein with a triple helix structure given by the winding of three peptide chains α1, α2 and α3, with the repetition of the pattern glycine-XY, where X and Y are other aminoacids, usually proline and hydroxyproline. The different arrangement of the collagen molecules form aggregates with different structure: collagen type I, II, III and V has fibrillar structure; the type IV, the main component of the basal lamina form, however, a two-dimensional network. The collagen is suitable to be processed in order to obtain different shapes, such as sponges and porous gels and can be cross-linked with chemical agents to modify compactness and degradability. Being an animal protein can induce immunological problems.

Chitosan is a polysaccharide obtained by N-deacetylation of chitin and its copolymers of D-glucosamine and N-acetyl-D-glucosamine (Ciardelli and Chiono, 2005); it is a cationic polymer and has a structure similar to the glycosaminoglycans of the basal lamina and extracellular matrix: this particular configuration allows the interaction between the polymer and the molecules of the extracellular matrix (such as laminin, fibronectin and collagen). It has several properties: low immunogenicity and easy to work with. The material was used in the regeneration of cartilage, nerves and liver but, despite the excellent properties, its low mechanical strength and poor adhesive properties for the cells do not make it a suitable material of choice. To improve the characteristics, the chitosan can be combined with other materials, such as poly-ethylene glycol or collagen, to increase resistance and improve the adhesiveness.

The agarose and alginates are linear polysaccharides obtained from algae; both polysaccharides must be subjected to purification to lower their degree of immunogenicity. Both materials promote cell growth, are biodegradable, non-toxic and thermostable; they have, however, low mechanical resistance (easily upgradeable by combining the material with other polymers capable of increasing this property). These materials have already been used in the repair of liver injury, nerve, heart and cartilage.

Fibronectin is a protein found on the outside and on the cell surface; is also present in blood and other body fluids. It is capable of binding to other extracellular matrix proteins such as fibrinogen, collagen, glycosaminoglycans and to receptors on the cell membrane. It can be processed in order to obtain gels with little immunogenic properties, biodegradable and promotes adhesion and release of neurotrophic factors.

Gelatin is a material obtained by thermal denaturation of the collagen. It is biocompatible, biodegradable, non-immunogenic, non-toxic, plastic, cheap and capable of binding neurotrophic factors. As other materials requires a cross-linking process in order to improve the mechanical, chemical and physical properties.

- ***Synthetic Materials***

Synthetic polymers have been used for more than twenty years in surgical sutures and many are approved for human use by the Food and Drug Administration (FDA) (Tabesh et al, 2009). Synthetic polymers are very workable and easy to obtain but not all of them are biodegradable and can often cause immune and inflammatory responses in the body. Generally, they are more expensive than natural polymer cause the extrusive process from raw materials.

Silicone is an inorganic polymer, is not biodegradable and non-permeable and creates an isolated environment for regeneration. It is elastic and resistant to aging and can be combined with other materials to increase the regenerative properties. The non-degradability can cause chronic inflammatory response with the onset of fibrosis.

The poly-lactic acid (PLA) is a biodegradable polyester obtainable by condensation of molecules of lactic acid with monomeric precursors obtainable from renewable resources. Lactic acid is a product of the metabolism of all animals and microorganisms and for this reason is degradable in a non-toxic metabolites. The polymer is biocompatible, biodegradable and has good mechanical properties.

The poly-caprolactone (PCL) is an aliphatic polyester, bioresorbable, biocompatible and has a slower degradation compared to poly-lactic acid derivatives. May be in combination with other materials, such as collagen.

The poly-ethylene glycol (PEG) is the most commercialized polyether, given by the condensation of ethylene oxide. It promotes cell adhesion and is poorly immunogenic. The material is easily cross-linkable and in this way it is possible to create materials with different degradation rates.

The poly-urethane (PU) is a polymer which is derived from the condensation of poly-isocyanate or the poly-caprolactone with a polyol, usually propylene glycol or a polyester (Ciardelli and Chiono, 2005). The material is biodegradable, biocompatible, and thermoplastic. The material is very expensive and the degradation process can release toxic molecules (this problem can be easily solved by using lysine or butane in the condensation process) (Ciardelli and Chiono, 2005).

The poly-vinyl alcohol (PVA) is a linear polymer produced by the partial or total hydrolysis of the acetate groups of poly-vinyl-acetate. The entity of hydroxylation determines the chemical, physical and mechanical properties of the material. It appears as a white solid and is soluble in water but is resistant to most organic solvents. Is not permeable to gas, is odorless, nontoxic and has adhesive properties, emulsifiers and film-forming .Because of its solubility in water, PVA must be cross-linked to allow the formation of hydrogels with an increase of tensile strength and flexibility. It is atactic because configurations of the carbon atoms bearing the hydroxyl group are altered randomly and crystallizes at very low temperatures.

The resistance of PVA to organic solvents and its solubility in water make it suitable for various applications, so much so that the polymer is commonly used in the textile industry, food and as a medical device. The latter is widely used for its biocompatibility, non-toxicity, non-carcinogenicity, for its swelling properties and adhesive. In fact hydrogels and membranes of PVA have found application in the construction of contact lenses, artificial pancreas, in the practices of hemodialysis and in the formulation of artificial tears. The material may be used also in the construction of implantable devices, usable, for example, in the reconstruction of cartilaginous and treating vascular embolism, as well as to promote nerve regeneration (Baker et al, 2012) (Fig. 9.).

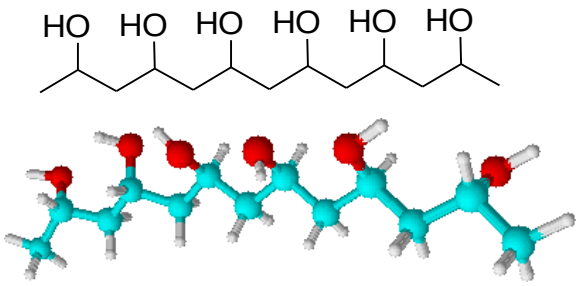

Fig. 9. Polyvinyl alcohol structural formula. Line and angle and ball and stick models.

2.3. Manufacturing techniques

The manufacture of a graft for nerve regeneration is based on the use of nanotechnology, which may allow the manipulation of biomaterials both at the atomic that macromolecular level in order to obtain scaffold with a specific geometrical structure, with strength, porosity, and reactivity for a better compatibility with cells.

There have been developed many techniques to work both synthetic materials that biological actions, including:

• Elettrospinnig: is a technique employed to produce scaffolds consist of nano-fibers. The diameter of the fibers ranging from nanometer to micrometer. The good relationship between surface area and volume promotes cell adhesion. The fibers may also be packaged within a defined volume in order to obtain a density of fiber that mimics that of the axons. In this technique, the polymers are dissolved in a suitable solvent and are subsequently subjected to magnetic field energized: this helps to lower the surface tension and viscoelastic forces and promotes the formation of fibers of different diameters. The fibers are formed to organize into a three-dimensional network with morphological characteristics similar to the extracellular matrix. The scaffolds obtained are porous (the size of the pores favor the passage of cells and factors pro-regenerative), resistant and cell adhesion permissive.

• Freeze-thawing (freezing and lyophilization): this procedure allows to obtain porous scaffolds without the use of chemicals. The machining conditions thrusts limit the possibility of incorporation of bioactive proteins and cells. The freezing leads to the formation of ice crystals which are then sublimated, contributing to the creation of a porous microarchitecture. The size of the pores can be controlled by the rate of freezing and pH (Tabesh et al, 2009).

• Molding: this technique allows to obtain grafts that can melt at temperatures lower than those of a normal graft. The structure of the graft is obtained using special tools capable of producing layers of matrix until it reaches the desired density. The limit of this procedure lies in the difficulty of accurately build the three-dimensional structure of the matrix in small scaffolds. Moreover, the cost is very high.

3) GROWTH FACTORS IN TISSUE ENGINEERING APPLICATION

3.1. The neurotrophic factors in peripheral nerves regeneration

As already mentioned earlier, neurotrophic factors play a fundamental role in the regeneration of peripheral nerves. The presence or absence of such factors, influence the mechanisms of neuronal survival and regrowth, as well as differentiation of Schwann cells and their remyelination (Chen et al, 2007).

The main neurotrophic factors are the neuregulins, which include factors such as NGF, BDNF, neurotrophin 3 (NT-3), and neurotrophin 4 and 5 (NT-4, NT-5): they regulate the phases of remyelination of Schwann cells and play a key role in promoting the survival and axonal regeneration (Chen et al, 2007).

Another very important thing is the neurotrophic factor fibroblast grow factor (FGF): it is overexpressed after nerve injury and has the task of promoting axonal growth and survival of sensory neurons in the process of nerve regeneration. Also contributes to the regulation of the proliferation and differentiation of Schwann cells after nerve injury.

GDNF can act both on motor neurons and sensory. After lesion may be an increase in the levels of mRNA, coding for this factor and its receptors on the distal part of the injured nerve. GDNF acts by stimulating the growth and promoting neuronal survival of these neurons.

The neuregulins 1 (NRG-1) are a family comprising more than fifteen isoforms of the protein. Based on the differences of the terminal amino acid sequence, can be divided into three sub-groups (I, II, III). The NGR-1 are potent regulators of the various phases that underlie the processes of alignment, proliferation and survival of Schwann cells.

3.2. Ciliary neurotrophic factor (CNTF)

The Ciliary neurotrophic factor (CNTF) is a protein of 23 kDa, expressed in both the CNS and PNS in the beginning of the last embryonic stage (Rezende et al, 2009). The protein is structurally related to some members of the family of cytokines such as leukemia inhibitory factor (LIF), interleukin 6 (IL-6), interleukin 11 (IL-11), oncostatin M (OSM) and cardiotropin 1 (CT-1) and for this reason it is often called "neurokin" (Rezende et al, 2009). Crystallographic studies and nuclear magnetic resonance (NMR) confirmed that the protein has a tetrameric structure composed of four subunits to α-helix, respectively called subunit A, B, C and D. The subunits A and B, and C and D subunits are joined by crosslinks, while between the subunits B and C is present a short bond (Sleeman et al, 2000) (Fig. 10A and B).

Fig. 10. Structure of TAT-CNTF from two different point of view (A and B).

The amino acid sequence of CNTF reveals that the protein is devoid of endogenous peptide-signal and a sequence for glycosylation, but presents only a free cysteine residue in position 17 (Sleeman et al, 2000).

CNTF has several tasks: centrally promotes the survival of motor neurons, sensory neurons, the neurons of the brain and hippocampus, promotes the differentiation of cholinergic neurons of the sympathetic and the glial progenitor cells in type 2 astrocytes and promotes the maturation and survival of oligodendrocytes. The protein prevents the degeneration of motor neurons after assonotmesis and, in mice, in cases of progressive neuropathies (Rezende et al, 2009). It has also protective effects against striatal neurons in pharmacological model for Huntington's disease (Sleeman et al, 2000). Its neural protective effects make it a potential therapeutic agent for the treatment of neurodegenerative diseases.

The CNTF is able to cause a reduction in body weight and appetite: in animal models manifest effects on body weight similar to leptin. The receptor subunits for the CNTF show, in fact, similar sequences to the receptor for leptin, a cytokine involved in the homeostasis of energy metabolism.

It seems that the effect on body weight induced by CNTF is due to the direct action of the protein on the cells of pro-opio-melanocortin, a group of neurons in the arcuate nucleus of the hypothalamus level, involved in energy metabolism. The arcuate nucleus is an area of the CNS accessible from the periphery by its proximity to the circumventricular organs (Sleeman et al, 2000). The protein would be capable of inducing a reduction of neuropeptide Y on neurons of this area (Rezende et al, 2009). The action of CNTF on the energy metabolism is still independent of leptin and this has been demonstrated by the ability of CNTF to correct obesity and diabetes associated with deficiency and/or resistance to leptin (Vieira et al, 2009).

Recent studies have demonstrated, moreover, that the CNTF can affect the regulation of body weight by adjusting the complex 1 and the factor A of the mitochondrial respiratory chain (Rezende et al, 2009).

In the peripheral nervous system there is a documented activity of CNTF on denervated skeletal muscle (atrophy reduction) and in the liver: the CNTF is able to promote the transcription of the genes coding for fibrinogen in primary liver cells and is capable of stimulating the metabolism of liver lipids (Sleeman et al, 2000).

The mechanism of signal transduction by the CNTF begins with the binding of factor to its receptor composed of the trimeric subunits α (CNTFRα), extracellular, not transductional and anchored to the membrane via a glycosyl-phosphatidylinositol bond or solubilized in it (thanks to the action of destruction of the bond, that anchors the subunit to the membrane, by the action of phosphatase C. In this form the receptor can also be found in the cerebrospinal fluid and in serum and can transduce signals mediated by other molecules) and two transmembrane subunits, transducers of signals, the leukemia inhibitory factor receptor (LIFR) and gp 130. The receptor is present at both central and peripheral level, especially at the level of skeletal muscle and to a lesser extent at the level of the sciatic nerve, skin, liver, kidney and testis (Sleeman et al, 2000).

Once the CNTF binds to CNTFRα, it induces heterodimerization between the subunit LIFR and gp 130 through the formation of a disulfide bridge (Marz et al, 2002). The heterodimer formed promotes the activation of protein JAK / TYK tyrosine kinase, associated to the receptor, which then promote the phosphorylation of STAT proteins, in particular STAT-3. The proteins STAT-3 phosphorylated in turn dimerize with themselves or with other STAT proteins and then migrate to

the nucleus, where they will bind to specific DNA sequences: in particular it has been demonstrated a particular affinity for the coding sequence for the gene tis-11 (Sleeman et al, 2000).

When the CNTF binds to the receptor, in addition to the signal transduction mediated by proteins JAK / STAT, there is another transduction pathway represented by the protein Ras-MAPK (ERK especially 1, a protein MAPK) found mainly in cell cultures of human neuroblastoma (Kuroda et al, 2001).

3.3. Protein engineering: TAT-CNTF

As a result of protein-engineering, it is possible to fuse part or the entire protein sequence to small peptides that can improve the effects or reduce the side effects of neurokin, such as CNTF.

TAT-CNTF was obtained by fusing the transductor domain of human CNTF with the transcriptional transactivator domain of the protein TAT of human immunodeficiency virus-1. The fusion protein obtained is able to cross the cell membrane and localize in the nucleus.

The fusion of CNTF sequence with the TAT has two purposes: first, it increases the speed of uptake of the protein by the cell after administration, and secondly, it efficiently promotes the intracellular translocation of the protein linked to it. Furthermore, it is shown that TAT-CNTF is equipotent to CNTF in stimulating nerve regeneration but unlike the latter, does not induce cachexia and does not stimulate the immune response (Rezende et al, 2009). Therefore, this factor promotes the survival of neurons of the embryonic chicken dorsal ganglia in culture; addition, local administration or subcutaneous administration of TAT-CNTF promotes the survival of motor neurons after sciatic nerve transection in young mice, as for CNTF while in cultures of human neuroblastoma cells incubated with the protein have shown an increase in the phosphorylation of STAT-3, as for CNTF (Rezende et al, 2009). These results take together means that TAT-CNTF maintains its neurotrophic activity, despite the presence of the TAT domain.

With regard to weight loss, TAT-CNTF administered in the subcutaneous tissue, induces a lower loss of body mass, unlike the CNTF (Rezende et al, 2009). The motivation for this may lie in the inability of TAT-CNTF to activate the phosphorylation of STAT-3 at the hypothalamic level and in adipocytes, due to structural and functional changes caused by the fusion of CNTF with TAT, notwithstanding the degree of phosphorylation of STAT -3, in vitro, is equal to that induced by CNTF. While assuming that the protein is capable of crossing the blood-brain barrier, probably the

subcutaneous administration prevents the protein to achieve concentrations comparable to those of CNTF that would ensure the activity at the hypothalamic level (Vieira et al, 2009).

It has been also studied the possible saturable transport systems for CNTF around the blood-brain barrier: their activation may alter the hypothalamic environment and make it more receptive to CNTF. This hypothesis requires, however, further investigation (Vieira et al, 2009).

AIM OF THE WORK

The serious consequences that may result from a non-optimal regeneration of peripheral nerves have shifted the focus in recent years on the techniques of microsurgery, especially as regards the use of tubular scaffolds. The tubulization can take advantage of both biological tissues and biomaterials.

The purpose of this thesis was therefore the conception, design and development of a prosthetic composite scaffold for peripheral nerves regeneration. Such a prosthesis is based on a synthetic biomaterial of tubular shape.

In the first phase of this work it has been studied and characterized the polyvinylalcohol, a synthetic polymer, resistant, biocompatible and low cost. This biomaterial has been modified chemically by an oxidation reaction in an acid environment, to facilitate the acquisition of two basic characteristics:

- the attack and release of therapeutic proteins to improve qualitatively and quantitatively the rate of regeneration; this make the scaffold a potential DDS

- improve the degradation rate compatible with a optimal tissue regeneration.

The experiment design was based, therefore, on mechanical, chemical, physical and biologic properties of the material, due to the collaboration with the University Tor Vergata (Rome), the Hospital S. Luca of Rovigo (Padua) and the center CUGAS of the University of Padua.

The second phase of the study was based on the study of a recombinant and engineered neurotrophic growth factor, TAT-CNTF, obtained by the fusion of the trascriptional transactivator domain of the human immunodeficiency virus with the functional domain of CNTF. The protein maintains the same characteristics of the human CNTF, but unlike the latter, does not manifest the secondary side effects, such as cachexia, anorexia and capacity to develop an immune response, sometimes very severe.

In the end, it has been studied and improved the characteristics of a synthetic biomaterial already currently on the market and engineered in order to be able to build a suitable scaffold for the regeneration of peripheral nerves, also as a drug delivery system (DDS), in a possible future optical marketing. From this point of view, this work ended with a patent deposit for multiuse tubular prosthesis.

MATHERIALS AND METHODS

1) PVA POLYMER AND OXIDATIVE REACTION

1.1. Oxidized PVA

The PVA (range 124000-186000, hydrolyzed 99 +) and PEG-1000 were purchased from Sigma-Aldrich (Sigma-Aldrich, St. Louis, MO, USA).

Potassium permanganate, 70% perchloric acid, sodium hydrogen phosphate and dihydrogen, sodium chloride, ethanol, methanol, acetone, ammonium acetate and DNFH (2,4-dinitrophenylhydrazine) were purchased from Fluka (Basel, Switzerland), while the sodium hydroxide and hydrochloric acid were obtained from Carlo Erba (Milan).

The dialysis membranes, cut-off 8000, were provided by SpectraPor (Philadelphia, PA, USA).

The RO water, used both in the preparation of solutions for dialysis, was produced by the instrument RO HDD 250 LM Elettracqua srl (Milan-Genoa) and includes a filter cartridge for reverse osmosis followed by ion exchange mixed bed.

MilliQ water was produced by a MilliQ Academic system of Millipore (Bedford, MA, USA).

For the filtration of aqueous solutions it has been used filter type GS in regenerated cellulose, having a pore diameter equal to 0.22 µM, manufactured by Millipore (Bedfor, MA, USA).

The nitrogen at a pressure of 6 kg/cm² has been provided by the network of the Department of Pharmaceutical Sciences, University of Padua, and is derived from liquid nitrogen.

Parafilm is produced by American National Can (Greenwich, Connecticut, USA).

1.2. Oxidized PVA preparation

The oxidized PVA was prepared based on the redox reaction, in environmental acid with potassium permanganate. The process is described by the following formula:

$$2KMnO_4 + 5[CH_2\ CHOH]n + 6HClO_4 \rightarrow 5[CH_2\ CO]n + 2\ Mn^{2+}\ (ClO_4\text{-})_2\ + 8H_2O + \downarrow 2KClO_4$$

The stoichiometric ratio is therefore two permanganate ions for every five secondary hydroxyl groups of the type which are oxidized to carbonyl group.

PVA were prepared with two different degrees of oxidation, respectively 1% and 2%, and a PVA native, not oxidized. Then, to obtain the degree of oxidation equal to 0, to one gram of PVA native, it was necessary to add 20 ml of MilliQ water and 0.60 ml of perchloric acid. Not being oxidized is not provided for the addition of potassium permanganate. Instead one gram of PVA with a degree of oxidation 1% (1% PVA) were added 20 ml of MilliQ water, 0.0144 g of potassium permanganate and, finally, 0.30 ml of perchloric acid, while, for a gram of PVA with a degree of oxidation of 2% (2% PVA) were added 20 ml of MilliQ water, 0.0287 g of potassium permanganate and 0.60ml of perchloric acid.

The procedure for the oxidation of PVA involves the following steps:

1. Solubilization of PVA in deionized water.

The polymer, that is a white granular powder, after having been accurately weighed, was placed in a Pyrex glass bottle with a wide neck, fitted with a cap, and, subsequently, has been added the deionized water provided by the formula. The container was then placed in an oven at 95-100°C for about two hours, stirring from time to time to promote a more homogeneous dissolution. When completely dissolved, the container was removed from the oven and left to cool to the temperature of 25°C.

2. Preparation of the solution of potassium permanganate in deionized water.

The potassium permanganate, after being weighed, is let to solubilize in deionized water while stirring for a few minutes, in relation 10 mg of salt per 1 ml of water.

3. Adding to the aqueous solution of potassium permanganate 60% perchloric acid

To the solution of potassium permanganate obtained, intensely colored in purple, are added some ml of 60% perchloric acid depending on the type of the oxidation rate.

4. PVA oxidation.

In the bottle containing the PVA dissolved and cooled to 25°C is poured, immediately after preparation, the acid solution of potassium permanganate. Close the bottle and proceed, then, with vigorous agitation for few minutes. Subsequently, the solution thus obtained, of purple colored, is left in a waterbath at 30°C until complete decoloration. The complete discolartion takes 60-90 minutes.

5. Dialysis in deionized water.

The obtained colorless solution is placed in a dialysis tube with a membrane cut-off of 8000 Da The solution was dialyzed against 4 liters of deionized water, operand changes every 4-6 hours. The water must be maintained under stirring with the aid of a magnetic stirrer.

After dialysis, we proceed by filtering the solution. After filtration, the solution is poured into containers type of polystyrene Petri dish with a diameter of 10 cm (BD Falcon, USA), in order to obtain a thickness of the liquid of about 3-4 mm, which are placed in the freezer at a temperature of -18°C until their complete freezing. Finally, the frozen material is placed in the lyophilizer. The process is completed in about 12-15 hours, at the end of which the material will be white, have a fibrous texture and satin appearance.

2) CHEMICAL, PHYSICAL AND MECHANICAL TESTS ON MODIFIED PVA

2.1. Chemical and physical tests on native and oxidized PVA

The various types of material (native PVA, 1% PVA and 2% PVA), once freeze-drying process have been completed, were dissolve in water at elevated temperature (90-95°C) and have been subjected to some physical-chemical evaluations.

2.1.1. Determination of the carbonyl groups by 2,4-dinitrophenylhydrazine (DNFH) reaction

This test is used to determine the percentage of carbonyl groups present in the three types of prepared PVA, due to the oxidation of the secondary alcohol groups of the polymer in carbonyl groups. The reaction occurs between the carbonyl group of an aldehyde or ketone and the hydrazinic group of DNFH, to give origin to a derivative phenyl-hydrazinic, colored in pale yellow. The diagram shows the reaction:

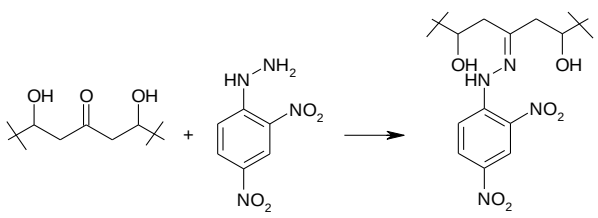

PVA + DNFH DNF-hydrazone

After weighing approximately 10 mg of each type of PVA (native PVA, 1% PVA and 2% PVA) and after their complete solubilization in boiling deionized water, were added 5 ml of 10 mM reagent. The above reagent is prepared by adding to 40 mg of DNFH 20 ml of hydrochloric acid and the solution thus obtained is allowed to react in the dark for 16 hours in rotation.

The three solutions were dialyzed into three tubes with a membrane cut-off of 8000 Da. The dialysis was performed against 4 liters of solution of ammonium acetate 0.05 M, changed 4 times throughout the whole procedure. The solution was then taken out from the tubes and was diluted to a final volume of 25 ml with the last buffer added to dialysis.

On the three samples obtained were carried out measurements of absorbance using a spectrophotometer Jasco mod V630 (JASCO, Japan) and in quartz cuvettes Suprasyl, having optical path of 1 cm. The molar extinction coefficient of the phenyl-hydrazonic derivate is 22000 (M x cm -1) at 375 nm as reported in the literature (Levine et al, 1990).

2.1.2. Dynamic Light Scattering (DLS)

To determine the degree of molecular dispersion in the polymer solution, respectively in the three study conditions, non-oxidized, oxidized 1% and 2%, the three PVA solutions have been prepared by heating for one hour at a temperature of 95°C the lyophilized material in MilliQ water. The resulting solutions were placed in 1.5 ml eppendorf and were centrifuged at 22°C at 20000 rpm for one hour in GS-15R centrifuge (Beckman, Brea, CA), equipped with rotor F2402H. For each sample were taken 150 µl of supernatant and were transferred to microcuvettes Kuvetten ZH 8.5 mm UV-transparent (Starstedt, Numbrecht, DE). The measurement was performed using Zetasizer Nano-ZS DLS instrument (Malven Instruments Ltd., Worcestershire, UK) in triplicate using as an index of refraction of the PVA that of polystyrene, set as default in the program of the instrument, and the index of refraction of water regarding the dispersing medium.

2.1.3. Differential Scanning Calorimetry (DSC) characterization

DSC was conducted in order to determine the degree of crystallinity and the melting temperature of the polymers. The analysis, carried out at the Research Center INSTM Tor Vergata University of Rome, was made on tubular scaffolds of PVA in the three study conditions (native, 1% and 2% oxidized PVA). From these materials were obtained few mg of material which were then air-dried

and subjected to analysis by using the Netzsch DSC 200 PC (Netzsch-Gerätebau GmbH , Selb, Germany).

2.2. Preparation of PVA scaffolds

In carrying on this work, two types of scaffolds with different shapes were prepared. The first, of tubular shape, was designed to facilitate mechanical tests and to resemble the shape of the peripheral nerves. The second, disk-shaped (to favor an easier insertion into the wells of cell culture plates) has been prepared with the aim of favoring *in vitro* biological and degradation tests of the material itself. Both types of scaffolds were prepared by applying the process of Freezing-Thawing in three cycles.

2.2.1. Native and oxidized tubular scaffolds

The tubular scaffolds were prepared using a cylindrical mold of stainless steel with a diameter of about 4 mm. The native and oxidized PVA, all at 16%, were prepared following the procedure explained above (section 1.2.).

The native PVA and the two oxidized, once the freeze-drying process has ended, were cut into small pieces and placed in a Pyrex glass bottle, equipped with a sealing stopper and teflon seal. At each of the three types of PVA has been added deionized water and PEG 1000, in amounts calculated according to the table 1 (Tab.1.).

Sample	**Oxidation (%)**	**Quantity (g)**	**H_2O (g)**	**PEG 1000 (g)**
Native PVA	0	16,0	83,0	1,0
1% PVA	1	16,0	83,0	1,0
2% PVA	2	16,0	83,0	1,0

Tab.1. Preparation of native and oxidized PVA tubes. Quantity referred to 100 g of total mixture.

To facilitate a more rapid melting of the material, the bottles have been placed in an oven at a temperature of 95-100°C, stirring from time to time, to favor a more homogeneous dispersion and to avoid the formation of lumps. It is important to pay particular attention to not prolonging the dissolution time of oxidized PVA at the above temperature since the material tends to take a yellow coloration and get dry.

The materials have been cooled taking care to keep them in a fluid state; thereafter every type of PVA was introduced, without forming bubbles of gas, in the mold tube in which it was introduced also a cylindrical bar of stainless steel, maintained concentric to the mold by means of the use of small rubber centering devices placed at the ends, to create the internal lumen.

At this point was followed the process of Freezing-Thawing: the molds are cooled to -20°C for 4 hours and then are conditioned between -3°C and -5°C for 48 hours. The molds are again reported to the temperature of -20°C for 12 hours and again at temperatures between -3°C and -5°C for another 12 hours. The latter step is repeated once more and only after this the molds can be brought to room temperature.

Scaffolds, once extruded from the molds, are stored at 4°C in tubes containing a 1% solution of mixture antifungal-antibacterial and PBS.

2.2.2. Preparation of disks scaffolds for cell cultures

Scaffolds were prepared following the procedure described in paragraph 1.2., followed by the preparation mode indicated in Table 1. of the tubular scaffolds. Once obtained the three types of PVA (native, 1% and 2% oxidized) of fluid consistency, about 200 µl of each material is poured into a 24-well multiwell plate (BD Falcon, USA) and leveled to obtained disks with a diameter of 15 mm and a thickness of approximately 1 mm.

The plate was then subjected to a Freezing-Thawing process, as shown above, and was stored under the same conditions as tubular scaffolds.

2.2.3. Preparation of disks scaffolds for degradation tests

For these scaffolds have followed the methods of preparation set out in paragraph 1.2. and Table 1.

Once obtained three different types of material (native, 1% and 2% oxidized PVA) it was poured a volume of 1 ml per type of material and leveled in a 6-well multiwell plate (BD Falcon). The plate was then subjected to the process of Freezing-Thawing, as set above.

2.3. Mechanical characterization

Mechanical properties of tubular PVA grafts (native, 1% and 2% oxidized PVA) were evaluated up to break by means of uniaxial tensile tests at 5 mm/min using a universal testing machine equipped with a 100 N load cell (Lloyd LRX). Specimens were obtained by longitudinally cutting the original samples and measurements were carried out at ambient conditions directly after withdrawal of the grafts out of the storage solution. Stress was defined as the measured force divided by the initial cross-section area, while the strain as the ratio between the grip displacement and the initial gripping distance. Secant modulus, at 50% strain at break, tensile strength and strain at break were determined.

3) POLYMER DEGRADATION ABILITY

The disc-shaped scaffolds prepared for this purpose were first sterilized with 70% alcohol and UV and then resized in order to analyze two different modes of degradation

3.1. Static degradation test

There were taken two portions for each type of PVA dish under examination and were placed divided into a new 6-wells multiwell plate (BD Falcon). In three of its wells were added 2 ml of Phosphate-Buffered Saline (PBS) 1X of Invitrogen Corporation (Gibco - Carlsbad, CA USA), composed as follow: 80 g of NaCl (final concentration 1.37 M), 2 g of KCl (final concentration 27 mM), 11.5 g of $Na_2HPO_47H_2O$ (final concentration 81 mM; alternately, it can be used 80 ml of a 100 mM solution), 2.59 g of KH_2PO_4 (final concentration 19 mM, alternatively it can be used 20 ml from a 100 mM solution) and was brought to one liter with demineralized/distilled water and pH of 7.4. The solution has been diluted 10 times to use it to 1X concentration.

In the other three remaining wells were added 2 ml of culture medium DMEM/F12 (1:1) 1x (+ L-glutamine + 15MM HEPES), antibiotic (penicillin-streptomycin-glutamine 100x) in a concentration equal to 0.1% and PBS (Phosphate-Buffered Saline) of Invitrogen Corporation (Gibco - Carlsbad, CA USA), while 15% FBS (Fetal Bovine Serum), Trypsin (0.25% Trypsin-EDTA solution) and 1% nonessential amino acids (NEAA) were supplied by Sigma-Aldrich.

The plate was placed in an incubator (Memmert) at 37°C, in an atmosphere containing 5% CO_2 and 90% humidity. The two solutions were changed regularly once a week and photos were taken every two months by Nikon Digital Sight DS-SMc (Nikon Corporation) camera..

3.2. Dynamic degradation test

Two portions of each type of PVA have been taken and weighed. In this case the two portions were placed into two eppendorfs (BD Falcon), one containing PBS, and the other one containing culture medium (the same composition as that one used for static tests), and it was proceeded with the determination of the final weight.

After that, the samples were placed in a rotating device Labquake (Labindustries, CA). At each time point solutions were changed and the PVA pieces were weighed in order to plot the weight difference on time scale.

4) DECELLULARIZED HUMAN NERVE MATRIX

4.1. Human nerve decellularization

Human median and ulnar nerves were kindly provided by Dr. Leonardo Sartore of the University Hospital of Padua.

For this procedure it has been followed the method of decellularization of Meezan (Meezan et al, 1975). The nerves, carefully cleaned using few ml of PBS, were placed in a closed container with water MilliQ previously sterilized. The MilliQ water was changed every two hours for three days.

The third day the tissue was placed in a solution of sodium deoxycholate (Sigma-Aldrich) to 4% w/v for four hours. The solution was obtained by dissolving 10 g of powder in 250 ml of MilliQ water. The solution was then filtered with a suitable device for vacuum filter.

At the end of the four hours, the tissue was washed with sterile PBS. Subsequently, the sample was treated with a Dnase solution for two hours at room temperature (Sigma-Aldrich) (obtained by dissolving the enzyme in 40 ml of 1M sterile sodium chloride) and left in sterile MilliQ water at 4°C.

4.2. Decellularized nerve analysis

To ensure the successful decellularization of nerve tissue, some test has been performed.

4.2.1. 4-6 Diamidino-2-phenylindole (DAPI)

A portion of nerve tissue has been embedded into ice and cut in longitudinal sections of 12 µm using cryostat Leica CM1850UV (Leica, DE). The samples were then placed in the freezer at -80°C for at least 6 hours. The samples were then mounted with coverslip-object using the Fluorescence Mounting Medium with DAPI (Vecta-Shield).

4.2.2. Hematoxylin-Eosin (H & E) staining

To perform the analysis it was used a solution of hematoxylin and eosin (Bio Optica, Milan) filtered with a filter paper at the time of use, on sections of 12 µm previously cut with cryostat and stored at - 80°C.

The procedure was as follows:

• the sample has been treated with a solution of hematoxylin for 8 minutes;

• then rinsed in MilliQ and tap water and left to air dry;

• the sample has been treated with a solution of eosin for 3 minutes;

• it has been proceeded to washing the sample in tap water and left it to air dry;

At this point the sample has been mounted and was viewed with an optical microscope Matic AE 2000 (Ted Pella-INC., USA).

4.2.3. Pentachromic staining

To perform this staining it was used the kit Diapath (Diapath, Bergamo) on sections of 12 µm previously cut with a cryostat and frozen at -80°C.

The procedure was as follows:

• to the sections have been added the Reagent A (Alcian blue) for 20 minutes and then washed with deionized water;

• it has been added the Reagent B (an alcoholic alkaline solution) for 6 minutes and then proceeding with a wash in tap water for 10 minutes;

• in the meantime it has been prepared the Reagent C, obtained by the union of the C1 Reagent (a solution of hematoxylin 1) with the C2 Reagent (a solution of hematoxylin 2) and it has been placed immediately on the slide for 15 minutes and then they have been washed in deionized water;

• it has been added the Reagent D (ferric chloride) and it has been proceeded to immediately rinse slides in water;

• reagent E was added (sodium thiosulfate) for 1 minute and the slides were washed 10 minutes in tap water, followed by one in deionized water;

• it has been added the Reagent F (acid fuchsin) for 3 minutes and the slides were washed with 0.5% acetic acid;

• it has been added the Reagent G (phosphotungstic acid) for 10 minutes, and the slides were then washed with 0.5% acetic acid and, subsequently, rapidly immersed twice in absolute alcohol;

• finally it was added the Reagent H (safranin alcoholic) for 15 minutes. Then slides have been washed in absolute alcohol for 2 minutes. Once the slides dried, they were mounted in balsam and analyzed by light microscopy.

4.2.4. Proteomic characterization

About 3 mg of lyophilized decellularized human nerve matrix were dissolved in 300 µl of a rehydration buffer (containing 9 M urea, 1% CHAPS, 30 mM DTT, 0.1% Bio-Lyte 3/10 and 0.001% bromophenol blue), applied on a ready Strip IPG (length 17 cm, linear pH gradient 3-10) and focused at 60000 Vh in a Protean IEF cell apparatus (Bio-Rad, Richmond, CA).

The strip was incubated in a SDS and DTT-containing buffer and allowed to run down a precast 2D polyacrilamide gradient gel (6-18%) using a Mod. V161 vertical gel electrophoresis apparatus

(BRL, Inc., Rockville, MD). After Coomassie R250 staining, several spots were excised and digested in the gel with trypsin sequencing grade.

The extracted tryptic peptides were analyzed by LC-MS/MS (QTof, Micromass UK, Ltd.). Protein identification was made by Mascot (www.matrix-science.com) using a NCBInr 20101016 (mammalia) database.

4.3. Preparation and use of decellularized human nerve matrix

In a 50 ml falcon (BD Falcon, USA) was weighed 1 g of the decellularized tissue and were added 15 ml of 10% acetic acid. The sample was then triturated in an ice bath. The grinding lasted 20 seconds, after which the sample was left at rest, always in an ice bath, for 5 minutes.

This operation has been repeated repeated eight times.

Once obtained the matrix, it has been proceeded by pouring 300 µl of product in a 24-well multiwell plate and 500 µl of the same product in cylindrical molds of plastic material, closed at one end, taking care to not let air in it. Both, plate and cylindrical molds, were placed in a freezer at -20°C and, once frozen, they were lyophilized for 12 hours. The disks and cylinders thus obtained were stored in a freezer at -80°C prior to use.

To evaluate the protein composition and the actual efficiency of the decellularization process on human nerve, it was made a Sodium Dodecyl Sulfate Gel-Polyacrilamide Electrophoresys (SDS-PAGE), using a pre-cast gel gradient 4-20, supplied by GE Healthcare.

5) TAT-CNTF

5.1. Bacterial transformation, expression, amplification and protein purification

The plasmid pTAT-CNTF was constructed in order to express TAT sequence of HIV-1 fused with human CNTF. The coding sequence for human CNTF has been inserted into a plasmid pT7.7 and was cloned in the sites of the plasmid pTAT-Ngb, NheI and EcoRI. (Rezende et al, 2009).

Cells of Escherichia coli BL21 (DE3) LysS have been transformed with the plasmid coding for the protein by heat shock. Subsequently to the bacterial colture was added 1 ml of SOC medium (for 1

liter of medium: 950 ml of water, 20 g of Bacto-Tripton, 5 g of Bacto-Yeast extract, 0.5 g of sodium chloride –Applichem- and glucose 20 mM), the cells were placed in an incubator at 37 ° C degrees on a shaker device IKA Labortechnik (DE); it has been proceeded centrifuging the cell solution for 5 minutes at 4000 rpm with Beckman Coulter Avant J-25. The pellet obtained was resuspended in 20 µl of supernatant; the culture was performed on Petri dishes with a diameter of 10 cm with agar and antibiotic (ampicillin) 1%; and as culture medium was used Luria broth 1X (sodium chloride, tryptone and yeast extract-Applichem-). The plates were placed in incubator at 37 ° C overnight.

The plates were then washed with a few ml of LB medium 1X, the recovered cells were suspended in Luria broth in flasks of 2 liters, placed in incubator at 37°C, under stirring, until it was obtained optical density at 600 nm (OD_{600}) equal to 0.6, index of reached confluence, measured with a spectrophotometer (Jenway).

Protein expression was induced by adding to the confluence bacterial culture isopropyl-β-D-tiogalactopiranoside (IPTG) (Applichem) 100 mg/ml for 3 hours at room at 37°C, under stirring.

At this point the cultures were spun at a temperature of 4°C, for 20 minutes at 6000 rpm with Beckman Coulter Avant J-25. The pellet obtained was resuspended in 15-20 ml of PBS (Invitrogen Corporation, Gibco - Carlsbad, CA USA).

It has been proceeded, therefore, with the lysis of cells: the cell pellet resuspended in PBS was sonicated (Sonifier 250/450, Branson, DE) with Buffer A (a solution of sodium chloride and 200 nM Tris/HCl at pH 20 nM 8). The lysate obtained was centrifuged for 30 minutes at 11000 rpm.

The protein purification was conducted by Imobilyzed Metal ion Affinity Chromatography (IMAC), based on affinity binding between Nickel ions, immobilized on the resin, and a tag of histidines fused with the protein to be purified.

The resin Hys-Select-Nickel (Sigma-Aldrich) was washed with MilliQ water and then with Buffer A sonicator. The resin thus obtained was put under stirring, for one hour, with the supernatant obtained by centrifugation of the bacterial lysate, in a way to enhance the binding of the protein, dispersed in the supernatant, with the resin.

The resin, therefore, has been allowed to settle for about half an hour and then was loaded into a 1 x 10 cm column; the resin was then washed again with Buffer A and then eluted with Buffer B (a solution of sodium chloride 200 nM, Tris/HCl 20 nM and 250 nM imidazole at pH 8).

We proceeded, therefore, with a dialysis overnight, at a temperature of 4°C, against Buffer A, collecting the protein solution and purified using membranes with cut-off equal to 12000 Da.

High Performing Liquid phase Chromatography (HPLC) (in reverse phase) using a Vydac C4 column (4.6 x 150 mm, Experia, CA) instrument of LKB (Uppsala, Sweden) to remove impurities, such as urea, small peptides and reduction agents. The sample obtained after dialysis was centrifuged at 15000 rpm for 10 minutes in an eppendorf of 1.5 ml, and the supernatant was separated from the pellet and discarded. The pellet was washed with 200 µl of water, and then were added 28 mg of Dithiothreitol (DTT) (Fluka), 100 µl of anhydrous trifluoroacetic acid (TFA) (Fluka) and 5 mg of potassium iodide (Fluka). The solution assumed a yellow-orange color which, after addition of 25 µl of βmercaptoetanolo (Fluka), the tended to decrease. After 20 minutes at room temperature to the reaction mixture were added 1000 µl of 6 M guanidinium chloride (Fluka, microselect) and 200 mg of ammonium acetate to increase the final pH to 5. After centrifugation at 15000 rpm for 5 minutes the sample was loaded on Vydac C4 and eluted by a gradient of increasing concentration of acetonitrile (MeCN) in water containing 0.05% TFA. The protein fraction collected by reverse phase chromatography was subjected to UV spectrophotometry, using a spectrophotometer mod V630 Jasco (Tokyo, Japan), to determine the concentration through the value of absorbance at 280 nm. It was used a quartz Suprasil cuvette having an optical path of 1 cm. The coefficient of molar absorptivity was calculated to 15000 (M x cm-1).

The purity grade of TAT-CNTF was then evaluated by SDS-PAGE. It has been proceeded to the realization of the solution of the two gels:

• 3% stacking gel, constituted by MilliQ water, acrylamide-bisacrilamide (Applichem), 10% Ammonium Persulfate (APS) (Applichem) and tetramethylethylenediamine (TEMED) (Sigma-Aldrich);

• 10% separating gel, constituted by MilliQ water, acrylamide-bisacrilamide, 1.5 M Tris/HCl at pH 8.8, 10% SDS, 10% APS and TEMED.

For the preparation of samples to be loaded into the gel, the protein solution was centrifuge using GS-15R centrifuge (Beckman, Brea, CA), equipped with rotor F2402H; pellet and supernatant were separated and were treated as follows, adding 50nm Tris-HCl pH 6.8, 2% SDS, 10% glycerol, 5% β-Mercaptoethanol (Fluka), 0.03% Bromophenol Blue (Fluka) and by boiling them for 5 minutes. At the end of this operation, 40 µl of the two samples (TAT-CNTF precipitate and TAT-CNTF surnatant) were loaded into wells, previously obtained in the gel by placing a small upper comb of plastic material. The electrophoretic run was made by applying an electric current of 25 mA for

about two hours. At the end of the run it has been proceeded with the staining of the gel in a solution of Coomassie brilliant blue (Coomassie Blue, Methanol-water in a 1:1 ratio and 10% glacial acetic acid-Fluka-) for about half an hour; after this the gel was placed in a decolorizing solution (consisting of 7% methanol, 5% acetic acid and water MilliQ) and was examined.

The protein TAT-CNTF recovered from the chromatography was analyzed by mass spectrometry using MarinerTM ESI-TOF spectrometer (Applied Biosystems, Foster City, CA, USA). The solution was infused in the spray by a transport stream of 20 µl/min consisting of MeCN-Water 1-1 with 1% formic acid (Fluka). The calibration was performed using three peptides: bradichinia, neurotensin and angiotensin. The obtained multiptotic spectrum was deconvoluted to show the molecular mass.

It has been proceeded with the measurement of the absorbance of the protein using a spectrophotometer at 280 nm, in order to have an idea of the concentration of the protein in solution.

5.2. TAT-CNTF releasing from native and oxidized PVA

The experiment was carried on preparing two disks (3 mm of diameter) per each of polymer under study.

The disks samples were treated as follows. In three eppendorf of 1 ml volume was added 1 ml of a solution of TAT-CNTF 0.3 mg/ml collected with reverse phase chromatography (seen in Chapter 3.3.1.); it has been proceeded by evaporating the solutions up to the achievement of a volume of 500 µl; finally in each eppendorf were added 500 µl of phosphate buffer at pH 5 (obtained by dissolving calcium phosphate -Carlo Erba- in deionized water and bringing the solution to pH 5 with sodium hydroxide). In this way was made a binding solution in which two disks per type of PVA were immersed. The discs were left in the solution of bindings for 24 hours in rotation, after which, the solution was removed completely and replaced by 1 ml of PBS, always in agitation.

The release assessment was made after 1, 24, 96 and 240 hours by measuring the absorbance of PBS (in which there were left pre-incubated disks) in a spectrophotometer, with λ from 280-350 nm. The resulting data were then normalized with the dry weight of the analyzed disks, obtained by lyophilization of the disk itself.

6) CELL CULTURE

The experiments were conducted on cell cultures stabilized of human neuroblastoma (SHSY5Y), purchased from ECACC (European Collection of Cell Cultures) and rat pheochromocytoma (PC12), also purchased from ECACC. For the preparation, amplification and the use of SHSY5Y cell cultures were used the following products: DMEM/F12 (1:1) 1x (+ L-glutamine + 15MM HEPES), antibiotic (penicillin-streptomycin-glutamine 100x) and PBS (Phosphate-Buffered Saline) of Invitrogen Corporation (Gibco, CA, USA), and FBS (Fetal Bovine Serum), Trypsin (0.25% Trypsin-EDTA solution) and non-essential amino acids (NEAA) were provided by the company Sigma-Aldrich. For PC12 cells was used RPMI (Gibco, CA, USA), supplemented with 5% FCS (Fetal Calf Serum) (Sigma), 10% HS (Horse Serum) (Sigma), glutamine 2mM and 1% antibiotic (penicillin-streptomycin).

6.1. SHSY5Y cell line

The stabilized culture of human neuroblastoma (SH-SY5Y) were prepared using the culture medium DMEM/F-12 (1:1), supplemented with 15% FBS, 1% NEAA and 0.1% of antibiotic (penicillin-streptomycin -glutamine). The cells were cultivated in suitable flask (having an area of 75 cm^2) in an incubator (Memmert) at 37°C, in an atmosphere containing 5% CO_2 and 90% humidity. The culture medium was changed every two days. Reached confluence, the cultured cells were detached with 0.25% Trypsin-EDTA and centrifuged at 1200 rpm using centrifuge Beckman Coulter AllegraTM 64R. The pellet thus obtained was resuspended in culture medium and re-sown in flasks or plates depending on the experiment.

6.2. PC12 cell line

The stabilized culture of rat pheochromocytoma (PC12) were cultured in flasks (having an area of 75 cm^2), and placed in an incubator (Memmert) at 37°C, in an atmosphere containing 5% CO_2 and 90% humidity. They were previously conditioned with collagen IV (Sigma-Aldrich) for 2 hours and an half in incubator and then allowed to dry. The culture medium was changed every two days. Reached confluence, the cultured cells were detached with 0.25% Trypsin-EDTA and centrifuged at 150000 rpm with a centrifuge Beckman Coulter AllegraTM 64R. The pellet thus obtained was

resuspended in culture medium and re-seeded in multiwell plate or Petri dish, depending on the type of experiment.

6.3. The MTT assay

In order to quantify the cellular adhesion and proliferation rate was use the MTT assay on both SHSY5Y and PC12 cell lines.

The MTT reagent is used to measure the activity of enzymes capable of reducing the same reactive to a formazan salt; this is optically visible for the color change, from yellow to dark blue-violet. Salts of formazan form insoluble crystals in the intracellular environment to which the membranes are substantially impermeable: is then allowed the entry of the molecule into the cell, but not the output of the product if it has been properly metabolized. Infact if the mitochondrial electron transport chain is still metabolically active and have an active reducing power, the mitochondrial enzyme succinate dehydrogenase is in fact active only in living cells. This reaction and its product, the solubilized color, is measured using spectrophotometer at a wavelength of 570 nm.

The MTT (5mg/ml) solution was prepared by dissolving the powder substance in PBS, under constant stirring and then filtered with a syringe filter with a cut-off of 0.22 μm. To this solution was added culture medium (specifically for the type of cells in used) in order to have a MTT final concentration of 10%. For the SHSY5Y the MTT solution was added to DMEM F12 while for PC12, to RPMI. The reagent was placed on the cells in the multiwell plates and then in the incubator with 5% CO_2 and 90% humidity for 3 hours. After incubation, the formazan crystals were solubilized with 100 μl per well of cold isopropyl alcohol maintained under stirring for about 15 minutes. Subsequently, the color solubilized salt was then collected and transferred into a 96 multiwell plate to perform optical reading of the pigment using the reader Microplate Autoreader EL311SX (Bio-tek Instruments, Winooski, VT) at 560 nm.

6.4. Adhesion and cell morphology experiments

The experiment was conducted both on simple “naked” biomaterials and them with added disks of matrix of decellularized human nerve matrix on the surface. The fixing of the matrix disk takes place immediately after pouring the biomaterial into the mold and prior to the process of Freezing-Thawing.

SHSY5Y cells were seeded at a density of 200000 cells/well in three 24-wells multiwell plates. In two of them there were placed naked biomaterials (one incubated with collagend and the other one incubated with laminin) while in the last one there was placed biomaterials with added matrix. There was also a control condition, consisting on the wells in plates without any biomaterials.

The naked biomaterials and control glasses disks in one of the two multiwell plates, before seeding, were conditioned with 100 µl of a laminin solution (10 µg/ml in PBS) for one hour in the incubator at 37°C, in order to have a coating concentration of 1µg/cm^2. In the other plate, the naked biomaterials and control glasses disks were coated using 500 µl of a collagen solution (1mg/ml) for two hours and a half in the incubator at 37°C, in order to have a coating concentration of 1µg/cm^2. Then the solutions were removed and the materials were washed with PBS to eliminate the excess of proteins.

Cell adhesion was evaluated on naked and matrix added biomaterials after 24, 72 and 96 hours after seeding, leaving the biomaterials incubated with cell suspension at 37°C, in an atmosphere containing 5% CO_2 and 90% humidity (Memmert incubator). At each time points, the materials were washed using 1X PBS and added the MTT solution prepared as previously described in order to have a real quantification.

In order to have also images of the adhesion rate, some biomaterials (naked and with matrix) and glasses disks (placed in some wells of the plates in order to mimic the control conditions but easily removed to be prepared for SEM observation) were taken out from plates at the same time points of them used in MTT experiment and prepare to be observed by SEM.

6.5. Cellular proliferation

The proliferation experiments, using MTT as well, was conducted on the following samples:

• biomaterials with decellularized human nerve matrix, placed in a 24 multiwell plates. On them were seeded SHSY5Y cells at a density of 60000 cells/well. After 1, 3 and 4 days was performed MTT assay, according to the modalities previously described. In these experiments, some biomaterial and glass disks were taken out from plate in order to be observed using SEM.

• SHSY5Y cells plated on polystyrene plates BD Falcon, to evaluate a difference in proliferation induced by TAT-CNTF. The cells were seeded at a density of 60000 cells/well in a 24 multiwell plate. To these cells was added 100 nM TAT-CNTF, compared to a control group of the same cells

without any growth factor. The MTT assay was run after 1, 3, 6 and 24 hours after addition of the growth factor.

• SHSY5Y cells plated on polystyrene plates BD Falcon, to assess the proliferation induced by NGF. The cells were seeded at a density of 60000 cells/well in a 24-wells multiwell plate (BD Falcon). To these cells was added 100 nM NGF, compared to a control group of the same cells without any growth factor. The MTT assay was run after 1, 3, 6 and 24 hours after addition of the growth factor.

• PC12 cells were plated and stimulated with TAT-CNTF in order to understand the possible proliferation effects of the growth factor. The cells were seeded in a 24-wells multiwell plate (BD Falcon)with a density of 60000 cells/well. To this group of cells was added 100 nM TAT-CNTF and they were compared to a control conditions where it wasn't added any factor. The possible cell proliferation was evaluated by MTT assay after 1, 3, 6, 24, 48, 72, 96 hours after addition of growth factor.
In the last three experiments some pictures were taken by Nikon Digital Sight DS-SMc (Nikon Corporation) camera mounted on the optical microscope Leica DM2000 (Leica Microsystems, Wetzlar, Germany).

6.6. Morphological differentiation induced by NGF or TAT-CNTF

To understand the reactivity of SHSY5Y cells toward growth factor stimuli and study their morphogenetic activity, it has been used NGF growth factor in order to have a comparison with the effects induced by TAT-CNTF. The experiment was carried on in a Petri dish of 10 cm diameter (BD Falcon) in which were seeded cells at a density of 60000 cells/plate. In one Petri dish was added NGF concentrated 100 nM, while in other one was added TAT-CNTF at the same concentration. For both of these conditions there was set also a control condition, with the same cells without the growth factors. Through the use of the optical microscope was evaluated the effect of NGF and TAT-CNTF after 48 hours, 6 and 10 days.

In was study also the morphological activity of TAT-CNTF on PC12 cellular line. In this case, cells were seeded in a Petri dish (diameter 10 cm) (BD Falcon) with a density of 60000 cells/plate. To the culture was added 100 nM TAT-CNTF and there was set also a control condition represented by a cell culture analogous, without any factor. The growth factor activity was monitored after 1, 4 and 7 days through the use of the optical microscope.

In these two experiments were taken some pictures by Nikon Digital Sight DS-SMc (Nikon Corporation) camera mounted on the optical microscope Leica DM2000 (Leica Microsystems, Wetzlar, Germany).

6.7. Cellular trafficking

6.7.1. Cellular treatment with TAT-CNTF

Cells of human neuroblastoma SH-SY5Y and PC12 were cultured, respectively, in enriched DMEM/F-12 and RPMI media at a temperature of 37°C in a humidified atmosphere and with 5% CO_2.

To determine the presence of TAT-CNTF by western blotting, SHSY5Y and PC12 cells were seeded in T-75 flasks (Sarstedt) at a density of 5 x 104 cell/cm^2, while for the localization by confocal microscopy the cells were seeded at the same density on coverslip diameter of 1 cm. For both experiments, after 24 hours from seeding the cells were treated with medium without serum in the presence and in the absence of TAT-CNTF 100nM for 30 minutes, at the end of this period the medium was removed and replaced with medium without serum.

6.7.2. Preparation of cell lysates

At the end of the treatment with TAT-CNTF 100nM and after 3, 6, 24 hours the medium was removed from cells. They were washed 3 times with 1X PBS at 4°C. Subsequently were detached mechanically and centrifuged for 5 minutes at 1200 rpm and 4°C. After removing the supernatant, the cells were treated with 120µl of lysis buffer (1% v/v Triton-X100, 0.5% w/v Sodium Deoxycholate, 0.15 M NaCl, 10mM Tris-HCl pH 7.6, 1% cocktail of protease inhibitors (Sigma-Aldrich)), and centrifuged at 14000 rpm for 15 minutes at 4°C. The supernatant was then collected for subsequent quantification.

6.7.3. Quantification of cell extracts

To quantify the cell extracts was used the BCA Protein Assay kit (Pierce) which exploits the bicinchoninic acid colorimetric method. The solutions A (Na2CO3, NaHCO3, sodium tartrate, bicinchoninic acid in a 0.1 M solution of NaOH) and B (4% Cu2So4 solution) were mixed in

proportion 50:1 respectively for a final volume of 1 ml. It was prepared a calibration curve using standard samples of known concentration of bovine serum albumin (BSA) and considering 8 points from 0µg/ml to 2000 micrograms/ml. Standards and samples were added to the mixture by volume of 50ul of reactive A + B and after stirring for 30 seconds were incubated for 30 minutes at 37°C. The spectrophotometric reading was performed using the instrument DU 530 Life Science UV / Vis (Beckman) at a wavelength of 562nm.

6.7.4. Sodium Dodecyl Sulfate Polyacrylamide Gel Electrophoresis (SDS-PAGE)

On the gels were loaded 50µg of each sample. After reduction in a solution containing 50nm Tris-HCl pH 6.8, 2% SDS, 10% glycerol, 5% β-mercaptoethanol, 0.03% Bromophenol Blue and subsequent boiling at 96°C for 5 minutes, a total volume of 50µl of mixture was loaded on a discontinuous polyacrylamide gel consisting of 10ml of Staking gel (4% Solution Acrylamide / Bis-Acrylamide 37:1, 125 mM Tris-HCl pH 6.8, 10% SDS, 100 µl Ammonium persulfate (APS), 16µl TEMED (Sigma Aldrich)) and 20ml of Running gel (10% -12% Solution Acrylamide / Bis-Acrylamide 37:1, 375mm Tris-HCl pH 8.8, 10% SDS, 70ul APS, 15 ul TEMED), cast and mounted on cell for electrophoresis VP-140 (Elettrofor). The samples were subjected to a constant current of 60 mA for 2 hours and 30 minutes in running buffer consisting of: 25 mM Tris-HCl pH 8.3, 192 mM glycine, 0.03% SDS. After separation by electrophoresis the proteins were transferred onto nitrocellulose membranes (GE Amersham) with porosity 0.45 uM, hydrate in mQ water and equilibrated for 15 minutes in transfer buffer containing 25 mM Tris-HCl pH 8.3, 192 mM Glycine, 0.03% SDS, 20% Methanol. Subsequently it has been assembled the transfer apparatus and a constant electric field orthogonal to the gel of 400 mA was generated for a time of 90-240 minutes.

6.7.5. Immunoblotting

The nitrocellulose membranes were incubated overnight at 4°C in TBS-T solution (Tris HCl pH 7.6, NaCl, 0.1% Tween) 10% skimmed milk in order to block nonspecific sites. Subsequently, the membranes were incubated 1 hour at 37°C with different antibodies, according to the table 2 (Tab. 2.).

After incubation was performed a washing of the membrane of 15 minutes and three from 5 minutes with TBS-T. At this point the membrane was incubated with different secondary antibody (Tab. 2.)

for 1 hour after which it was performed a washing of the membrane of 15 minutes and three from 5 minutes with TBS-T.

Cell line	**Antigen**	**Primary Antibody**	**Secondary Antibody**
SHSY5Y	His-tag	Monoclonal Anti-poly Histidine Clone HIS-1, (Sigma-aldrich), diluted 1:2000.	Anti-mouse conjugated with peroxidase (HRP), (GE Healthcare), diluted 1:5000.
SHSY5Y	P-STAT3	Anti-PSTAT-3 (Tyr 705, Cell Signaling), diluted 1:2000.	Anti-rabbit conjuncted with peroxidase (HRP), (GE Healthcare) diluted 1:5000.
SHSY5Y	CNTFRα	Anti-CNTFRα (AN B2, Santa Cruz Biotechnology), diluted 1:200.	Anti-mouse conjugated with peroxidase (HRP) (GE Healthcare), diluted 1:3000.
PC12	hCNTF	Anti-hCNTF (FL 200, Santa Cruz Biotechnology), diluted 1:200.	Anti-rabbit conjuncted with peroxidase (HRP) (GE Healthcare) diluted 1:3000.
PC12	P-STAT3	Anti-PSTAT-3 (Tyr 705, Cell Signaling), diluted 1:2000.	Anti-rabbit conjuncted with peroxidase (HRP), (GE Healthcare) diluted 1:3000.
PC12	CNTFRα	Anti-CNTFRα (H 182, Santa Cruz Biotechnology), diluted 1:200.	Anti-mouse conjuncted with peroxidase (HRP) (GE Healthcare), diluted 1:3000.

Tab. 2. List of antibodies used in the immunoblot experiments.

6.7.6. Revelation

The revelation was performed according to the protocol of ECL kit (GE Amersham) and involved the incubation of the membrane for 1 minute with 0.125 ml/cm^2 of revelation solution, consisting of the solutions A and B in proportion 1:1. Once dried, the membrane was placed in the cell of exposure, in the dark, and in contact with a slab autoradiographic (GE Amersham) for a time varying from 1 to 30 minutes. Subsequently the plate impressed was developed by incubation in liquid development X-OMAT EX II and fixing RP X-OMAT LO (Kodak).

6.7.7. Immunofluorescence and Confocal Microscopy

At the end of the treatment with TAT-CNTF 100nM and after 3, 6, 24 hours the medium was removed and the cells were washed in PBS 1X cold, fixed in methanol for 10 minutes, and for 1 minute in acetone at -20°C. After running 3 washes of 5 minutes at room temperature with 1X PBS, the cell membranes was permeabilized by treatment for 6 minutes at room temperature with a solution of distilled water to 1% of Triton X-100 (Sigma-Aldrich). Subsequently, the samples were washed with 1X PBS and incubated with a 10% solution of bovine serum albumin (BSA) in PBS 1X and maintained at room temperature for 10 minutes.

At this point, the samples were incubated for 1 hour at room temperature with primary antibody mouse anti-His-tag (Sigma-Aldrich), mouse anti-h-CNTF (Santa Cruz Biotechnology), diluted 1:100 in PBS 1X supplemented with 1% BSA. After three washes of 5 minutes with 1X PBS, was added the secondary antibody anti-isotype conjugated to Alexa 488 or 594 (Invitrogen Life Technologies) diluted 1:200 in 1X PBS supplemented with 1% BSA, for 30 minutes at room temperature environment. The preparations thus obtained were mounted with aqueous upright for fluorescence containing 4-6 Diamidino-2-phenylindole (DAPI) (Vecta-Shield). Negative controls were set up by omitting the primary antibody. The preparations were observed with a Leica TCS-SP5 confocal microscope (Leica Instruments), with objectives with magnifications HCXPL Fluotar 20X/0.5, HCXPL Apo 40X/1.25, HCXPL Apo 63X/0.5 both oil immersion. The acquisition of images is realized by means of the program staat LAS AF (Leica Instruments).

7) STATISTICAL ANALYSIS

All cellular proliferation and adhesion experiments were conduct in technical and biological triplicate in order to assess statistical analysis. Data were analysed using commercially available software (SPSS version 18.0 for Windows; SPSS Inc, Chicago, IL). Statistical analysis was performed using one-way ANOVA followed by Bonferroni's post-hoc test for multiple comparisions. $P < 0.05$ was considered statistically significant.

8) PREPARATION OF A PVA TUBULAR SCAFFOLD STRUCTURE WITH A LYOPHILIZED DECELLULARIZED HUMAN NERVE MATRIX FILLER

After the various tests performed on the three types of PVA and on decellularized human nerve matrix, it has been constructed a tubular scaffold of 2% PVA, based on the procedures mentioned in paragraph 3.1.1. and 3.1.3. The filler of decellularized human nerve matrix was obtained according to the methods specified in paragraph 3.2.1. and was mechanically inserted into the tubular scaffold. The composite scaffold thus obtained was analyzed by SEM.

9) SAMPLES PREPARATION FOR SCANNING ELECTRON MICROSCOPY (SEM) OBSERVATION

Some samples of the proliferation and adhesion experiments (glass disks, naked and matrix added biomaterials), pieces of decellularized human nerve and scaffolds (tubular and disks) were prepared for SEM observation. All of the samples were previously fixed in 3% glutaraldehyde and stored at 4°C. After 48 hours the glutaraldehyde was removed and the samples were subjected to dehydration with increasing alcohol content process (from 30% to 100% v/v ethanol in water). The samples were dried in the air and were fixed on a metal support with double-sided adhesive tape. Subsequently, they were metallized with a thin gold layer by sputtering (to make them conductive and protect the more delicate structures), and were observed using the instrument Stereoscan S-205 (Cambridge Instruments, Cambridge, MA), located at CUGAS of the University of Padua.

RESULTS

1) CHEMICAL, PHYSICAL, MORPHOLOGICAL AND MECHANICAL CHARACTERIZATION OF OXIDIZED PVA

1.1. Chemical characterization

In order to assess the oxidation degree occurred in the material, the assay was performed using 2,4-dinitrophenylhydrazine (DNFH). The test is used to determine the percentage of carbonyl groups present in the three types of PVA prepared, due to the oxidation of the secondary alcohol groups of the polymer in carbonyl groups. DNFH reacts with the hydrazinic groups of DNFH to form derivatives that absorb in the UV spectrum at 375 nm. In Figure 1 (Fig.1.) it can be observed that with the increase percentage of oxidation, there is a proportional increase in absorbance.

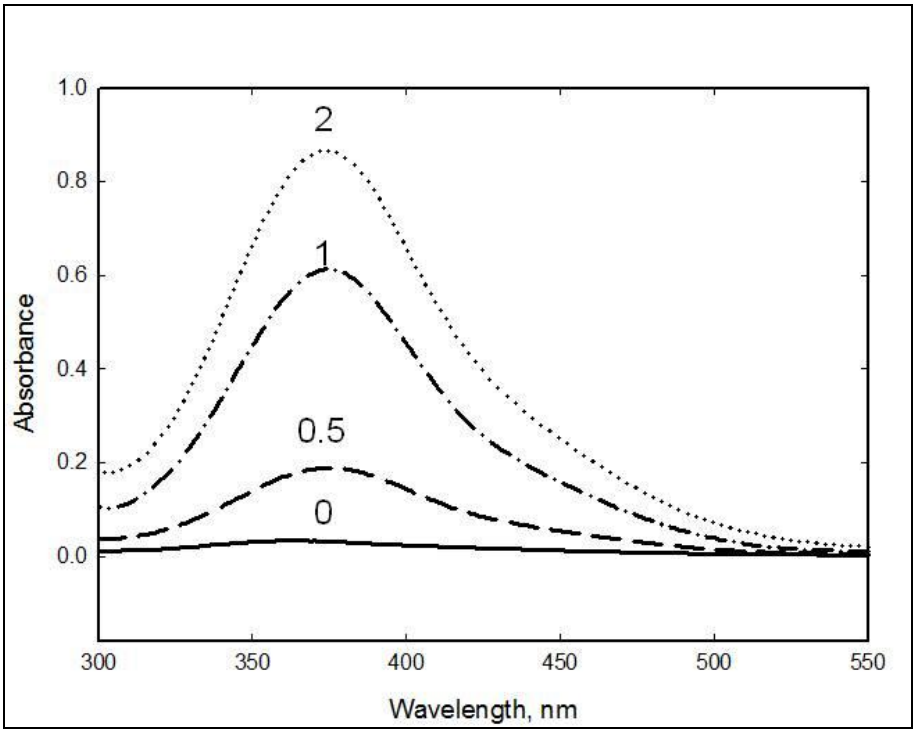

Fig.1. UV spectrum of oxidative reaction on native, 0.5%, 1% and 2% PVA with DNFH.

Based on the absorption values at 375 nm, since the coefficient of molar absorptivity of the DNF-hydrazone is 22,000 $M^{-1}cm^{-1}$ and a volume of each solution of 25 ml, it is possible to derive the moles of carbonyl groups present and by these also the rates of experimental oxidation as shown in Table 1 (Tab. 1.). It can therefore be noted that the increase in the oxidation percentage correspond to the increase of the moles of CO.

Sample	Quantity (mg)	Vynil alcohol (µM)	Theoretical CO (µM)	A_{375} (nm)	Experimental CO (µM)	Experimental CO percentage (%)
Native PVA	10,5	238	0	0,0320	0	0
1% PVA	12,1	375	2,27	0,6128	0,660	0,24%
2% PVA	11,4	259	5,18	0,8665	0,948	0,37%

Tab.1. Determination of carbonyl content by DNFH assay. The last column shows the percentage of carbonyl groups experimentally determined.

On native, 1% and 2% oxidized PVA were then performed a DLS analysis (Fig. 2.) to understand the degree of particles homogeneity and dispersion that constitute the materials. The shift between the three curves represents the hydrodynamic volume reduction of particles instead the areas below the curves represent the dispersion amount. The sample of 2% PVA (red curve) is polydispersed and has a hydrodynamic volume reduction compared to the others.

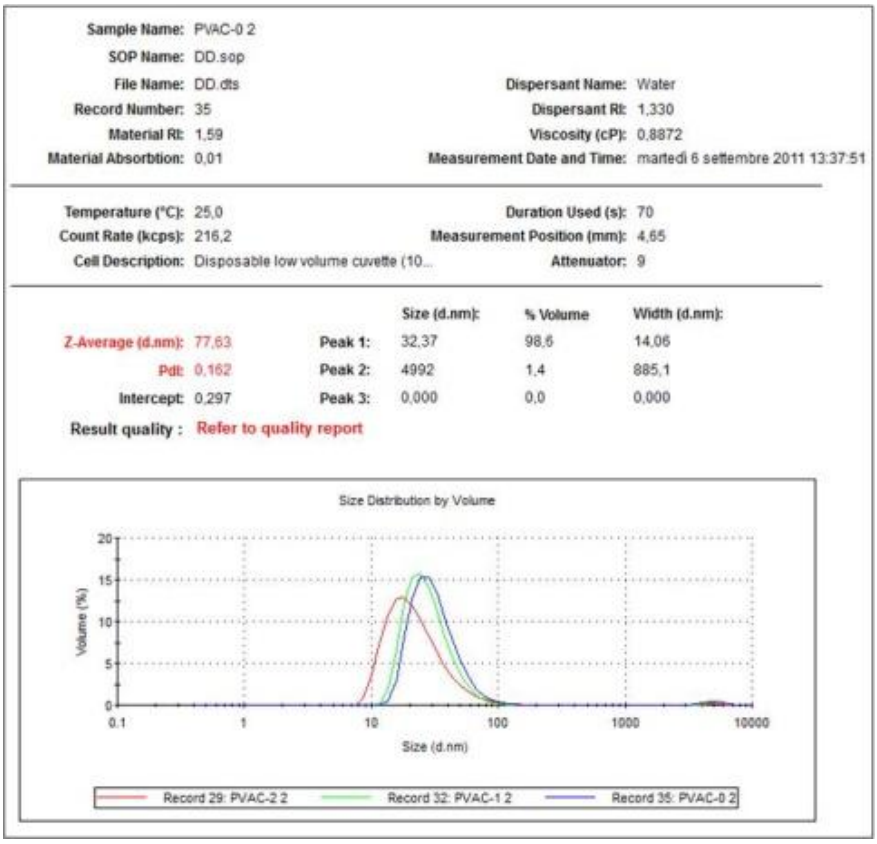

Fig. 2.. DLS of native (blue), 1% (green) and 2% PVA (red).

1.2. Physical characterization

The DSC analysis studies the variation of the degree of cristallinity and the melting point temperature of the 3 polymers to vary the percentage of oxidation (Fig. 3. AND Tab. 2.).

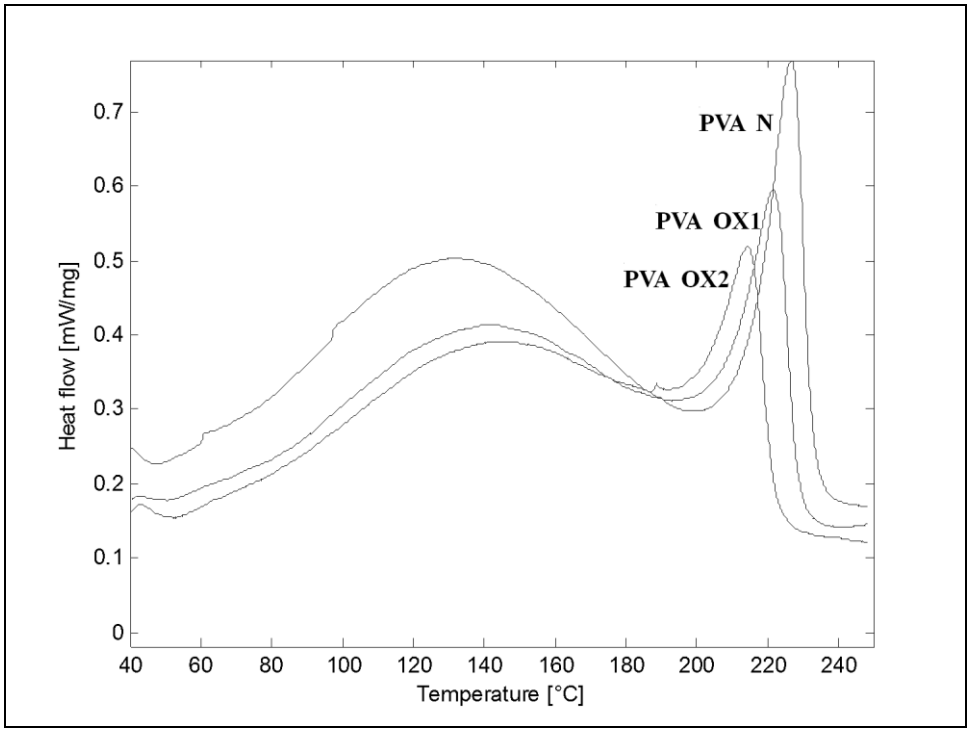

Fig. 3. DSC chart of the three samples of PVA (native, 1% and 2%).

SAMPLE	MELTING TEMPERATURE (°C)	CRYSTALLINITY DEGREE (%)
NATIVE PVA	226,8	31,07
1% PVA	221,8	24,55
2% PVA	214,6	18,01

Tab. 2. Melting point temperature and the degree of crystallinity of the three polymers.

As can be seen from Fig. 3. and Tab. 2., the melting temperature decreases proportionally to increase in the percentage of crystallinity. The more enlarged curves represent the melting temperature of the amorphous part of the polymer, instead of the peaks that represent the purest part. The area below the curves and peaks represents the amount of crystallinity. The increase in the oxidation rate coincides with the decrease in the percentage of crystallinity that's because there are

a lower number of OH groups available to form H bonds e so to build the polymer crystallinity structure.

The degree of crystallinity was calculated by considering a value of ΔH equal to 138.6 J/g for a 100% crystalline sample of PVA (Hassan and Peppas, 2000: Millon et al., 2006) and not considering the ΔH relative to the water content remaining.

1.3. Tubular and disks scaffolds morphology

Once achieved the oxidized material, the material was used for the construction of tubular scaffolds (diameter of 2 and 4 mm) (Fig. 4.) and the disk-shaped scaffold (diameter of 15 mm), through the freeze-thawing process.

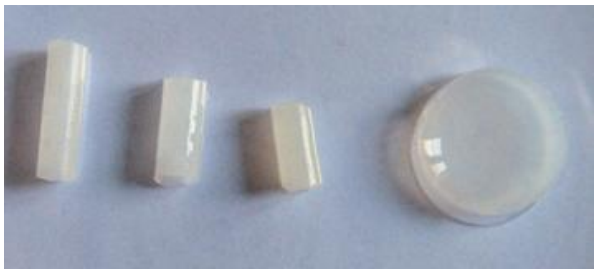

Fig. 4. Tubular (diameter 2 mm) and disk-shaped (diameter 15mm) scaffold.

The SEM images (Fig. 5.) of the outer surface of tubular and disk-shaped scaffolds of native PVA appears smooth and oriented, effect probably due to the mold, and there were no interruptions or porosity of the material. The inner surface appears to be less uniform and presents spread microporosity, of diameter between 0.5 and 10 microns.

The surfaces of the tubular and discoid scaffolds of 1% PVA are visible in Figure 6 (Fig. 6.). Externally the surface of these scaffolds is less uniform compared to that of native PVA and there are dips and rises clearly visible, bordered by small surface grooves. The inner surface, in the tubular scaffolds, looks smooth, randomly crossed by microroughness raised and non-porous.

In Figure 7 (Fig. 7.). it is possible to see the SEM images of the scaffolds 2% PVA. The outer surface is heterogeneous, characterized by a jagged appearance, rich in reliefs oriented in only one way and arranged in a regular manner. There are some microcavities, but the material appears to be devoid of porosity. The inner surface of the tubular scaffolds presents, instead, areas of microporosity extended, spaced by a few smooth area. There are some pores, of dimensions ranging between 2 and 5 microns.

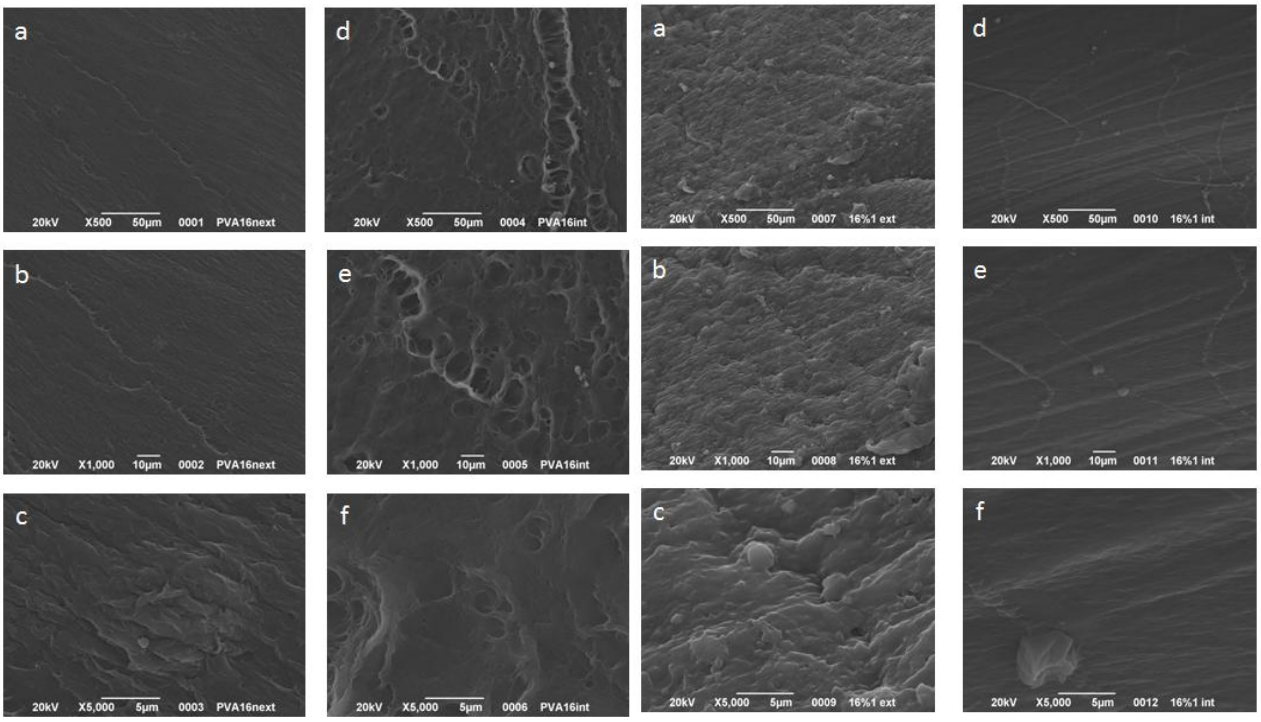

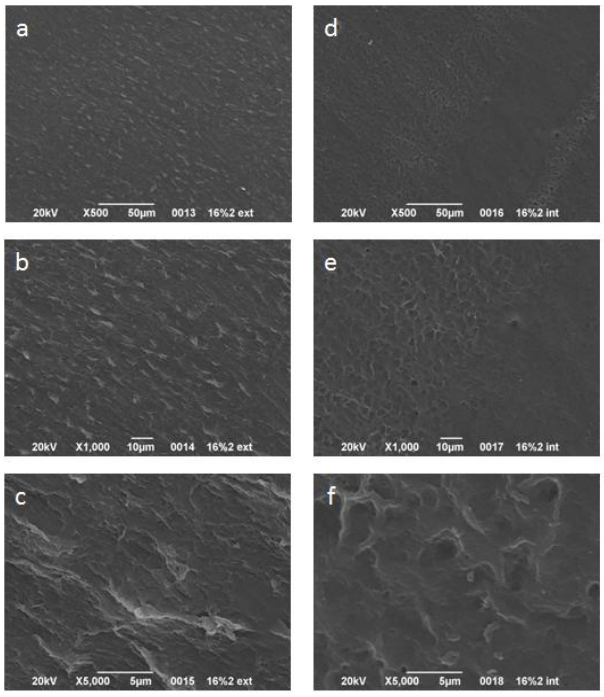

Fig. 6 (above panel on the left) . Outer surface of tubular and disk-shaped scaffold of native PVA at different magnifications (a, b, c). The images d, e and f show the inner surface.

Fig. 7 (above panel on the right). Outer surface of tubular and disk-shaped scaffold of 1% PVA (images a, b, c); figures d, e, f show the inner surface.

Fig. 8 (below panel on the left). Outer surface tubular and disk-shaped scaffold of 2% PVA (images a, b, c); figures d, e, f show the inner surface.

1.4. Mechanical characterization

The tubular scaffolds were, therefore, subjected to mechanical tests at the Research Center INSTM University Tor Vergata (Rome).

It was evaluated the uniaxial tensile strength of individual tubular samples of native, 1% and 2% PVA. The curves obtained are shown in Figure 8 (Fig. 8.), whereas the resistance are shown in

Table 3 (Tab. 3.). The tests show that native PVA has a tensile strength higher than the oxidized materials, which decrease the resistance with increasing percentage of oxidation.

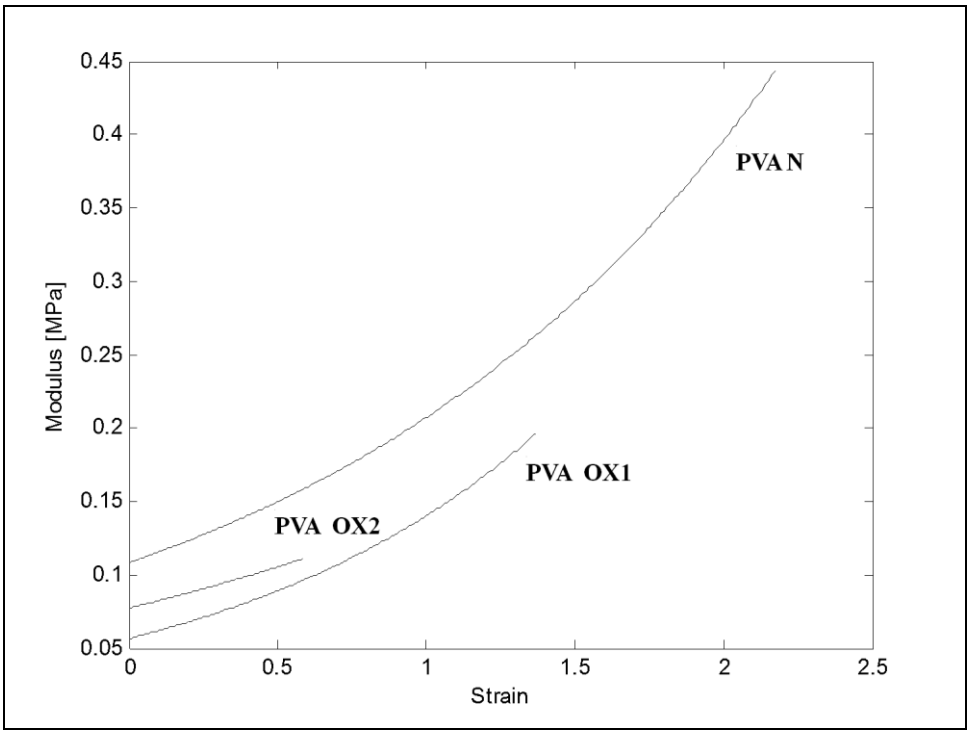

Fig. 8. Graph of tensile strength of native, 1% and 2% PVA.

SAMPLE	S[MPa]	TS[MPa]	Strain at breack (%)
Native PVA	0,11 +/- 0,03	0,33 +/- 0,12	192 +/- 23
1% PVA	0,06 +/- 0,02	0,15 +/- 0,02	162 +/- 18
2% PVA	0,06 +/- 0,02	0,07 +/- 0,02	78 +/- 15

Tab. 3. Values of native, 1% and 2% PVA resistance.

2) POLYMER DEGRADATION

Some disks scaffolds were prepared to study the rate of degradation. The degradation tests were carried out according to two methods: the static degradation, in which the three types of PVA are put in incubator both with PBS and culture medium of SHSY5Y cells. Degradation rate was qualitatively observed by the more or less presence of pores and holes (Fig. 9A, B, C and D). The dynamic degradation comprises the treatment of the three types of PVA with the same solutions of

the degradation static test, but the materials are kept in continuous rotation by means of the use of a special device.

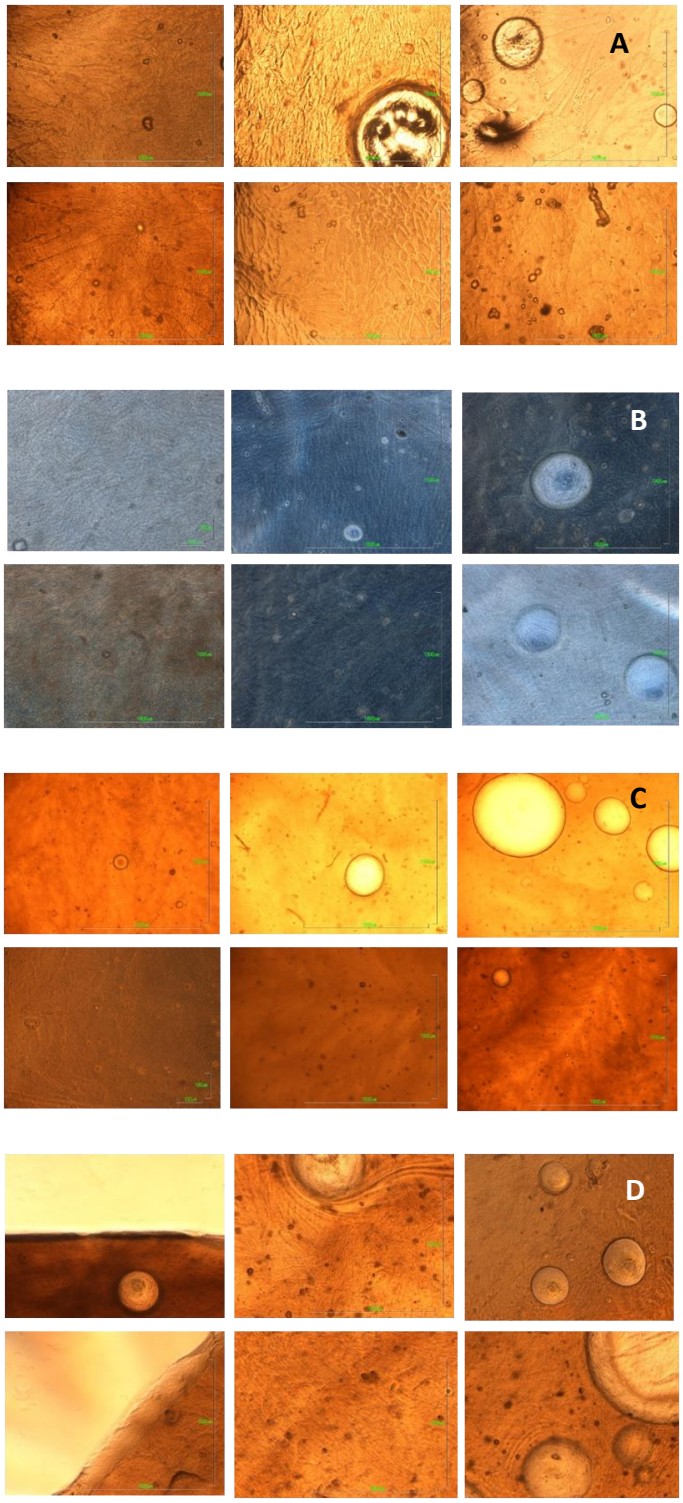

Fig. 9. Static degradation test. The four panels (A, B, C and D) represent, respectively, the PVA materials after 1, 2, 4, and 6 months. Pictures in the upper part of each panel represent, from left to right, native, 1% and 2% PVA in DMEM; in the lower part, with the same order, there are the materials in PBS.

The PVA pieces are collected, dried and weighed at the beginning and end of each time points in order to have a quantitative measure plots in time. fragments were. They were compared to the weight of the fragments with the respective weights of the experimental points earlier and also with the native sample of PVA which has not been put to degrade so as to have a weight difference, expressed as a percentage, plots in elapsed time. Compared to the sample of native PVA and to the 1% PVA, 2% PVA has a degradation rate clearly higher (Fig. 10A and B).

Figures 9 (Fig. 9A, B, C and D) respectively show the visible rate of degradation suffered by the materials of static tests after 1, 2, 4 and 6 months. From the static tests, it can be noted only a greater propensity of 2% PVA to form holes. There aren't significantly differences between PVA DMEM and PBS conditions.

Figures 10A and B (Fig. 10A. And B.) show graphs of dynamic degradation tests. There are substantial differences in the behavior of three biomaterials if placed in DMEM or in PBS. As regards the DMEM condition, 2% PVA maintains a degradation rate constant growing. Regarding the PBS condition, all the materials exhibit the same degradation rate

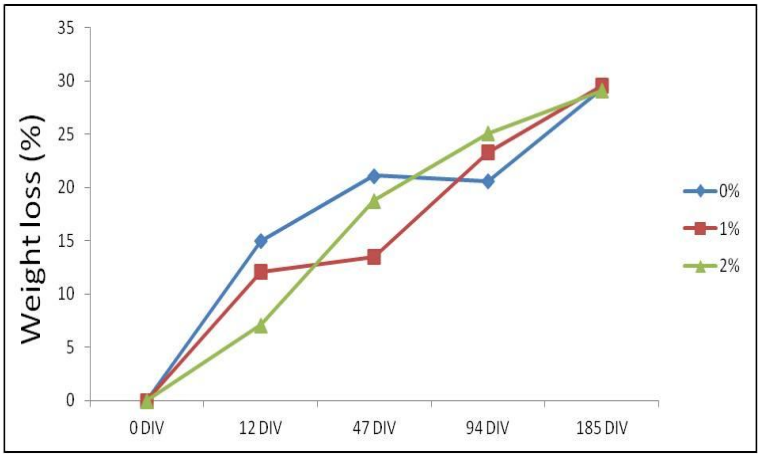

Fig. 10A. Graph of dynamic degradation test in DMEM.

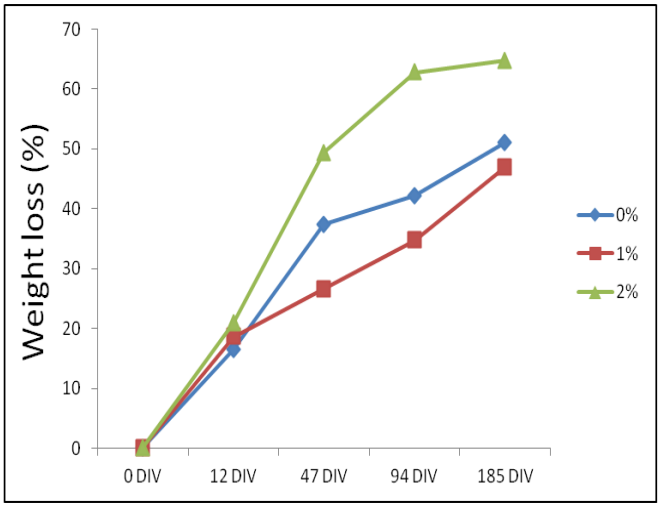

Fig. 10B. Graph of static degradation in PBS.

3) DECELLULARIZED HUMAN NERVE MATRIX

As described in the experimental section 2.2.1. the human median and ulnar nerve, were decellularized according to the Meezan method to eliminate immunogenic component.

To assess the obtained decellularization degree were performed the following tests:

1. DAPI to highlight the nuclei presence or not. As can be seen in Figure 11 (Fig. 11.). there is complete absence of signal from the 3rd cycle of decellularization.

2. Hematoxylin staining with eosin, to highlight the acidophilic (by eosin) and the basophilic (with hematoxylin) cellular components. As can be seen from Figure 12 (Fig. 12.). there is an increase in the degree of vacuolation from 2nd to 3rd cycle of decellularization.

3. Pentachromic staining to highlight the protein composition of the matrix. The black color corresponds to the nuclei and elastic fibers, yellow for collagen, blue for mucins, dark red for fibrin and light red for muscle tissue. Even in this case, as can be noted from the images (Fig. 13.), there is an increase in the degree of vacuolation in 3rd cycle of decellularization.

4. Morphological analysis using SEM in order to highlight the ultrastructural changes of the decellularized tissue samples. It is observed in Figure 14 (Fig. 14.) a greater loss of texture of the decellularized sample compare to the native one.

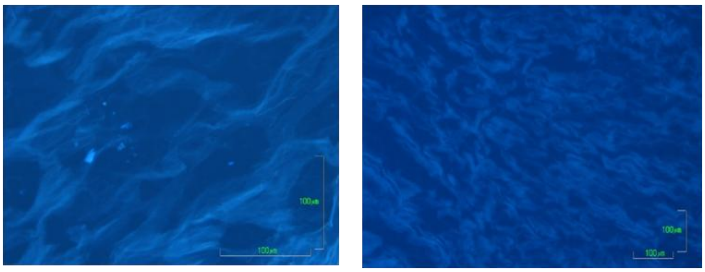

Fig. 11. DAPI staining.

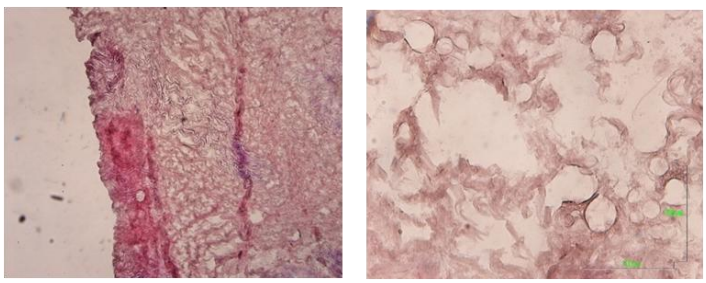

Fig. 12. Hematoxylin-eosin staining.

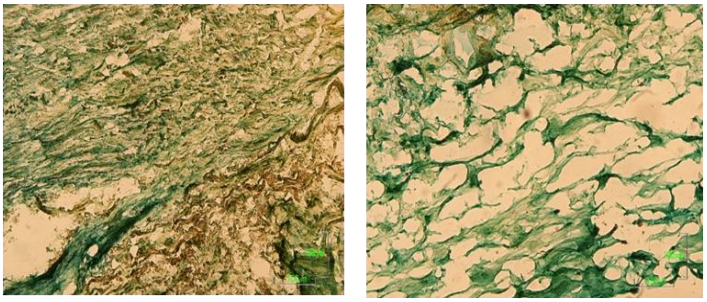

Fig. 13. Pentachromic staining.

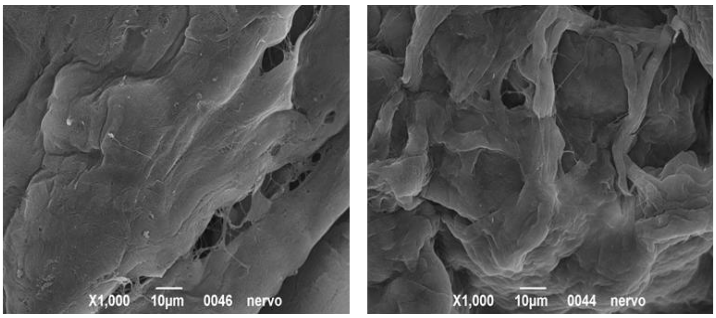

Fig. 14. SEM images of nerve tissue.

Once confirmed the morphological decellularization, it has proceeded by analyzing the protein composition of the extracellular matrix of human nerve. It has been performed a SDS-PAGE where it can be seen (Fig. 15.), in correspondence of the samples 2, 3 and 4 (corresponding to the decellularized human nerve matrix) the triple band typical of collagen (125 Kda). Samples 1 and 5 correspond to murine collagen, 7 to the standard (Amersham prestained A8889).

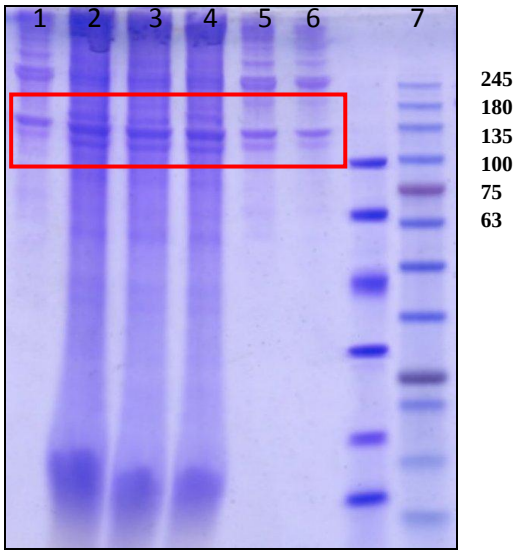

Fig. 15. SDS-PAGE of the decellularized human nerve matrix. Samples 2, 3, 4 correspond to the nerve samples, 1 and 5 to murine collagen, 7 to the standard (Amersham Prestained A8889).

4) TAT-CNTF GROWTH FACTOR

The fused protein, after been expressed was purified using Immobilized Metal ion Affinity Chromatography (IMAC).

The protein was subsequently analyzed by reverse phase chromatography, using a Jupiter C4 column in order to eliminate impurities such as peptides, urea and reduction agents. The Figure 16 (Fig. 16.). shows the chromatogram obtained where it is possible to observe the peak of the protein at approximately 90% acetonitrile.

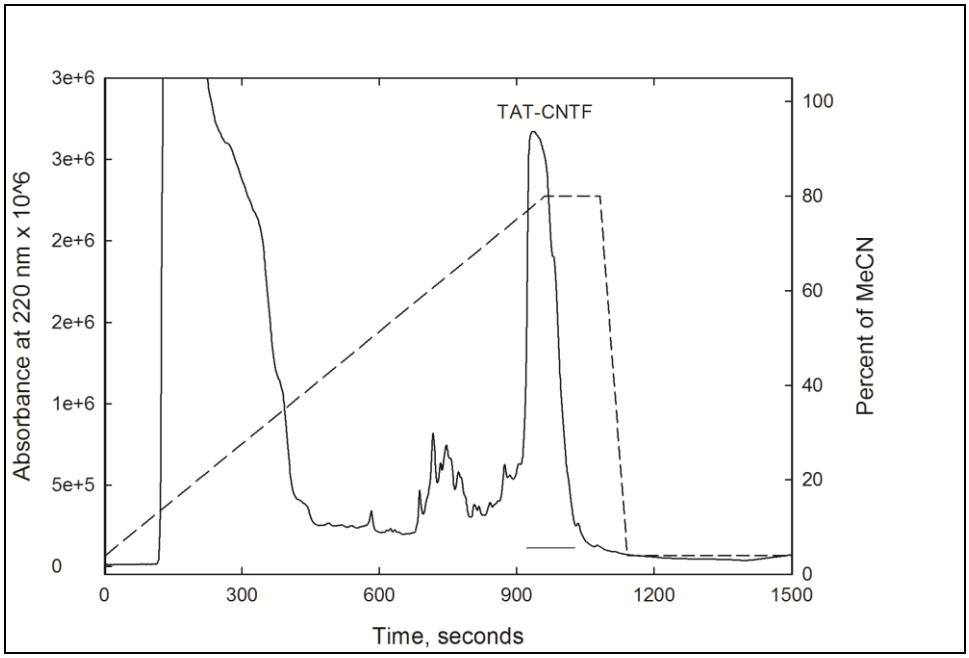

Fig. 16. Chromatogram on the recovery of TAT-CNTF obtained with reverse phase chromatography using a Vydac C4.

In order to evaluate the purity degree, the neurotrophic growth factor TAT-CNTF was loaded on SDS-PAGE. As can be seen in Figure 17 (fig. 17.)., in samples where the growth factor has precipitated (P) and, more markedly, in the supernatant (S) there is the presence of a single band of approximately 26 KDa corresponding to the effective weight of the factor.

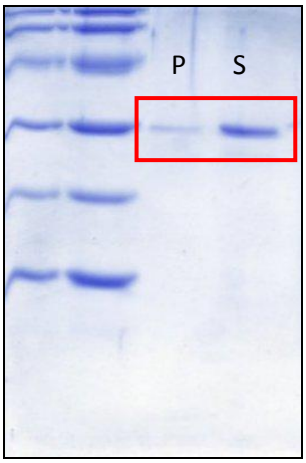

Fig. 18. SDS-PAGE of TAT-CNTF. P is the precipitated protein fraction, while S is the supernatant protein fraction.

To verify the molecular mass of the purified protein, it has been used MarinerTM ESY-TOF spectrometer and the obtained multiprotic spectrum has been deconvoluted in order to show only one peak which represents the molecular mass. (Fig. 19A and B).

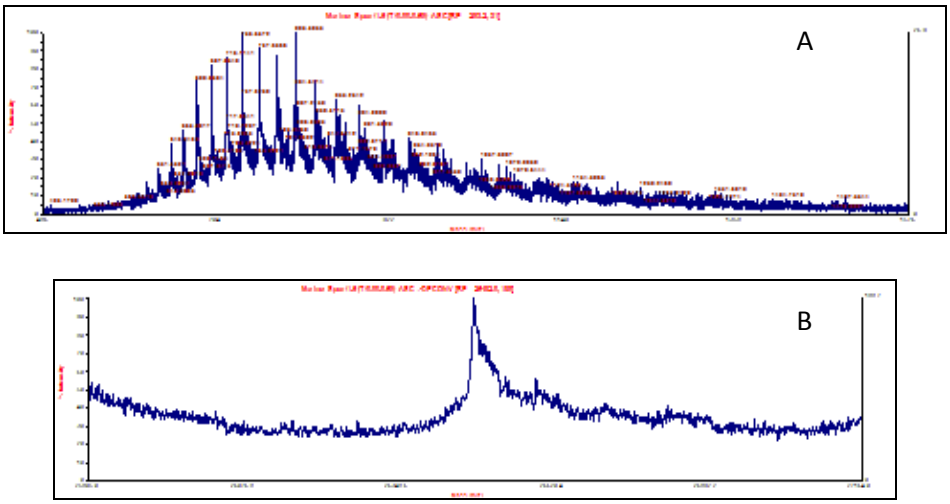

Fig. 19. Multiprotic spectrum (A) and deconvoluted spectrum (B) of TAT-CNTF after recovery with reverse phase chromatography using Vydac C4.

The collected protein fraction after reverse phase chromatography (HPLC) was used to measure the UV absorbance of the protein in order to quantify its concentration in solution. The peak in the image (Fig. 20.) shows the presence of the protein at 280 nm.

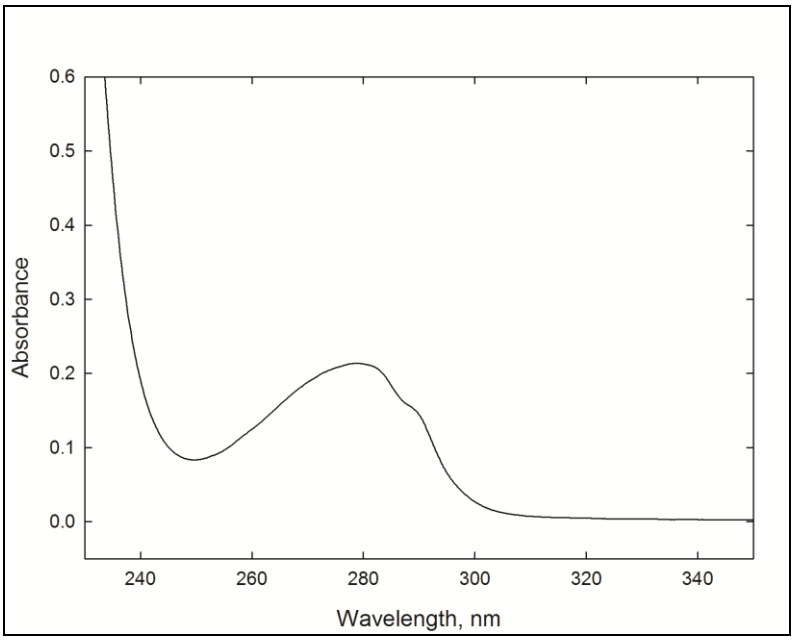

Fig. 20. UV spectrum of TAT-CNTF.

Once obtained the purified protein, in order to confirm the hypothesis that the chemical modification made on the material can promote the neurotrophic factor attack and release, it has been evaluated the release of TAT-CNTF, incubated with the three different types of PVA.

The release was assessed after 1, 24, 96 hours and after 10 days (Fig. 21.) incubation using UV spectrophotometer measures, placing λ from 280-350 nm. The results obtained were normalized using the dry weight of disks. The oxidation affects the release of the protein in a different manner. The sample 2% PVA (green curve) appears to be the best sample in releasing the protein over the time.

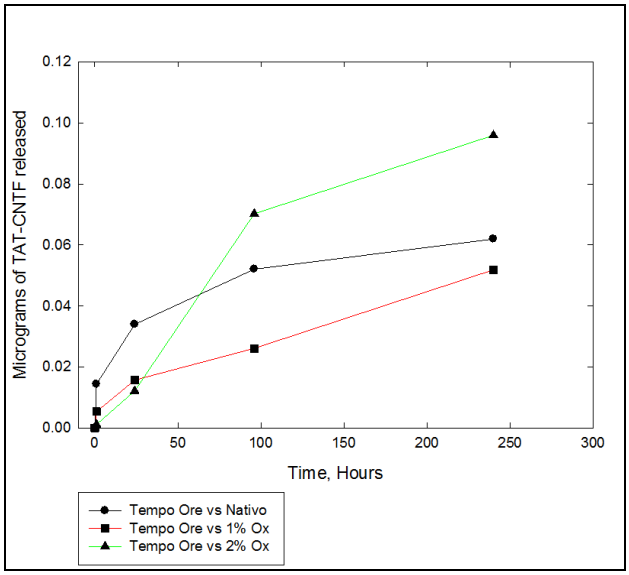

Fig. 21. Graph of protein release from native (blue curve), 1% (red curve) and 2% PVA (green curve).

5) CELL CULTURE

5.1. SHSY5Y cell adhesion and morphology

The first experiments were conducted with the aim to determine any adhesion properties of the three types of PVA. The cells were seeded onto disks scaffolds of the three types of PVA under examination (native, 1% and 2% PVA), previously incubated with laminin and collagen. The adhesion was evaluated by SEM after 24, 72 and 96 hours after seeding.

Figures 22 and 24 (Fig. 22. and 24.) show SEM images relating to cellular adhesion on the three types of material (respectively with laminin and then with collagen) after 24, 72 and 96 hours. In all the cases the cellular adhesion is poor, except for the control glass disks where cells adhere well and increase in number through time, as confirmed by the MTT test performed on the same materials (Fig. 23. And 25). Moreover, cells on biomaterials maintain a globular shape, meaning a negative qualitatively adhesion.

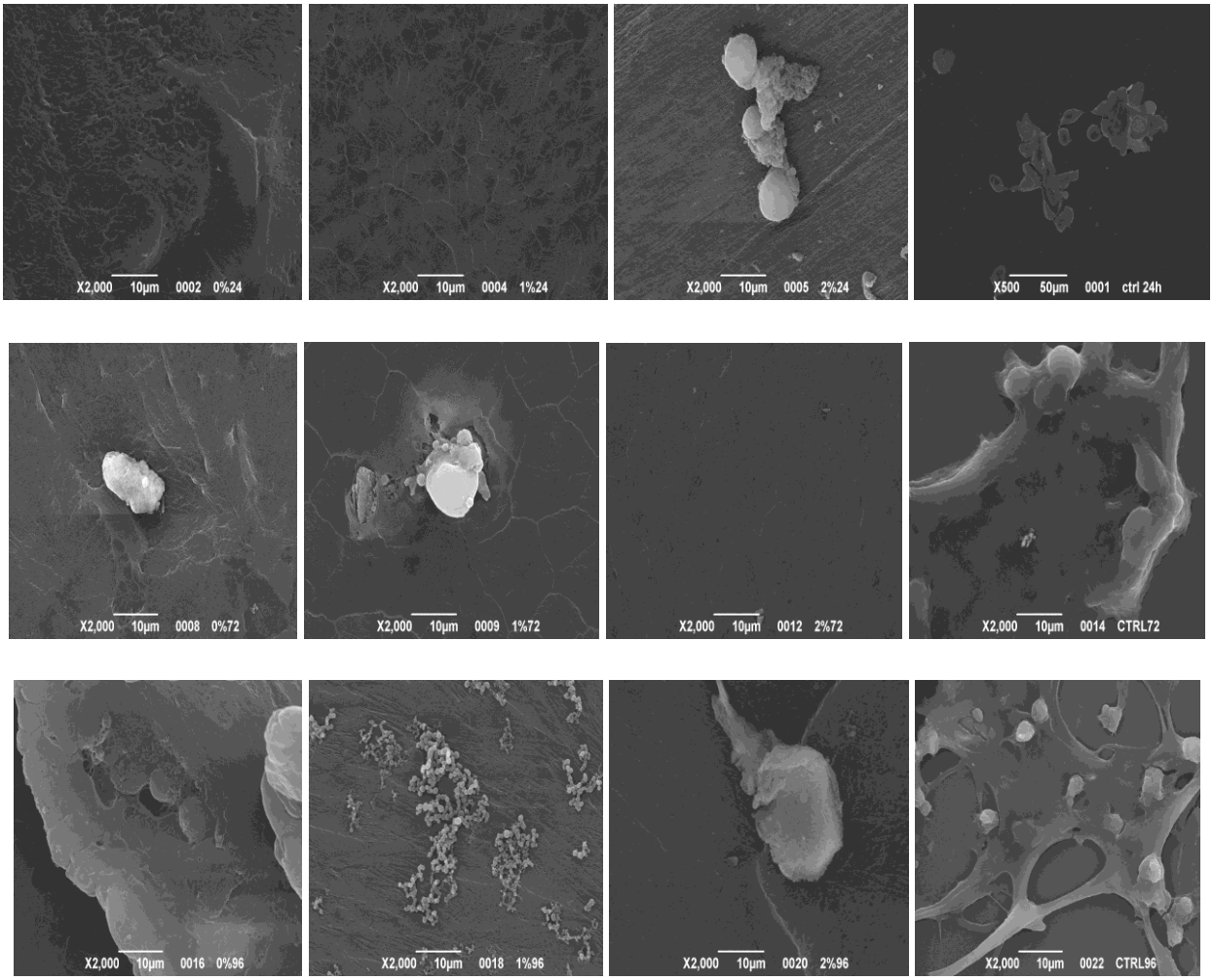

Figure 22. SEM images of SHSY5Y adhesion on native (first row), 1% (second row), and 2% PVA (third row) conditioned with laminin. Images, from left to right, represent cellular adhesion at 24 hours (first column), 72 hours (second column) and 96 hours (third column). Last column represents cellular adhesion on control glass disks.

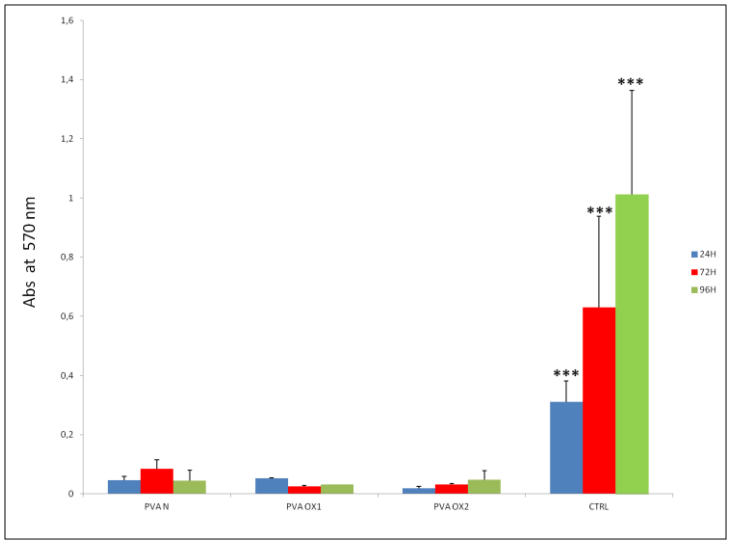

Fig. 23. MTT assay at 24, 72 and 96 hours. From left to right are indicated, respectively, the cellular adhesion on native, 1% and 2% PVA incubated with laminin. Statistical analysis was performed using anova test with post hoc Bonferroni test (SPSS program V.18). Three, two and one asterisks indicate, respectively, a p value <0.001, 0.01 and 0.05.

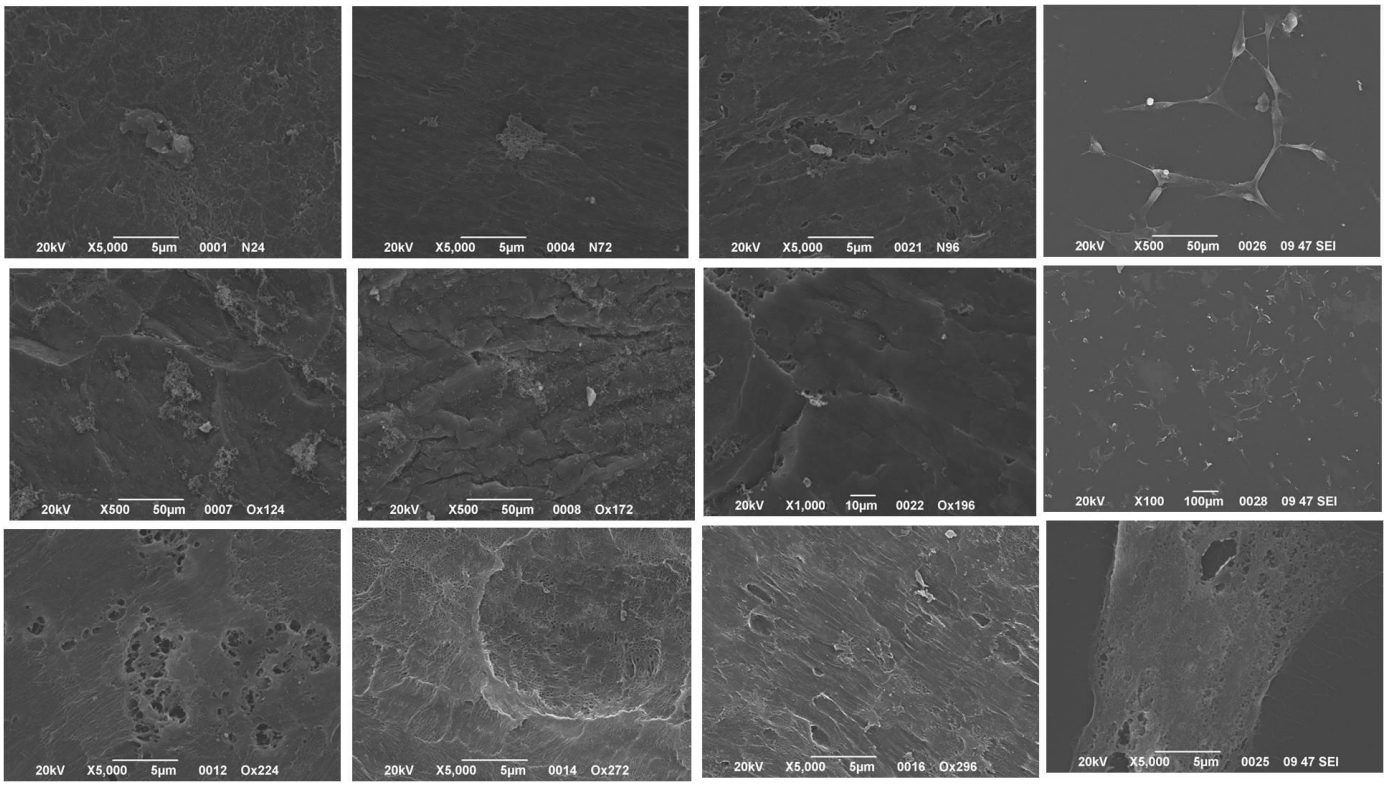

Fig. 24. SEM images of SHSY5Y adhesion on native (first row), 1% (second row), and 2% PVA (third row) conditioned with collagen. Images, from left to right, represent cellular adhesion at 24 hours (first column), 72 hours (second column) and 96 hours (third column). Last column represents cellular adhesion on control glass disks.

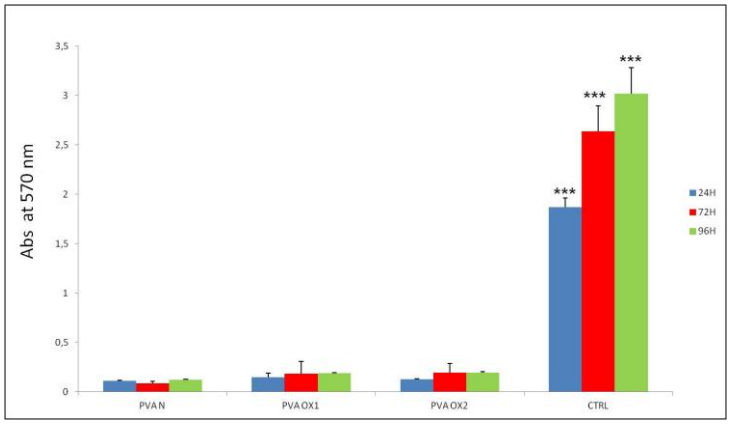

Fig. 25. MTT assay at 24, 72 and 96 hours. From left to right are indicated, respectively, the cellular adhesion on native, 1% and 2% PVA incubated with collagen. Statistical analysis was performed using anova test with post hoc Bonferroni test (SPSS program V.18). Three, two and one asterisks indicate, respectively, a p value <0.001, 0.01 and 0.05.

The experiment was then performed in the same way, by seeding cells on three types of biomaterial with added decellularized human nerve matrix (Fig. 26.), thus increasing the irregularity of the surface and creating a more favorable environment for cellular adhesion and proliferation.

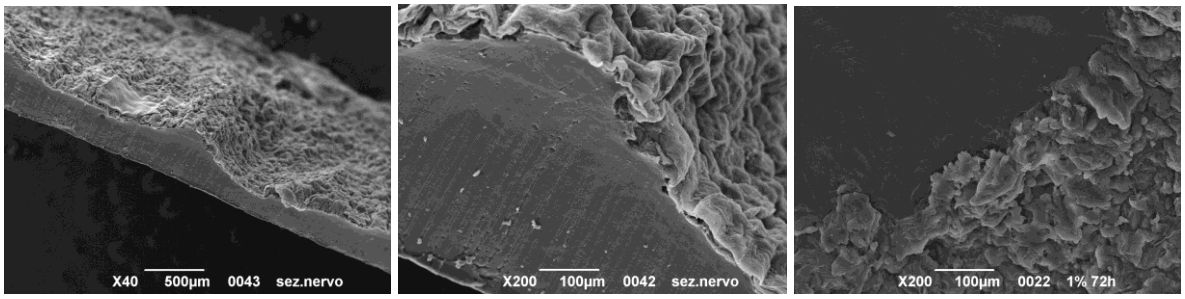

Fig. 26. SEM images of PVA supplemented with decellularized human nerve matrix.

In Figures 27 (Fig. 27.), SEM images show scaffolds with matrix added at 24, 72 and 96 hours after seeding. As can be seen, in all three cases there is a greater increase in cell adhesion compared to the same scaffolds without matrix and greater than the controls themselves, until reaching the confluence. This is also reflected in the MTT assay (Fig. 28.). However, as it can be seen, the increase in vitality do not depend on the different oxidation degree of the PVA.

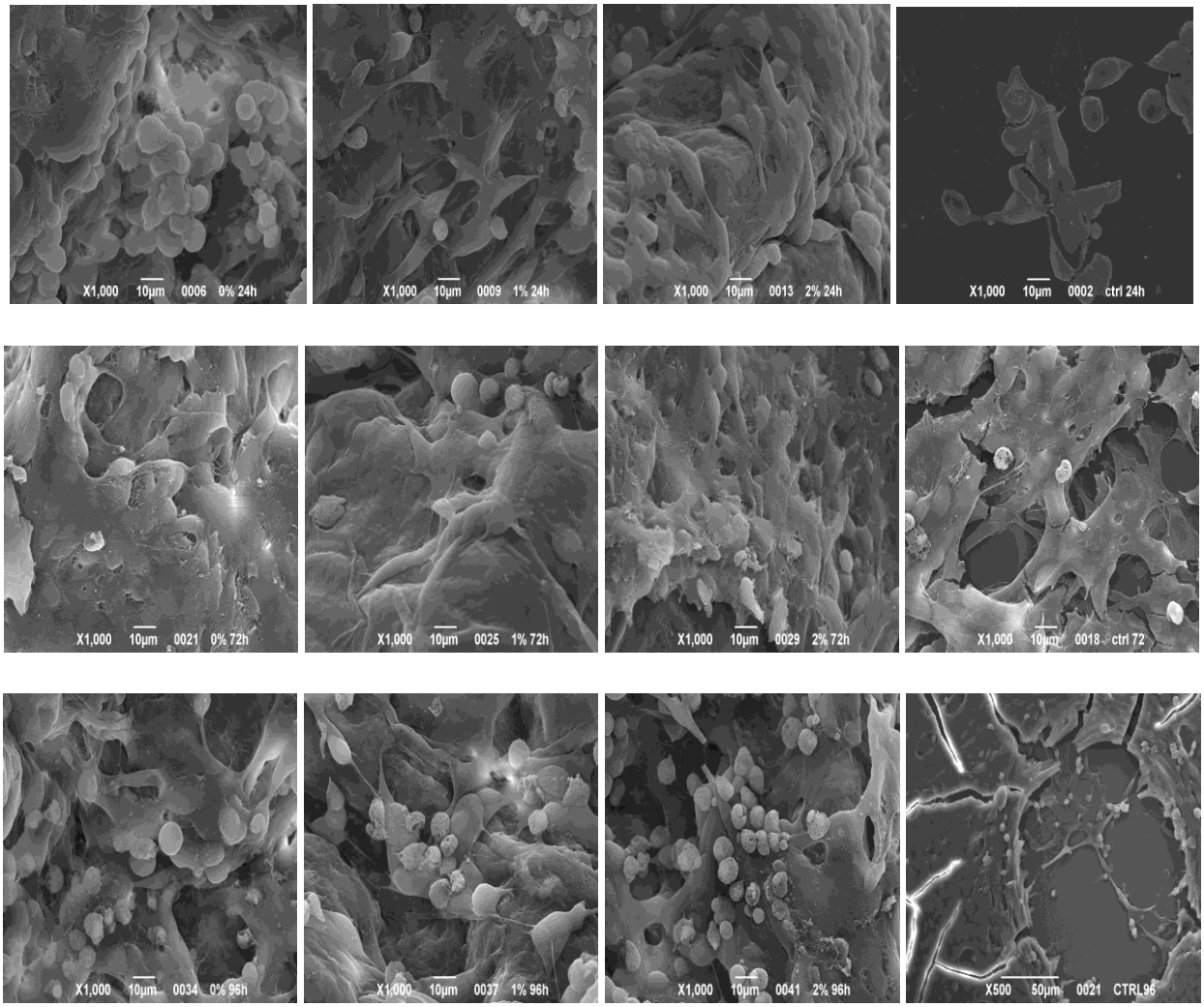

Fig. 27. SEM images of SHSY5Y adhesion on native (first row), 1% (second row), and 2% PVA (third row) with lyophilized decellularized human nerve matrix on disks surface. Images, from left to right, represent cellular adhesion at 24 hours (first column), 72 hours (second column) and 96 hours (third column). Last column represents cellular adhesion on control glass disks.

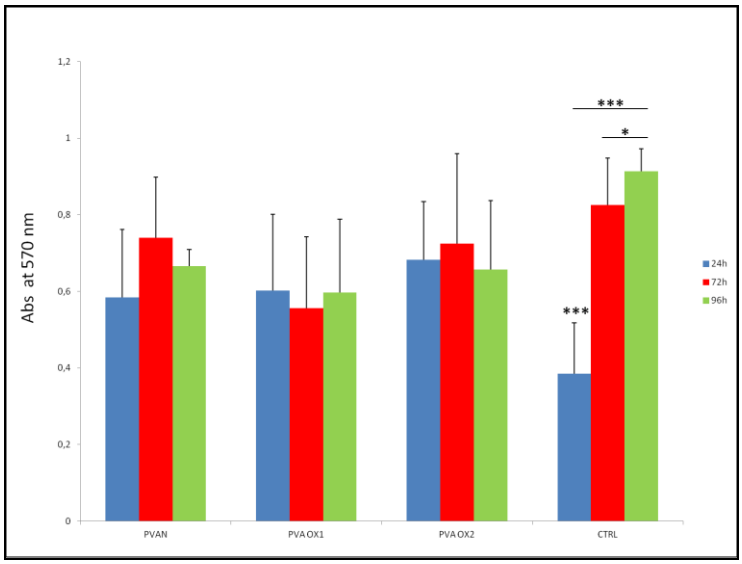

Fig. 28. Cell adhesion asses by MTT experiment at 24, 72 and 96 hours after cell seeding (from left) on native, 1%, 2% PVA (with lyophilized decellularized human nerve matrix on disks surface) and controls. Statistical analysis was performed using anova test with post hoc Bonferroni test (SPSS program V.18). Three, two and one asterisks indicate, respectively, a p value <0.001, 0.01 and 0.05

5.2. Cellular proliferation

It has been evaluated the proliferation degree of SHSY5Y cells, plated in less quantity on PVA materials added with decellularized matrix, than in previous experiments. Since cells don't adhere on naked materials it wasn't important study this property on this type of materials.

As can be seen from SEM images (Fig. 29.) and from the MTT graph (Fig. 30.), there is a proportional increase in cell number, through time in vitro, on biomaterials with added matrix. However, the proliferation degree does not depend from the different oxidation degree of the polymer, since the growth trend is comparable between the different materials in the same time points (that's the reason in showing the images relating only to one of three types of biomaterial).

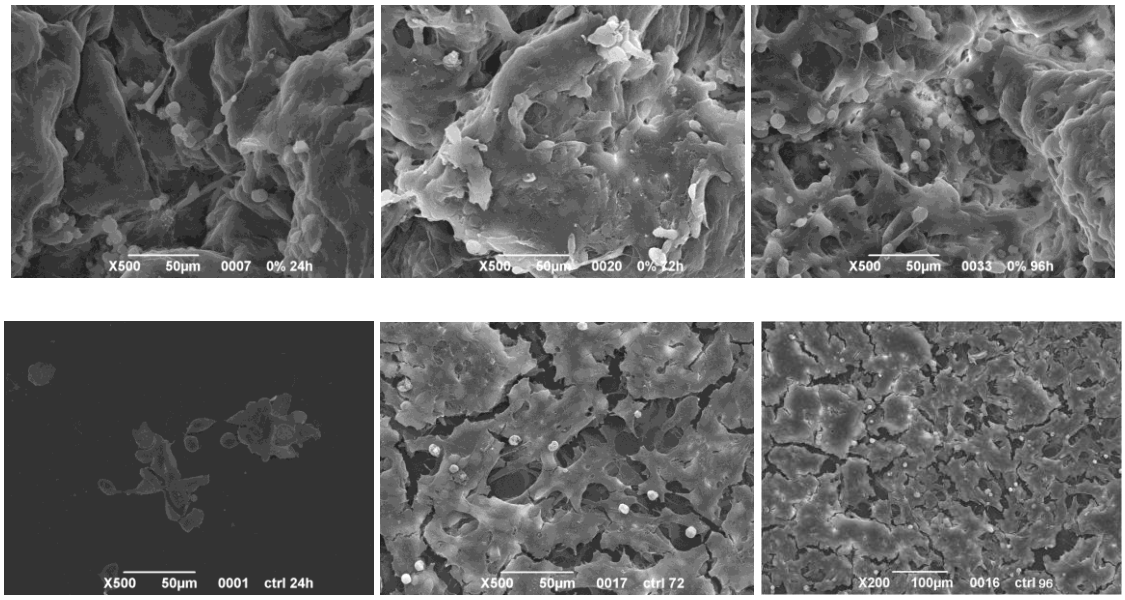

Fig. 29. SEM images of SHSY5Y proliferation on PVA with added matrix. First row, from left to right, represent cellular proliferation, respectively, at 24, 72 and 96 hours on native PVA. Last row represent the control glass disks at the same time of analysis.

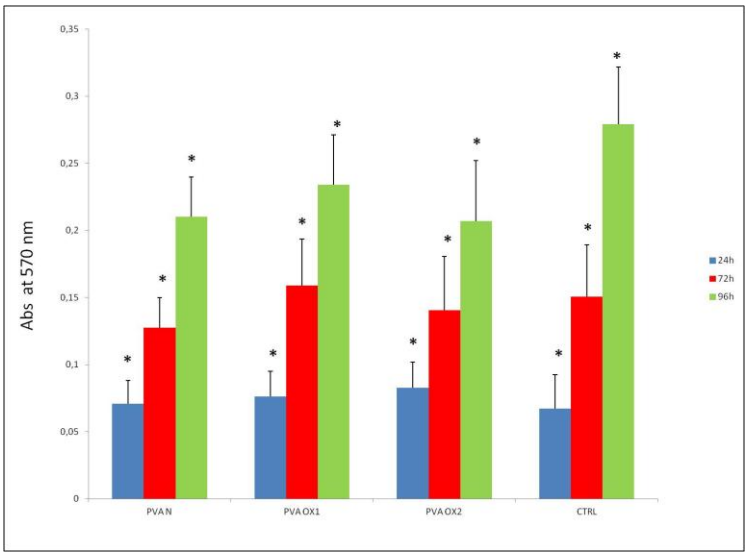

Fig. 30. MTT graph of SHSY5Y proliferation on the biomaterial with added matrix. From left to right, native, 1%, 2% PVA and control glass disks. Statistical analysis was performed using anova test with post hoc Bonferroni test (SPSS program V.18). The three, two and one asterisks indicate, respectively, a p value <0.001, 0.01 and 0.05.

As regards the proliferation, both in the presence of TAT-CNTF (Fig. 31A) and NGF (Fig. 31B.) at the same concentrations, there isn't significant increase in the cellular proliferative activity in the period of time taken into consideration (from 1 to 24 hours after stimulation).

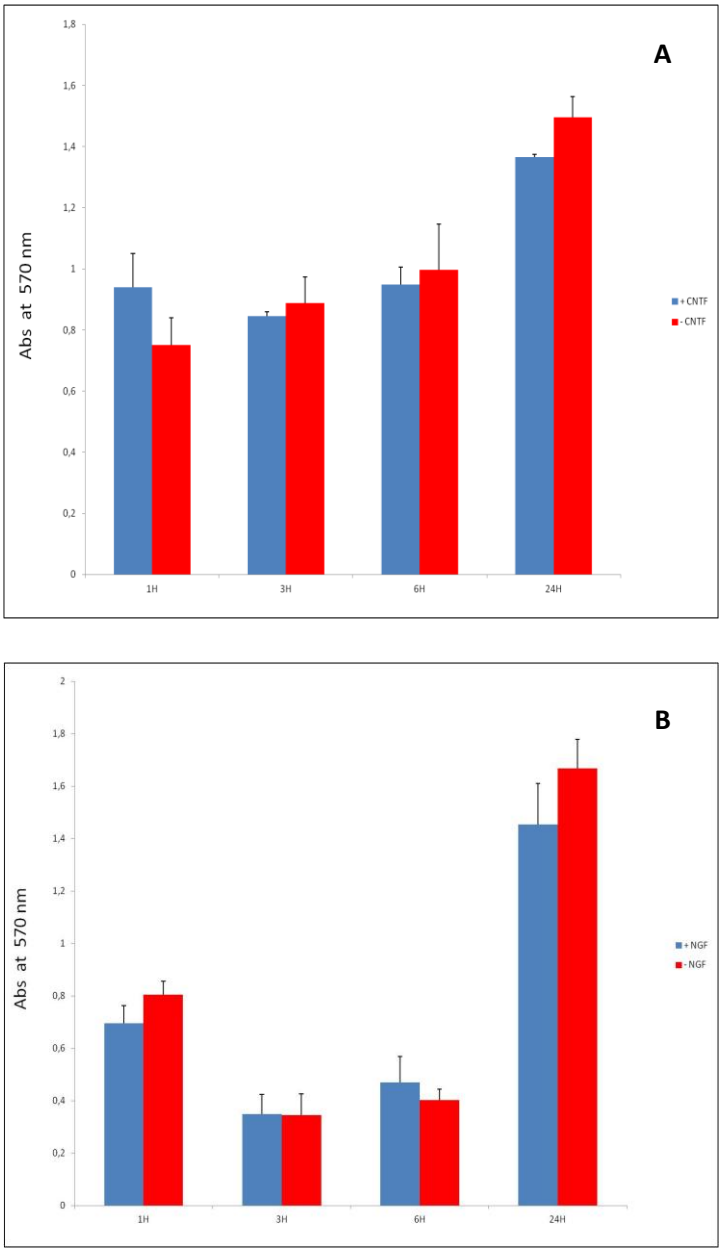

Fig. 31. MTT graph of SHSY5Y proliferation in the presence (blue column) or absence (red column) of TAT-CNTF (A) and in the presence or absence of NGF (B).

Despite the lack of proliferation there is the presence of CNTFRα subunit and STAT 3 activation by phosphorylation, as it can be seen by western blots (Fig. 32A and B.)

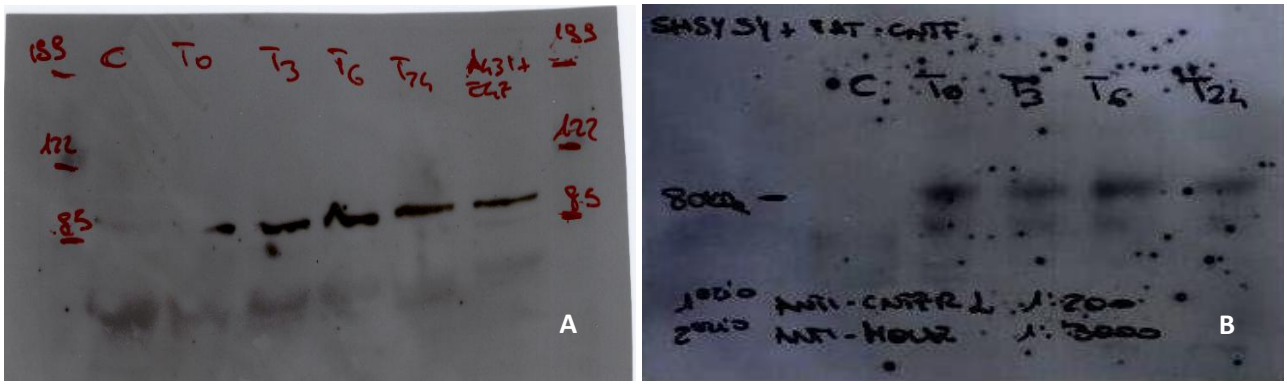

Fig. 32. SHSY5Y western blots of A) anti-STAT3 (85 KDa) and B) anti-CNFTRα (80 KDa).

In the last part of the work it has been used also PC12 cells treated with TAT-CNTF in order to verify the functionality of the neurotrophic factor. Through the use of the MTT assay (Fig. 33.), it was noticed as the factor induces a significant increase in proliferation from 6 to 48 hours after stimulation. Subsequently, the difference between the treated and not treated cells tends to vanished because the first reach the full confluence faster than the other and therefore stop their proliferation activity for the contact inhibition (Fig. 34.).

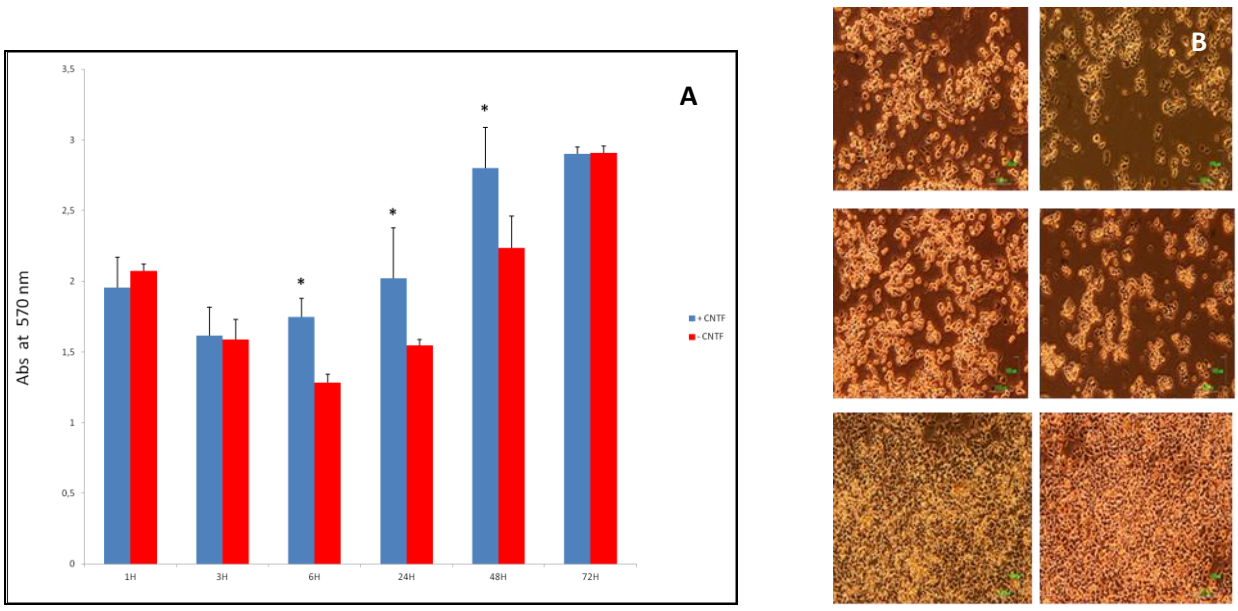

Fig. 33. MTT graph of PC12 proliferation stimulated with TAT-CNTF (A). Statistical analysis was performed using anova test with post hoc Bonferroni test (SPSS program V.18). The three, two and one asterisks indicate, respectively, a p value <0.001, 0.01 and 0.05. Images of PC12 proliferation under the optical microscope (B). First column represents cellular cultures with TAT-CNTF while second column represents cellular cultures without neurotrophic factor. The images are referred at 24, 48 and 72 hours after growth factor stimulation.

The obtained above results are further substantiated by western blots (Fig. 34A and B.) showing a strong expression of the CNTFRα subunit which lead to the STAT-3 phosphorylation.

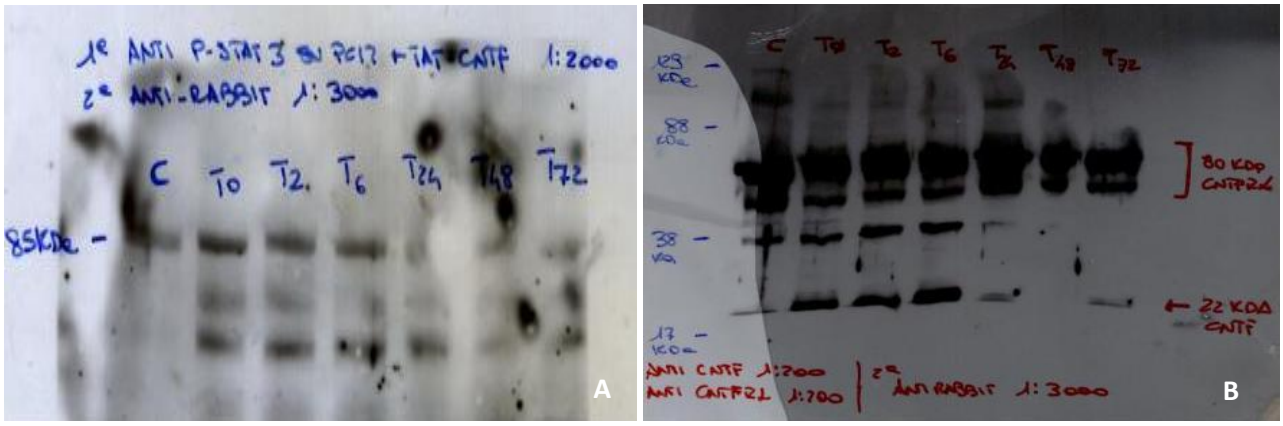

Fig. 34. PC12 western blots of A) anti-STAT3 (85 KDa), B) Western blot anti-hCNTF (22 KDa) and anti-CNFTRα (80 KDa).

5.3. Cellular morphogenetic differentiation

It has been rated also the morphological differentiation activity induced by TAT-CNTF and NGF on SHSY5Y using the same cell density and the same concentration of factor seen in the proliferative experiments. The cells treated with TAT-CNTF, observed using light microscopy after 1, 6 and 10 days, show no morphological differences compared to the control, in contrast to cells treated with NGF. (Fig. 35.).

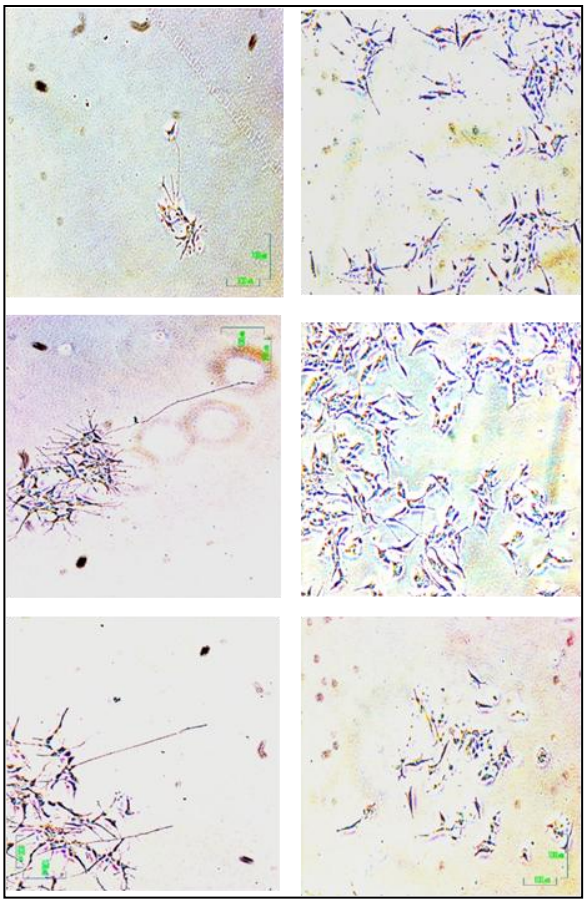

Fig. 35. Optical microscope images of SHSY5Y cells. Images of the first column show cells treated with NGF after, respectively, 1, 6 and 10 days. Images of the second column show the same cells treated with TAT-CNTF at the same concentration and in the same period.

Also on PC12 cells was carried out the same experiment in after stimulation with TAT-CNTF. Also in this case there aren't any differences between treated cells and controls without factor (Fig. 36.).

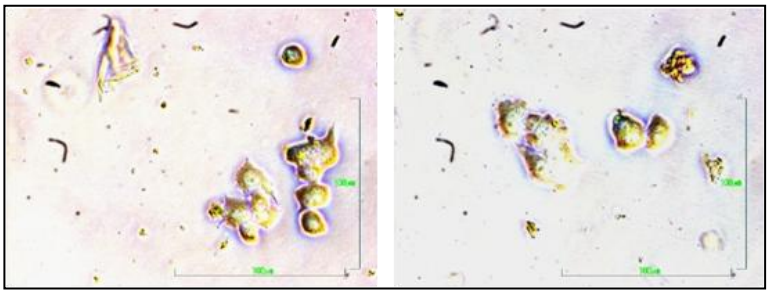

Fig. 36. Optical microscope images of PC12 morphogenetic differentiation. The images are related to 1 and 10 days after stimulation with TAT-CNTF.

5.4. Cellular trafficking

The experiment was carried out both on SHSY5Y and PC12 cell lines in order to be able to locate the TAT sequence and the CNTF protein inside cells. As can be seen in the images of immunofluorescence (Fig. 37A and B), the recombinant protein is immediately internalized into cells. Subsequently, the bond between TAT sequence and CNTF is cleaved thus allowing TAT to go to the nucleus, while CNTF is exocitate out of the cells, binding its receptor thereby activating the cascade of signal transduction. Immunofluorescence images and previous western blots experiments (for CNTFRα subunit and STAT 3) confirm this hypothesis.

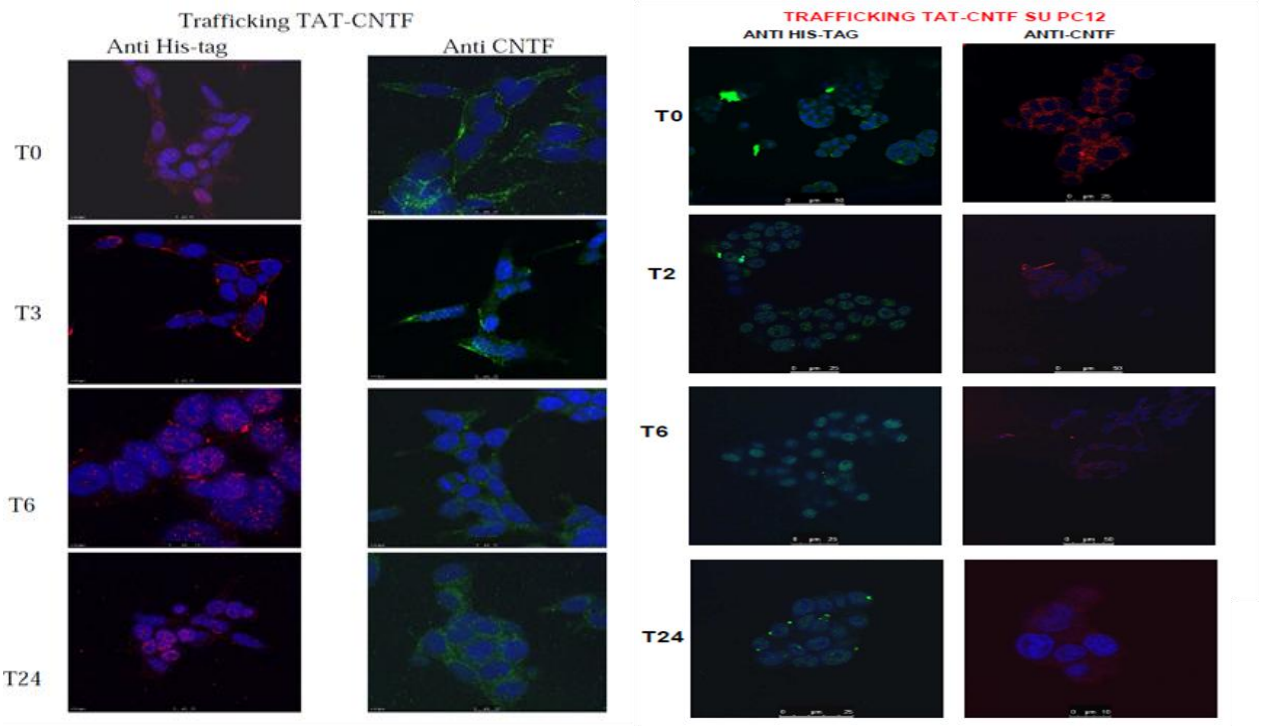

Fig. 37. Trafficking immunofluorescence images of SHSY5Y (A) and PC12 (B). In both of the panels, the first column shows the hys-tag location inside cells, while the second column shows the cellular CNTF position.

6) CONSTRUCTION OF A TUBULAR SCAFFOLD WITH AN INTRALUMINAL FILLER

After the various tests performed on biomaterials and decellularized human nerve matrix, it has been constructed a tubular scaffold of 2% PVA with an intraluminal filler made up of human nerve decellularized matrix manually inserted inside the scaffold. The choice of 2% PVA was motivated by its greater degradability and its best ability to release proteins. The SEM images (Fig. 38.) clearly show the structure of the device.

The polymer tube of the scaffold, from the material oxidation to the solid form, through the freeze thawing technique, is a patented industrial invention (No: **VI2013A000019,** class: A61K) deposited in "Camera di Commercio Industria, Artigianato e Agricoltura" of Vicenza, Italy.

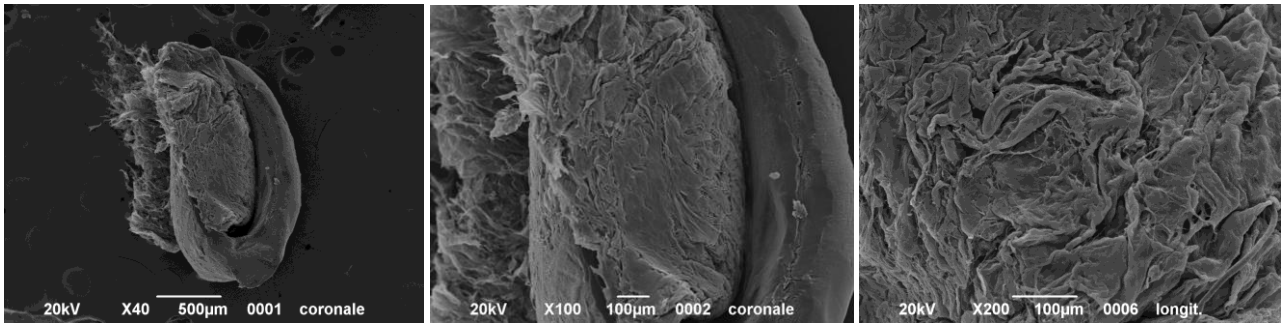

Fig. 38. SEM images of the 2% PVA tubular scaffold with decellularized human nerve matrix as internal filler.

DISCUSSION

Peripheral nerves injuries affect approximately 2.8% of all injuries (Ciardelli et al, 2005). They are more common in the upper parts of the body and are often due to common causes such as cuts, accidents, sports injuries. The incidence of a permanent or temporary disability due to a lack or incorrect regeneration is very high and often leads to drastic changes in lifestyle and work activity, having so an important socio-economic impact (Lohmeyer et al, 2008).

Over the past 25 years, the concept of "tube" for nerve regeneration has evolved from a simple tool to study this phenomena to a regenerative device used in clinical practice as an alternative to the use of autograft of nervous origin (De Ruiter et al, 2009). This was possible by an increase in knowledge about biomaterials, both natural and synthetic (Tabata et al, 2009). Despite the use of tubulization technique is temporarily limited to the repair of lesions of small size (3-4 cm) in nerves of small caliber, the potential of this technique can be extended also to the repair of more severe injuries, especially to the motor nerves.

In this work it has been studied and characterized, from a chemical, physical, mechanical and biological point of view the synthetic biomaterial polyvinyl alcohol (PVA). The material is obtained by hydrolysis of polyvinyl acetate, prepared by polymerization of vinyl acetate. PVA is a biocompatible material, resistant, flexible and low-cost and is not degradable if not in an artificial manner (Xin et al, 2011). In order to make it physiologically degradable and usable also as DDS, it has been studied a chemical modification that favors the presence of more chemical groups for electrostatic interactions: the selective oxidation carried out has therefore made possible the transformation of some secondary alcohol groups, abundant in the material, in more labile ketone groups, but also hemiacetal and acetal groups (due to the binding of the keto groups with secondary alcohol). After then, three different types of PVA has been prepared, two of which with nominal oxidation degree equal to 1% and 2% (1% PVA and 2% PVA), and one non-oxidized (native PVA).

The oxidation degree was evaluated in the materials, from a chemical point of view, through the DNFH assay, a reactive typically indicated for the determination of carbonyl groups, aldehyde and ketone (Levine et al, 1990). The assay showed a quantity of carbonyl groups less than expected, considering also the amount of oxidizing agent employed. The result could be explained by the possibility that the massive dialization suffered by the samples have favored, in some way, the hydrazone partial dissociation, which would result in a lower recovery of ketone groups. Another hypothesis could involve an excessive lowering of the equilibrium constant of the reaction, favored by the highly acid environment. It is also not negligible the possible formation of acetal and hemiacetal groups, which would involve a considerable decrease of the carbonyl groups. However, the amount of carbonyl groups is directly proportional to the oxidation degree.

The DLS analysis showed a proportional decrease of the material hydrodynamic radius as the increase of oxidation degree. The explanation could be the increased compactness, acted by oxidation on the material, due to the formation of intramolecular acetal and hemiacetal bonds. These bonds, in addition, may cause a folding of the molecular chain, normally linear, on itself. The results may also be due to breakage of the CC bonds intrachain during the oxidation reaction: this would result in the presence of molecular species of lower weight, perhaps responsible, in fact, in the decrease in hydrodynamic radius. In any case the 2% PVA appears to be composed of lower weight particles compared to the native and 1% PVA, while all the three materials have an eterogeneous particle dispersion, as indicated by the area below the curves.

Subsequently, the materials were studied by a mechanical point of view, through uniaxial tensile test and DSC.

The uniaxial tensile tests, carried out on tubular scaffolds, showed a greater resistance of the not oxidized material, and in general, a decrease in stress resistance with increasing percentage of oxidation. Also the DSC test showed a decrease in the polymer crystalline component to the increases oxidation (in fact, the area below curves is greater as much the presence of crystal group), so it is possible to deduce that the chemical process makes the material less resistant because the decrease of the hydroxyl groups in favor of those carbonyl subtracts hydrogens atoms for the formation of intramolecular hydrogen bonds thereby reducing the polymer crystalline structure and so reducing also stress resistance.

However, since the chemically modified biomaterial has been thought as a prosthesis for use on the trauma of peripheral nerves and so be a type of lesion where pressures and tractions forces are mild, even a more rigid tube can be suitable as well to be sutured between two stumps and ensure an optimal nerve regeneration. In addition, this disadvantage is further passed by the extreme elasticity of the polymer.

With regard to biodegradation, it is known that the long permanence of a material on the site of nerve injury can result in chronic inflammation, fibrosis and adverse immune responses resulting in failure of recover functionality. The three types of PVA under examination, native, 1% and 2% PVA were then studied using static and dynamic degradation tests in two different solutions, complete DMEM culture medium and physiological saline buffer PBS.

The observation of the static tests allows purely qualitative analysis, where it can be noticed only a greater propensity of 2% PVA to form holes, indistinguishably between the condition in DMEM and the other one in PBS. The dynamic tests instead provide quantitative data and put a light on a

completely different behavior of the three biomaterials in two different solutions. After six months, regarding the condition in DMEM, all the materials lose a 30% of their weight while in PBS conditions they lose approximately a 60% of weight even if in this case, 2% PVA has the greater degradation rate. However, the experimental period in which the materials have been tested is insufficient to have a clear idea and a complete data set to elucidate the polymer degradation behavior. In fact, for DMEM condition it could be necessary to pass more time over six months since notice a difference in the degradation rate between the three materials, also because a complete quantitatively and qualitatively nerve regeneration occurs in years and most of the common commercialized regenerative scaffolds degradate in 2/4 years (De Ruiter et al, 2009).

The polymer adhesive and proliferation properties were evaluated by SEM observation and MTT analysis. Both SEM images and MTT data clearly showed the limited, or almost non-existent, ability of the material, in all its degrees of oxidation and functionalized with different adhesion proteins to promote cell adhesion. All the materials don't or scarcely show adherent cells on the surface. Moreover the globular cellular morphology is an index of qualitatively unsatisfactory adhesion and therefore it has not been possible to study the proliferation. One possible explanation for this phenomenon may lie in the high water content of the material. The hydrophilic, although it is fundamental for cell adhesion, if too strong, could act as an inhibiting environment for cellular adhesion (Young et al, 2005) and in fact both the oxidized and non oxidized PVA have a water content in water higher than 88%. Subsequently it has been highlight the difference (in terms of adhesion, cell proliferation and vitality) between the naked biomaterials respect the type with added decellularized human nerve matrix. Both SEM images and MTT data confirmed the increased adhesion and cell proliferation in all three types of PVA with extracellular matrix, compared to the same naked materials. However, these increases are not dependent on the oxidation degree, emphasizing how the biological properties of the composite material depend exclusively from the organic matrix. The literature confirms as a composite scaffold, of a different nature and composition, can increase the capacity of regeneration through the stabilization of the fibrin network that is formed within the scaffold. Furthermore, the presence of an internal structure increases the adhesion possibility, structurally supports the axonal regrowth and the local release of neurotrophic factors (De Ruiter et al, 2009; Daly et al, 2012). The matrix also provides proteins, such as collagen, also detected with SDS-PAGE, essential for the formation of basal lamina, a pivotal structure in the early stages of regeneration process.

Secondly, the oxidative modification of PVA has been thought with the aim of increasing the possible sites of nucleophilic attack on the material, in order to favor the binding and release of

neurotrophic factors, which are essential for the entire regeneration process, both anatomical that functional. For this purpose, was study the protein release from the three types of materials, incubated under suitable conditions in the presence of the growth factor TAT-CNTF. As expected, the 2% PVA has shown a better capacity to release the factor than the other two types of material, native and 1% PVA. This confirms the fact that the oxidation promotes the ability to create electrostatic bond, as much as the increase in oxidation rate and so it will also be able to release more factors in the lesion area. However, as confirmed by previous experiments conducted in our laboratory, the kinetics of protein release also depends on the weight and amount of the protein incubated with the material.

The growth factor used in this work, the TAT-CNTF has been employed on SHSY5Y and PC12 cells, two cell lines of different species, in which the factor receptor is expressed and preserved, in order to study the induced effects neurotrophic. TAT-CNTF was obtained by fusing a human CNTF domain with the transduction protein domain derived from TAT (transcriptional transactivator) protein of human immunodeficiency virus-1 in order to facilitate the crossing of the plasma membrane and the localization in the nucleus, unlike the CNTF not engineered. Therefore, the TAT domain is able to increase, after local administration, the cellular uptake rate of the protein domain CNTF and promote its cellular translocation, maintaining the neurotrophic activity but not the negative side effects, such as cachexia, anorexia and severe immune response (Rezende et al, 2009). Like all proteins belonging to the cytokines family, TAT-CNTF and CNTF have a tetrameric structure, consisting of four subunits to α-helix: UV-CD measurements have shown that the combination between CNTF with TAT does not involve changes in the protein structure (Rezende et al, 2009).

The signaling transduction mechanism involves the binding between CNTF and its receptor composed of three subunits: the α domain (also known as CNTFRα), not transductional, extracellular and anchored to the membrane by a phosphatidylinositolic bond; gp 130 subunit and Leukemia Inhibitory Factor Receptor β (LIFRβ), which are transmembrane and signal transductor (Vieira et al, 2009).

The neurotrophic factor, once bound to CNTFRα, promotes the activation, by dimerization of the two signal transduction subunits, protein JAK/TYK tyrosine kinase (particularly JAK-1 and JAK-2, as reported by Rossino et al, 1995). The activated JAK proteins induce STAT proteins phosphorylation, in particular STAT-3. STAT-3 in turn dimerize and promote the transcription of different DNA sequences. It has been also identified another group of proteins, the Ras-MAPK proteins, activatable after phosphorylation of gp 130 following the signal transduction (Kuroda et

al, 2001). CNTF and other cytokines are also able to induce tyrosine phosphorylation at the level of other proteins such as phospholypase Cγ, ERK 1 and ERK 2, PP120 (Sleeman et al, 2000). This data confirm the complexity of the transduction mechanisms underlying cytokine activity.

To assess the cellular localization of TAT-CNTF, it has been performed trafficking experiment on SHSY5Y and PC12 cell lines, using anti hys-tag (amino acid domain present on TAT sequence) and anti human CNTF antibodies: observation by confocal microscopy showed an increasing migration of TAT within the cell nucleus through the passing hours, and human CNTF from inside to outside the cell. This data support the hypothesis that TAT-CNTF is immediately internalized, thanks the TAT domain, the bond is cleaved promoting nuclear translocation of TAT and the CNTF exocytosis, which can bind to its receptor in order to start the signal transduction, as shown by western blot data (regarding the STAT 3 phosphorylation). In fact, the experiment shows that the phosphorylation of STAT-3 protein increases in cells after stimulation up to 24 hours. However, despite the receptor presence and the STAT 3 activation, TAT-CNTF does not induce increase in neurite morphogenesis, viability and proliferation in SHSY5Y, except for PC12 cells between the 6 and 48 hours after stimulation. In agreement with the results obtained by Kuroda et al, 2001, these may be explained on the basis of a failure of the signal transduction of other ways, such as the Ras-MAPK transduction way.

To understand whether the non-proliferation activity was attributable to the poor cellular reactivity, it has been used the NGF on SHSY5Y at the same concentrations of TAT-CNTF. The choice of NGF was motivated by its ability to induce positively three genes present in the neuroblastoma cell line: NGF 1A, c-fos and GAP 43; the latter is involved in the neurite growth cone development (Rossino et al, 1995). In fact the NGF stimulation has developed some neurites, but did not increase the cellular viability and proliferation compared to untreated controls. It is reasonable to think, therefore, that the non-proliferation activity and absent morphological differentiation is not due to cell line (Rossino et al, 1995), but in transductional mechanisms related to TAT-CNTF same. At this point, in order to understand the TAT-CNTF activity it has been used another cell line, such as the rat pheochromocytoma PC12 cell line. Having demonstrated the presence of CNTFRα receptor and the STAT-3 phosphorylation (as shown by western blot experiments), it has been performed the same previously cellular biology experiments on SHSY5Y cell. Unlike the latter, there is a significant difference in the proliferation and cell viability from 6 to 48 hours after stimulation with the factor. This difference, however, is not visible in the first 3 hours of incubation or at 72 hours. This can be explained by the fact that at the beginning there is a minimum time threshold before appreciate the effect due to the transduction of the signal, while at the end of the experimental

period, cells treated with TAT-CNTF reaching the confluence faster respect the non-treated cells, so arresting their growth for contact inhibition and be reached from the other cells. One possible explanation for the different behavior between the SHSY5Y and PC12 cells can be attributed to the greater expression of the CNTFRα receptor in the latter, but this hypothesis request further experimental confirmation. However, even for PC12 cells, there isn't a morphogenetic effect induced by TAT-CNTF.

In conclusion, the various elements analyzed in this experimental study were able to highlight the positive aspects of the chemical modification on the PVA polymer, from a chemical, physical and mechanical point of view. To increase the polymer biological properties it has been necessary the addition of decellularized human nerve matrix, previously lyophilized and then disk shaped in order to put on the surface polymer, and later used as filler for the composite tubular scaffold. These positive results, although preliminary, support the creation of a tubular scaffold of modified PVA modified, more degradable and able to function as DDS and so release pro-regenerative proteins. With these data has been possible obtained an industrial patent deposit and submit some papers.

REFERENCES

Baker MI, Walsh SP, Schwartz Z, Boyan BD. *A review of polyvinyl alcohol and its uses in cartilagine and orthopedic applications.* J Biomed Mater Res Part B. 100 B: 1451-1457. 2012.

Battiston B, Geuna S, Ferrero M, Tos P. *Nerve repair by means of tubulization: literature review and personal clinical experience comparing biological and synthetic conduits for sensory nerve repair*. Microsurgery.25: 258-267. 2005.

Bellamkonda R. *Peripheral nerve regeneration: an opinion on channels, scaffolds and anisotropy. Journal of biomaterials*. 27: 3515-3518. 2006.

Beris A, Lykissas M, Korompilias A, Mitsionis G. *End-to-side nerve repair in peripheral nerve injury*. Journal of neurotrauma. 4(5): 909-916. 2007.

Campbell W. *Evalutation and management of peripheral nerve injury. Clinical Neurophysiology*. 119: 1951-1965. 2008.

Chen ZL, Yu WM, Strickland S. *Peripheral regeneration*. Annu. Rev. Neuroscience. 30: 209-233. 2007.

Ciardelli G, Chiono V. *Materials for peripheral nerve regeneration*. Macromolecular bioscience. 6: 13-26. 2006.

Daly W, Yao L, Zeugolis D, Windebank A, Pandit A. *A biomaterials approach to peripheral nerve regeneration: bridging the peripheral nerve gap and enhancing functional recovery*. J. R. Soc. Interface. 9: 202-221. 2012.

De Ruitter GCW, Malessy MJA, Yaszemski MJ, Windebank AJ, Spinner RJ. *Designing ideal conduits for peripheral nerve repair*. Neurosurg Focus. 26(2): E5. 2005.

Geuna S, Nicolino S, Raimondo S, Gambarotta G, Battiston B, Tos P, Perrotau I. *Nerve regeneration along bioengineered scaffolds*. Microsurgery. 27:429-438. 2007.

Hall S. *The response to injury in the peripheral nervous system*. J. Bone Joint Surg. 87-B: 1309-1319. 2005.

Hassan CM, Peppas NA. *Structure and morphology of Freeze/Thawed PVA Hydrogels*. Macromolecules 33: 2472-2479. 2000.

Ichiara S, Inada Y, Nakamura T. *Artificial nerve tubes and their application for nerve repair of peripheral nerve injury: an update of current concepts*. Injury, Int j.Care Injured. 3954: 529-539. 2008.

Ijkema-Passen J, Jansen K, Gramsbergen A, Meek MF. *Transection of peripheral nerves, bridging strategies and effect evaluation*. Biomaterials. 25: 1583-1592. 2004.

Johnson EO, Zoubos AB, Soucacos PN. *Regeneration and repair of peripheral nerves*. Injury, Int. J. Care Injured. 365: 524-529. 2005.

Johnson EO, Soucacos PN. *Nerve repair: experimental and clinical evaluation of biodegradable artificial nerve guides*. Injury, Int. J. Care Injured. 395: 530-536. 2008.

Kuroda H, Sugimoto T, Horii Y, Sawada T. *Signaling pathway of ciliary neurotrophic factor in neuroblastoma cell lines*. Medical and pediatric oncology. 36: 118-121. 2001.

Leach JB. *Tissue-engineered peripheral nerve*. Wiley Encyclopedia of biomedical Engineering. 2006.

Levine RL, Garland D, Oliver CN, Amici A, Climent I, Lenz AG, Ahn BW, Shaltiel S, Stadtman ER. *Determination of carbonyl content in oxidatively modified proteins*. Methods Enzymol. 186 :464-478. 1990.

Lohmeyer JA, Siemers F, Machens HG, Mailander P. *The clinical use of artificial nerve conduits for digital nerve repair: a prospective cohort study and literature review*. J Reconstr Microsurg. 25: 55-62. 2009.

Marz P, Ozbek S, Fischer M, Voltz N, Otten U, Rose-John S. *Differential response of neuronal cells to a fusion protein of ciliary neurotrophic factor/soluble CNTF-receptor and leukemia inhibitory factor*. Eur. J. Biochem. 269: 3023-3031. 2002.

Meezan E, Hjelle JT, Brendel K.. *A simple, versatile, non disruptive method for the isolation of morphologically and chemically pure basement membranes from several tissues*. Life Sci. 17:1721-1732. 1975.

Millon LE, Mohammadi H and Wan WK.. *Anisotropic polyvinyl alcohol hydrogel for cardiovascular applications*. J Biomed Mater Res Part B: Appl Biomater 79B: 305–311. 2006.

Navarro X, Vivò M, Valero-Cabré A. *Neural plasticity after peripheral nerve injury and regeneration*. Progress in Neurobiology. 82: 163-201. 2007.

Orive G, Anitua E, Pedraz JL, Emerich DF. *Biomaterials for promoting brain protection, repair and regeneration*. Nature Reviews/ Neuroscience. 10: 682-692. 2009.

Plun-Favreau H, Elson G, Chabbert M, Froger J, deLapeyrière O, Lelièvre E, Guillet C, Hermann J, Gauchat JF, Gascan H, Chevalier S. *The ciliary neurotrophic factor receptor α component induces the secretion of and is required for functional responses to cardiotrophin-like cytokine*. The EMBO Journal. 20(7): 1692-1703. 2001.

Rezende AC, Peroni D, Vieira A, Rogerio F, Talaisys RL, Costa FTM, Langone F, Skaper SD, Negro A. *Ciliary neurotrophic factor fused to a protein transduction domain retains full neuroproctective activity in the absence of cytokine-like side effects*. Journal of Neurochemistry. 109: 1680-1690. 2009.

Rossino P, Volpe G, Negro A, Callegaro L, Altruda F, Tarone G, Silengo L. *Ciliary neurotrophic factor-induced gene expression in human neuroblastoma cell lines*. Neurochemical research. 20(6): 675-680. 1995.

Sleeman MW, Anderson KD, Lambert PD, Yancopoulos GD, Wiegand SJ. *The ciliary neurotrophic factor and its receptor, CNTFRα*. Pharmaceutica Acta Helvetiae. 74: 265-272. 2000.

Tabata Y. *Biomaterial technology for tissue engineering applications*. J. R. Soc. Interface. 6: 311-324. 2009.

Tabesh H, Amoabediny G, Salehi Nik N, Heydari M, Yosefifard M. *The role of biodegradable engineered scaffolds seeded with Schwann cells for spinal cord regeneration*. Neurochemistry International. 54: 73-83. 2009.

Vieira AS, Rezende ACS, Grogoletto J, Rogério F, Velloso LA, Skaper SD, Negro A, Langone F. *Ciliary neurotrophic factor infused intracerebroventricularly shows reduced catabolic effects when linked to the TAT protein transduction domain*. Journal of Neurochemistry. 110: 1557-1566. 2009.

Xin D, Xu X, Wang H, Gao Y. *Advanced oxidation of polyvinyl alcohol wastewater by O_3/UV*. IEEE. 978(1): 1424-1427. 2011.

Young TH, Hung CH. *Behavior of embryonic rat cerebral cortical stem cells on the PVA and EVAL substrates*. Biomaterials. 26: 4291-4299. 2005.

PUBBLICATIONS

Borgio L, Dalzoppo D, Stocco E, Lora S, Grandi C. Different adhesion properties of modified composite PVA scaffolds for neural regeneration. 2013. In Preparation.

Borgio L, Dalzoppo D, Del Gaudio C, Negro A, Stocco E, Lora S, Grandi C. Chemical, physical and mechanical characterization of modified PVA hydrogels for nerve regeneration. 2012. In Preparation.

Borgio L, Sartore L, Dalzoppo D, Stocco E, Lora S, Grandi C. Blood vessels reconstruction using PVA hydrogels tube-shaped scaffolds. 2012. Submitted.

Borgio L, Bridi D, Venturini M, Dalzoppo D, Negro A, Stocco E, Lora S, Grandi C. Trafficking, proliferation and neuromorphological effects of recombinant human TAT-CNTF on PC12 and SHSY5Y cells. 2012. Submitted.

2013. Deposit of industrial patent application "Biomaterial for medical device, in particular prosthesis", Camera di Commercio Industria, Artigianato e Agricoltura di Vicenza. Number: **VI2013A000019**; Class: A61K.

2010. Cloning and sequencing of the Fatty Acid Amide Hydrolase (FAAH) gene of *Carassius auratus* (for sequence details, see www.ncbi.nlm.nih.gov, accession number: HM231167).

I would like to thank my Supervisor, Prof. Claudio Grandi for the opportunity I had in learning so many things which allowed me to grow up not only as men but also as young scientist. Without him I will never arrive here.

Special thanks to Dr. Daniele Dalzoppo, for his precious and wise advises along these years not only like GREAT researcher, like he is, but also like dear person.

Thanks to Prof. Pier Paolo Parnigotto, Prof. MariaTeresa Conconi and Dr. Silvano Lora for their contribution in my human and scientific training and growth.

Thanks to Prof. Maria Fosca Franzoni, to force me to meet new and more honestly people and to experience an excellent work environment. I learned a lot from her.

I sincerely thank my family for always believing in me, for the many right words at the right time, for the support in all the difficult times and for his patience.

I sincerely thank all the friends from Turin and Bassano and my girlfriend for their physical and moral presence in remember me why I am here and for what purposes.

I would like to thank my Lab and courses friends and all the people I knew during these three important years of my PhD, with whom I shared intense and significant moments of this adventure.

Finally, I would like to thank myself, my attitude to the problem solving, stubbornness and the enormous patience to sustain all the things that happened during these last years.